UNIVERSIDADE DE LISBOA

Faculdade de Medicina

KYOTORPHIN AND ITS DERIVATIVES: UNVEILING ROUTES AND TARGETS

Juliana Rodrigues Perazzo

Orientador: Prof. Doutor Miguel Augusto Rico Botas Castanho

Tese especialmente elaborada para obtenção do grau de Doutor em Ciências Biomédicas, Especialidade em Bioquímica Médica

2018

UNIVERSIDADE DE LISBOA

Faculdade de Medicina

KYOTORPHIN AND ITS DERIVATIVES: UNVEILING ROUTES AND TARGETS

Juliana Rodrigues Perazzo

Orientador: Prof. Doutor Miguel Augusto Rico Botas Castanho

Tese especialmente elaborada para obtenção do grau de Doutor em Ciências Biomédicas, Especialidade em Bioquímica Médica

Júri
Presidente:
Doutor José Augusto Gamito Melo Cristino, Professor Catedrático e Presidente do Conselho Científico da Faculdade de Medicina da Universidade de Lisboa

Vogais:
- Doutor António Francisco Rosa Gomes Ambrósio, Investigador Principal com Agregação da Faculdade de Medicina da Universidade de Coimbra;
- Doutora Isaura Ferreira Tavares, Professora Associada da Faculdade de Medicina da Universidade do Porto;
- Doutora Dora Maria Tuna Oliveira Brites, Investigadora Coordenadora da Faculdade de Farmácia da Universidade de Lisboa;
- Doutora Ana Maria Ferreira de Sousa Sebastião, Professora Catedrática da Faculdade de Medicina da Universidade de Lisboa;
- Doutor Miguel Augusto Rico Botas Castanho, Professor Catedrático da Faculdade de Medicina da Universidade de Lisboa (orientador).

Bolsa de doutoramento financiada pela Fundação para a Ciência e a Tecnologia (SFRH/BD/52225/2013)

2018

As opiniões expressas nesta publicação são da exclusiva responsabilidade do seu autor

A impressão desta tese foi aprovada pelo Conselho Científico da Faculdade de Medicina da Universidade de Lisboa em reunião de 26 de Setembro de 2017.

Acknowledgements

I am so grateful I came this far and accomplished all that besides the difficulties. The years I spent working on this thesis have taught me a lot about who I am and what I want. Doing a PhD helped me to broaden my horizons and taught me valuable lessons for life. Many people helped me on this journey, in different ways, and I would like to thank them for that.

First I would like to thank my supervisor, Prof. Dr. Miguel Castanho, for giving me the opportunity to join his lab, to manage to find time for me in his very busy schedule and for being always open to my ideas. We both know that this pathway has not been easy for me, but if I got until here I must thank him because he was always supportive in the difficult moments and pushed me to continue with my work.

I also would like to thank Dr. Mônica Lopes-Ferreira that was my second supervisor. I spent a considerable amount of time in her lab, at Instituto Butatan and it was there that I developed big part of my research. Dr. Carla Lima together with Dr. Mônica provided me the technical and scientific guidance to develop my work and I am grateful for that.

To everyone that spent a bit of time to teach me a technique, to help me with an experiment (even the ones that did not work out) I would like to express my sincere gratitude. Here I want to mention specially Dr. Sónia Santos, Antónia Pinto, Dr. Diana Gaspar, Dr. Mônica Lopes-Ferreira, Dr. Lidiane Grund, Taís Matozo, Jéssica Araújo, Sara Cardoso and Keylla Domingues.

I do not know Dr. Eduard Bardaji and Dr. Monteserrat Heras in person, but I would like to thank them for the synthesis of kyotorphin analogues.

To my colleagues of MCastanho Lab and the technician Liliana Carvalho I want to thank them to provide me a very organized work environment and to guide me in the lab.

To NSantos group I want to thank the helpful discussions during the lab meetings and the companionship and informal chats, mainly during the lunch.

I acknowledge the LisbonBiomed PhD program, all the colleagues I did within the program and the financial support granted by Fundação para Ciência e Tecnologia through PhD scholarship SFRH/BD/52225/2013. Also, Marie Skłodowska-Curie Research and Innovation Staff Exchange (RISE) is acknowledged for funding: call H2020-MSCA-RISE-2014, Grant agreement 644167, 2015-2019.

I am thoughtfully grateful to my cousin Janaína and her family for welcoming me so warmly in their home when I arrived in São Paulo. I also would like to thank Leo for being more than a friend in the difficult moments.

The last, but not the least I thank my parents, Joyce and Luís, for their unconditional support, love and comprehension. They always encouraged me and gave me the strength to continue this journey. Without them I would never come this far.

Preface

I started my PhD on January of 2014 with the first edition of the LisbonBiomed PhD program. During the first two months, I had the chance to participate in the training module "Towards a creative and critical mind" developed specifically to the LisbonBiomed PhD students. This module comprised thematic weeks organized by different research groups at Instituto de Medicina Molecular (IMM) in which we were exposed to varied activities, such as seminars, talks given by inspiring figures, clinical case presentations and debates. During that period, we got to know better the work developed by the research groups that were interested in receiving a PhD student in their labs. I liked very much the work presented by Dr. Sónia Sá Santos entitled "beating the blood-brain barrier" where she presented a bit about the European Project PEP2BRAIN. I was fascinated with the work on the analgesic peptides developed by MCastanho team and then I decided to join the group to continue the work with the promising kyotorphin (KTP) derivatives. Although Professor Miguel Castanho had initially thought in a work related to Dengue virus, he supported my decision to work with the peptide KTP and its derivatives. Together, we have elaborated a project to better understand the routes and targets of KTP analogues.

This project allowed me to collaborate with the immunoregulation laboratory in the Laboratório de Toxinologia Aplicada, led by Dr. Mônica Lopes-Ferreira, at Instituto Butantan, where I spent 12 months in total.

My PhD work originated the following papers:

I. Pharmacological potential of the endogenous dipeptide kyotorphin and selected derivatives.
Perazzo J, Castanho M and Sá Santos S.
Front Pharmacol (2017), volume 7, 530, DOI: 10.3389/fphar.2016.00530

II. Endothelium-mediated action of analogues of the endogenous neuropeptide kyotorphin (Tyrosil-arginine): mechanistic insights from permeation and effects on microcirculation.
Perazzo J, Lopes-Ferreira M, Sá Santos S, Serrano I, Pinto A, Lima C, Badarjí E, Tavares I, Heras M, Conceição K and Castanho MARB.
ACS Chem Neurosci (2016), 7(8):1130-40. DOI: 0.1021/acschemneuro.6b00099

III. Neuropeptide kyotorphin impacts on lipopolysaccharide-induced glucocorticoid-mediated inflammatory response. A molecular link to nociception, neuroprotection, and anti-inflammatory action.
Perazzo J, Lima C, Heras M, Badarjí E, Lopes-Ferreira M, Castanho MARB.
ACS Chem Neurosci (2017), DOI: 10.1021/acschemneuro.7b00007. [Epub ahead of print]

IV. Improvement of the pharmacological properties of amidated kyotorphin by means of iodination.
Oliveira MC, Gano L, Santos I, Correia JDC, Serrano ID, Sá Santos S, Ribeiro M, **Perazzo J**, Tavares I, Heras M, Badarjí E and Castanho MA.
MedChemComm (2016), volume 7, pages 906-913, DOI: 10.1039/c6md00028b.

This thesis is written in a paper format and is divided into 5 sections. In the first section the reader can find a bibliographic revision about KTP and selected derivatives, mainly the ones designed and studied by us. Section 2 conjugates data obtained from permeability *in vitro*, analgesic tests and intravital microscopy of selected derivatives of amidated kyotorphin (KTP-NH_2) to help us to understand how simple structural modifications can impact the biological activity of the peptide. KTP-NH_2 is one of the most inexpensive and most interesting molecules developed by us. Therefore, we went a bit further to understand the mechanisms behind the analgesic and anti-inflammatory properties of this KTP analogue. Our efforts to address these questions resulted in the paper presented in section 3. A brief motivation for articles 2 and 3 were included at the beginning of sections 2 and 3, respectively. A general conclusion of the results is presented in section 4.

In this dissertation, two distinct referencing methods were followed. The references cited along the thesis (excluding articles) are listed in section 5, sorted alphabetically by first author's last name. Within each paper the format of the references cited comply with the guidelines defined by the respective journal and are listed in the end of each article.

Abbreviations

[I^{125}]MIK – mono-radioiodinated KTP-NH_2

[I^{125}]DIK – di-radioiodinated KTP-NH_2

2VO – bilateral common carotid artery occlusion

AI – angiotensin I

AII – angiotensin II

AIII – angiotensin III

ACE – angiotensin converting enzyme

AD – Alzheimer disease

ANP – atrial natriuretic peptide

BBB – blood-brain barrier

BK – bradykinin

Boc – tert-butyloxycarbonyl

BOP – benzotriazole-1-yl-oxy-tris-(dimethylamino)-phosphonium hexafluorophosphate

BSA – bovine serum albumin

Bzl – benzyl

CCK – cholecystokinin

cGMP – cyclic guanosine monophosphate

CNS – central nervous system

CSF – cerebrospinal fluid

DIEA – diisopropylethylamine

DMSO – dimethyl sulfoxide

DPP3 – dipeptidyl peptidase III

E.coli – *Eschericia coli*

EDTA – Ethylenediaminetetraacetic acid

e.g. – from latim *exempli gratia,* for example

EGTA – ethylene glycol-bis(2-aminoethylether)-N,N,N’,N’-tetraacetic acid

ERS – electrical resistance system

ESI – electrospray ionization

ET-1 – endothelin-1

ET-2 – endothelin-2

ET-3 – endothelin-3

GABA – aminobutyric acid

GCs – glucocorticoids

GEMSA – guanidinoethylmercaptosuccinic acid

GFAP – glial fibrillary acid protein

GR – glucocorticoid receptor

HBTU – O-(benzotriazol-1-yl)-N,N,N’,N’-tetramethyluronium hexafluorophosphate

HEPES – 4-(2-hydroxyethyl)-1-piperazineethanesulfonic acid

HO-1 – heme oxygenase-1

HOBt – N-hydroxybenzotriazole

HPLC – high performance liquid chromatography

I.A. g^{-1} – injected activity per gram of organ

IASP – International Association for the Study of Pain

Ib – ibuprofen

IbKTP – kyotorphin linked to ibuprofen

IbKTP-NH_2 – kyotorphin-amide linked to ibuprofen

i.c.v. – intracerebroventricular

i. e. – from latim *id est*, that is

IL-1 – interleukin-1

IL-1 – interleukin-10

i.p. – intra-peritoneal

i.pl. - intraplantar

Ind – indole

i.v. – intravenous

IVM – intravital microscopy

KTP – kyotorphin

KTP-NH_2 – kyotorphin amide

KTPr – kyotorphin specific receptor

LPS – lipopolysaccharide

LTA4 – leukotriene A_4 hydrolase

MCI – mild cognitive impairment

MGTA – 2-mercaptomethyl-3-guanidinoethylthiopropanoic acid

MD2 – myeloid differentiation protein 2

MS – mass spectrometry

NKA – neurokinin A

NKB – neurokinin B

NMM – N-methylmorpholine

NMR – nuclear magnetic resonance

NO – nitric oxide

NOP – nociceptin/orphanin receptor

NOS – nitric oxide synthetase

NSAIDs – non-steroidal anti-inflammatory drugs

NT – neurotensin

OT – oxytocin

PBS – phosphate buffer

PC18 – 2-amino4-methylsulfonyl butane thiol

PEPT2 – peptide transporter 2

PLC – phospholipase C

pmc – 2,2,5,7,8-pentamethyl-chroman-6-sulfonyl

P_R – relative permeability

RBCs – red blood cells

rpm – rotations per minute

rt – room temperature

S. aureus – *Staphylococcus aureus*

S.D – standard deviation

SEM – standard error of mean

SP – substance P

SS – somatostatin

SUVs – small unilamellar vesicles

TEER – trans-endothelial electrical resistance

TIS – triisopropylsilane

TRH – thyrotropin

UV – ultraviolet

Vis – visible

vs. – versus

VWF – von Willebrand factor

Resumo

O neuropéptido endógeno denominado quiotorfina (L-Tyr-L-Arg, KTP) tem demonstrado uma notável atividade analgésica, podendo ser até 4.2 vezes mais potente do que opióides endógenos quando administrados diretamente no cérebro, mas é ineficiente quando administrado sistemicamente. O nosso grupo tem desenvolvido e estudado vários análogos da quiotorfina, entre eles a quiotorfina-amida (L-Tyr-L-Arg-NH_2, KTP-NH_2), que é analgésica, anti-inflamatória e neuroprotetora após administração sistémica. Apesar deste conjunto interessante de propriedades biológicas, que tornam a KTP-NH_2 um candidato interessante para desenvolvimento farmacológico, o desconhecimento do seu mecanismo de ação torna-se muito limitativo. É necessário progredir no avanço do entendimento das suas bases moleculares de ação para conseguir depois executar um plano de desenvolvimento industrial do fármaco. Este avanço passa por conseguir uma melhor compreensão da relação estrutura-função, estrutura-eficácia e estrutura-farmacocinética do fármaco, bem como revelar e caracterizar os seus alvos.

O objetivo desta tese é contribuir para compreender os alvos e mecanismos de ação da KTP-NH_2. Para alcançar esse objetivo, desenvolveram-se derivados da KTP-NH_2 que contribuíram para elucidar novos aspetos da relação estrutura-atividade; e procuraram-se alvos específicos que pudessem explicar as atividades biológicas da KTP-NH_2.

Primeiro, introduziram-se pequenas alterações seletivas na estrutura química da KTP-NH_2 através da introdução de D-aminoácidos e/ou metilação N-terminal, de modo a aumentar a lipofilicidade e resistência à degradação enzimática. Observou-se que o péptido D-Tyr-L-Arg-NH_2 (KTP-NH_2-DL) tem um efeito anti-inflamatório pronunciado mas apresenta uma baixa atividade analgésica, provavelmente devido à baixa permeabilidade em membranas lipídicas. A KTP-NH_2 apresenta um comportamento semelhante, exceto pela sua potente ação analgésica em vários modelos de dor. Estes resultados suportam a hipótese de que a KTP-NH_2 utiliza transportadores específicos para atravessar a barreira hematoencefálica, transportadores esses que não são

capazes de transportar os seus análogos, como a KTP-NH_2-DL. Os isómeros metilados, quer seja em conformação LL ou LD, são bastante permeáveis em membranas lipídicas e provavelmente atravessam passivamente a barreira hematoencefálica. Este resultado, provavelmente associado a uma maior resistência à digestão enzimática, contribui para explicar o efeito analgésico prolongado desses derivados em comparação a KTP-NH_2. No entanto, os isómeros metilados (LL e LD) têm atividade pró-inflamatória, o que lhes retira potencial farmacológico.

Numa segunda fase, na tentativa de elucidar os mecanismos moleculares por detrás da ação da KTP-NH_2, utilizou-se uma abordagem baseada em microscopia intravital e inibidores farmacológicos. Demonstrou-se que o KTP-NH_2 é capaz de diminuir, em apenas 10 minutos, o número de leucócitos rolantes induzidos por lipopolissacáridos (LPS) ou CXCL-1, sugerindo um mecanismo de ação não genómico. No modelo de inflamação induzido por LPS, a KTP-NH_2 não conseguiu diminuir o número de leucócitos rolantes em ratinhos pré-tratados com metirapone, um inibidor da síntese de glucocorticóides (GCs), ou com um inibidor do receptor de interleucina-1. Além disso, o mesmo dipéptido não foi tão eficaz na redução do número de leucócitos rolantes em ratinhos estimulados com LPS e pré-tratados com um inibidor de heme-oxigenase-1 ou com um inibidor de interleucina-10. O pré-tratamento dos animais estimulados com LPS com um inibidor de MyD88 não afectou a ação da KTP-NH_2. No modelo de inflamação induzido com CXCL-1, o pré-tratamento com metirapone não afectou a ação anti-inflamatória da KTP-NH_2. Assim, concluiu-se que a KTP-NH_2 tem dupla ação: uma ação mediada por GCs, que é dominante em modelos de inflamação completos, e um mecanismo independente de GCs, que é predominante em modelos em que o rolamento de leucócitos é estimulado, mas a inflamação não está totalmente desenvolvida. Testou-se também a hipótese da KTP-NH_2 ser um inibidor de encefalinases. Ao contrário do dipeptídeo endógeno KTP, a KTP-NH_2 não inibiu a enzima conversora da angiotensina (ECA) nem a dipeptidil-peptidase III (DPP3). Contudo, não descartamos a possibilidade da KTP-NH_2 poder inibir outras encefalinases não testadas.

O trabalho nesta tese sugere que KTP-NH_2 é um péptido multifuncional que tem ações tanto a nível central como periférico. A KTP-NH_2 apresenta um mecanismo anti-

inflamatório muito rápido (10 minutos) que bloqueia a expressão/ativação de moléculas de adesão no endotélio e propõe-se que os GCs sejam o elo molecular que explica as propriedades analgésicas, anti-inflamatórias e neuroprotetoras deste péptido.

Abstract

The endogenous neuropeptide kyotorphin (L-Tyr-L-Arg, KTP) has remarkable analgesic activity, up to 4.2 fold more potent than endogenous opioids when administered directly into the brain, but is inefficient after systemic administration. Our group has designed and studied several KTP analogues, among them KTP-amide (L-Tyr-L-Arg-NH_2, KTP-NH_2), which is analgesic, anti-inflammatory and neuroprotective after systemic administration. Despite this interesting set of biological properties, what makes of KTP-NH_2 an interesting candidate for pharmacological development, the lack of knowledge on its mechanism of action is limiting. We need to improve our knowledge on the molecular basis of action of the peptide so then we can execute an industrial development plan for the drug. Understanding the relationships between the structure of the drug and its function, efficacy and pharmacokinetics as well as the identification and characterization of molecular targets will contribute to progress in that area.

The aim of this thesis is contribute to understand the mechanism of action of KTP-NH_2 and to identify molecular targets of this peptide. To achieve such aim, we have designed and studied KTP-NH_2 derivatives to elucidate new aspects of the structure-activity relationship; and we looked for specific targets that could explain KTP-NH_2 biological activities.

First, we introduced selective changes in the chemical structure of KTP-NH_2 by introducing D-amino acids residues and/or N-terminal methylation, in order to improve lipophilicity and resistance to enzymatic degradation. We found that D-Tyr-L-Arg-NH_2 (KTP-NH_2-DL) has a pronounced anti-inflammatory effect, but insignificant analgesic action probably due to its low permeation through lipid membranes. KTP-NH_2 has a similar behavior, except for its potent analgesic action in several pain models. The results support the hypothesis that KTP-NH_2 uses a specific transporter to cross the blood-brain barrier (BBB), which is not efficient to transport KTP-NH_2 analogues. Methylated KTP-NH_2 isomers, LL and LD, are very permeable through lipid membranes and probably diffuse passively across the BBB. They are also more resistant to enzymatic degradation. Therefore, they have a prolonged analgesic effect

in comparison with KTP-NH_2, but the pro-inflammatory activity jeopardizes their pharmacological potential.

In a second phase, to elucidate the mechanism of action of KTP-NH_2 at the molecular level, we used an approach based on intravital microscopy (IVM) and pharmacological inhibitors. We have demonstrated that KTP-NH_2 is able to decrease, within 10 minutes, the number of rolling leukocytes induced either by lipopolysaccharide (LPS) or CXCL-1, suggesting a nongenomic mechanism of action. In the inflammation model induced by LPS, KTP-NH_2 failed to decrease the number of rolling leukocytes in mice pre-treated either with metyrapone, an inhibitor of glucocorticoid (GC) synthesis, or with an inhibitor of interleukin-1 receptor (IL-1R). In addition, KTP-NH_2 was not as effective reducing the number of rolling leukocytes of LPS-stimulated mice pre-treated with an inhibitor of heme-oxygenase-1 (HO-1) or with an inhibitor of interleukin-10 (IL-10), but pre-treatment of the LPS-stimulated animals with an inhibitor of MyD88 did not affect the action of KTP-NH_2. In the inflammation model induced with CXCL-1, pre-treatment with metyrapone did not affect the anti-inflammatory action of KTP-NH_2. Thus, we concluded that KTP-NH_2 has dual action: a GC-mediated action, which is dominant in full-fledged inflammation models, and a GC-independent mechanism, which is predominant in models in which leukocyte rolling is stimulated but inflammation is not totally developed. We also tested the hypothesis that KTP-NH_2 could act as an inhibitor of enkephalinases. Unlike the endogenous dipeptide KTP, KTP-NH_2 did not inhibit angiotensin-converting enzyme (ACE) neither dipeptidyl-peptidase III (DPP3). However, we do not rule out the possibility that KTP-NH_2 can inhibit other untested enkephalinases.

The work in this thesis suggests that KTP-NH_2 is a multifunctional peptide that has both central and peripheral actions. KTP-NH_2 presents a very fast (10 minutes) anti-inflammatory mechanism that blocks the expression/activation of adhesion molecules on the endothelium and we propose that GCs might be the molecular link to explain the analgesics, anti-inflammatory and neuroprotective effects of the peptide.

Palavras-chave

Quiotorfina

Dor

Inflamação

Glucocorticóides

Mecanismo de ação

Keywords

Kyotorphin

Pain

Inflammation

Glucocorticoids

Mechanism of action

Contents

Section 1

Introduction

Kyotorphin: context and motivation

The endogenous neuropeptide composed by the amino acids L-tyrosine (L-Tyr) and L-arginine (L-Arg) was first isolated from bovine brain in 1979 and found later on in the brains of mice and rats, guinea pigs, squirrels and in human cerebrospinal fluid (CSF) (Takagi et al. 1979; Ueda et al. 1980; Nishimura et al. 1991; Santos et al. 2013). The dipeptide with morphine-like properties discovered in Kyoto was named kyotorphin (KTP) (Takagi et al. 1979).

If centrally administered, KTP shows a naloxone-reversible analgesic activity up to 4.2 times more potent than endogenous opioids (Takagi et al. 1979). However, KTP does not bind directly to opioid receptors (Takagi et al. 1979; Rackham et al. 1982). The opioid-dependent analgesic mechanism of action of KTP is mediated by the release of met-enkephalins and β-endorphins, which in turn activates δ- and/or μ-opioid receptors (Takagi et al. 1979; Shiomi et al. 1981; Rackham et al. 1982; Takagi et al. 1982; Janicki and Lipkowski 1983). The exact mechanism of action of KTP is not totally understood. Some authors suggest that KTP suffers a rapid degradation, originating L-Arg, a well-known substrate for nitric oxide synthase (NOS) (Kawabata et al. 1993; Kawabata et al. 1994). This would induce the production of nitric oxide (NO) and consequently the release of met-enkephalins. Other authors suggest that KTP induces met-enkephalin release after binding its receptor (Ueda et al. 1989; Ueda and Inoue 2000). Specific binding assays using radioactive KTP reveal the presence of a specific receptor to KTP functionally coupled to phospholipase C (PLC) through G-protein (Ueda et al. 1989). However, the putative KTP receptor (KTPr) has never been identified. In addition, there are evidences that KTP can protect met-enkephalins from degradation by inhibiting enkephalinases (Takagi et al. 1979; Hazato et al. 1986; Miguel et al. 2007).

Fifty percent of the total KTP found in the brain is concentrated in the cerebral cortex, a region with low content of opioid receptors and enkephalinases (Ueda et al. 1980). In addition to the unequal distribution of the peptide into the brain, several other naloxone-irreversible activities of KTP were reported (Sakurada et al. 1983; Inoue et al. 1997; Kolaeva et al. 2000), supporting the hypothesis that KTP also acts by a non-

opioid mechanism of action. The activity of KTP synthase was detected outside the central nervous system (CNS), in adrenal glands (Kawabata et al. 1996). Hereupon, it is reasonable to expect that KTP would also have peripheric activities. Pre-treatment with KTP, administered via intraplantar (i.pl.), inhibited the nociception caused by bradykinin (BK) in a peripheral pain reflex test (Inoue et al. 1997). The analgesic effect of KTP was completely abolished by leucine-arginine, an antagonist of KTPr, but was not affected by naloxone (Inoue et al. 1997). These data indicate that KTP blocked nociception in peripheral tissues through its binding to KTPr by an opioid-independent mechanism. KTP also plays a role in different physiological activities such as behavior modulator (Kolaeva et al. 2000), thermoregulatory (Sakurada et al. 1983), antiepileptic (Godlevsky et al. 1995), among others (Ignat'ev et al. 1998; Summy-Long et al. 1998). These activities are also not mediated by an opioid mechanism. For instance, the involvement of the thyrotropin-releasing hormone (TRH) neural system has been proposed instead of the opioid system to explain the role of KTP in thermoregulation (Sakurada et al. 1983), but little is known about the non-opioid mechanism of action on KTP.

Recently, our group have established a link between pain, Alzheimer disease (AD) and KTP. Pain is underestimated in AD patients due to the cognitive impairment; and these patients have decreased level of KTP in the CSF. Moreover, the level of KTP in the CSF correlated inversely with the phosphorylated-tau protein (p-tau) in AD patients (Santos et al. 2013). P-tau is released as consequence of neuronal cell destruction and therefore constitutes a biomarker of AD disease. Our group have proposed KTP as a biomarker of AD that could also be used to evaluate pain in patients with cognitive impairment (Santos et al. 2013).

KTP has shown a wide range of physiological activities, but the analgesic activity is by far the most studied. However, after systemic administration, KTP shows only a brief analgesic activity at high doses (Chen et al. 1998). The pharmacological potential of KTP is limited due to its inability of the peptide to cross the blood-brain barrier (BBB) and due to its susceptibility to enzymatic degradation (Chen et al. 1998). More recently, it has been proposed that the peptide could also be pumped out from the brain through efflux pumps (Jiang et al. 2009; Serrano et al. 2014; Serrano et al. 2015).

Peptide transporter 2 (PEPT2) is the proposed candidate. Within the brain, PEPT2 is expressed in astrocytes, ependymal cells and also in the apical membrane of choroid plexus (Berger and Hediger 1999; Dieck et al. 1999). The biodistribution of the transporter within the brain support the hypothesis that PEPT2 is implicated in the elimination of the peptide from the synapses and from the brain. The interaction between KTP and PEPT2 have been reported by different authors and methods (Fujita et al. 1999; Thakkar et al. 2008). More importantly, KTP showed enhanced analgesic response in PEPT2 null mice (Jiang et al. 2009).

Kyotorphin Derivatives

In 2009, our group joined a partnership with 2 other Universities and 2 companies in a project called PEP2BRAIN. The project aimed to develop safe KTP derivatives with analgesic efficacy, improved stability and ability to cross the BBB.

C-terminal amidation and/or the addition of lipophilic groups to the N-terminal were some of the strategies applied to improve the formal net charge of the peptides or to increase lipophilicity, respectively. These strategies resulted in the creation of the following peptides (Figure 1).

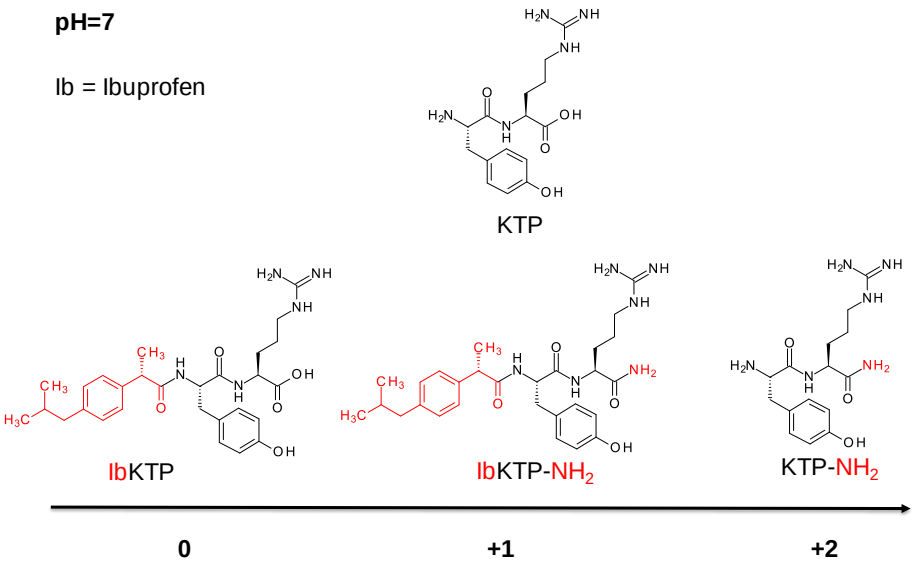

Figure 1. Kyotorphin (KTP), ibuprofen-KTP (IbKTP), ibuprofen-KTP-amide (IbKTP-NH_2) and KTP-amide (KTP-NH_2) distributed accordingly their formal net charge at pH=7.

Kyotorphin-amide (KTP-NH_2) has been extensively studied in several acute and chronic pain models after systemic administration. At a dosage of 32.3 $mg.kg^{-1}$, KTP-NH_2 showed an effect comparable to morphine at 5 $mg.kg^{-1}$ in acute pain models, meaning the equi-effective dose of KTP-NH_2 was about five fold that of morphine (Ribeiro et al. 2011). In chronic pain models antinociception induced by KTP-NH_2 was observed only after a week of daily treatment with 32.3$mg.kg^{-1}$ and unlike morphine, the peptide did not show tolerance effects (Ribeiro et al. 2011). The analgesic effect of KTP-NH_2 was reversed by naloxone but KTP-NH_2 showed low affinity to opioid receptors (Ribeiro et al. 2011). In addition, it was demonstrated that nociceptive activation of spinal neurons induced by formalin was inhibited by systemic administration of KTP-NH_2, as indicated by the lower number of Fos-immunoreactive neurons at the spinal dorsal horn (Ribeiro et al. 2011). This is a proof that KTP-NH_2 can block nociceptive transmission in the CNS after systemic administration. Nonetheless, biodistribution studies are needed to follow the biological fate of the peptide *in vivo*, after systemic administration.

The analgesic efficacy of KTP-NH_2 was reasonable, albeit not optimal. Chemical conjugation of KTP and KTP-NH_2 to the nonsteroidal anti-inflammatory drug ibuprofen (Ib) enhanced the analgesic activity of the peptide (Ribeiro et al. 2011). Naloxone decreased but did not completely abrogated the analgesic effect of IbKTP-NH_2 (Ribeiro et al. 2011). IbKTP-NH_2 also decreased the number of Fos-immunoreactive neurons providing an evidence for its central action (Ribeiro et al. 2011). The selectivity of IbKTP-NH_2 to brain endothelial cells supports the hypothesis that grafting Ib to KTP-NH_2 enhances BBB crossing (Ribeiro et al. 2011).

KTP-NH_2 and IbKTP-NH_2 have low affinity to opioid receptors, but their naloxone reversible effect suggests that they act, at least in part, by an indirect opioid mechanism (Ribeiro et al. 2011; Ribeiro et al. 2011). Despite the analgesic activity of KTP-NH_2 and IbKTP-NH_2 could be comparable to morphine, they do not have the major side effects associated to opioids such as constipation, increase in the blood pressure or food and water intake (Ribeiro et al. 2013). Both peptides have indeed a very safe profile. There are no evidences of *in vitro* cytotoxicity or hepatic lesions at effective doses (Ribeiro et al. 2013). KTP-NH_2 only showed a reduction in micturition and IbKTP-

NH_2 showed a moderate locomotion decline in rats (Ribeiro et al. 2013). Overall, these peptides might constitute advantageous alternatives over opioids.

Pain and inflammation are distinct physiological events, but they frequently coexist. The Ib moiety has previously shown to enhance KTP-NH_2 analgesic activity. Similarly, KTP-NH_2 was tested as an enhancer of Ib anti-inflammatory action. Using an intravital microscopy (IVM) approach it was demonstrated that KTP-NH_2, IbKTP and IbKTP-NH_2 did not cause damage in the microcirculation (Conceição et al. 2016). In addition, they were able to decrease the number of rolling leukocytes induced by lipopolysaccharide (LPS). Isothermal titration calorimetry studies showed that the peptides can bind to LPS, probably hampering its binding to Toll-like receptor 4 (TLR4) and jeopardizing signal transduction that triggers leukocyte rolling and recruitment to peripheral tissues (Conceição et al. 2016).

Recently, KTP-NH_2 and IbKTP-NH_2 have given proofs of their neuroprotective potential by improving cognitive deficits and preventing neuronal damage in a cerebral hypoperfusion dementia model (Sa Santos et al. 2016).

In contrast to the abundant data on the biological action of these peptides, little effort has been made to unravel their mechanism of action. KPT-NH_2 and IbKTP-NH_2 are promising compounds for future pharmaceutical development, but the pharmacodynamic of these drugs still is a major concern. Several other analogues were synthesized and tested for their potential to transverse lipid membranes *in vitro*, as well as for their analgesic efficacy *in vivo*. The structural modifications consisted in the addition of different groups at the N-terminus, such as tert-butyloxycarbonyl (Boc), γ-aminobutyric acid (GABA), acetyl, butanoyl and propanoyl or in the substitution of the tyrosine residue by an indole moiety (Serrano et al. 2015). In some cases, the peptide bond was replaced by a urea-like bond. This study was done with eight novel analogues and the results revealed that there was a correlation between analgesic efficacy and relative permeability, i.e. drugs with higher relative permeability (P_R) across lipid membranes had a higher analgesic effect at 30 minutes in the hot plate test (Serrano et al. 2015). KTP and KTP-NH_2 were exceptions to this correlation. While KTP presented a lower analgesic efficacy than predicted by P_R, KTP-NH_2 presented a

higher analgesic effect (Serrano et al. 2015). To explain these observations, the authors proposed that KTP might be pumped out from the brain by efflux pumps and KTP-NH_2 probably depended on a dipeptide transporter to translocate the BBB (Serrano et al. 2015). Most of the structural modifications resulted in drugs with a more enduring analgesic effect than KTP-NH_2, but we should be aware that the toxicity of these compounds has not been tested yet.

KTP-NH_2 gathers an interesting set of biological properties that makes of it an interesting candidate for pharmacological development, but the lack of knowledge on its mechanism of action is limiting. We need to improve our knowledge on the molecular basis of action of the peptide so then we can execute an industrial development plan for the drug. Understanding the relationships between the structure of the drug and its function, efficacy and pharmacokinetics as well as the identification and characterization of its molecular targets will contribute to progress in that area.

ARTICLE 1

Pharmacological potential of the endogenous dipeptide kyotorphin and selected derivatives

Frontiers in Pharmacology, 2017

I declare that the bibliographic research was conducted by me and Sónia Sá Santos under guidance of Prof. Miguel A.R.B. Castanho. This was written by me under advice and guidance of my supervisor Prof. Miguel A.R.B. Castanho.

frontiers in Pharmacology

REVIEW
published: 12 January 2017
doi: 10.3389/fphar.2016.00530

Pharmacological Potential of the Endogenous Dipeptide Kyotorphin and Selected Derivatives

*Juliana Perazzo, Miguel A. R. B. Castanho and Sónia Sá Santos**

Instituto de Medicina Molecular, Faculdade de Medicina da Universidade de Lisboa, Lisboa, Portugal

The endogenous peptide kyotorphin (KTP) has been extensively studied since it was discovered in 1979. The dipeptide is distributed unevenly over the brain but the majority is concentrated in the cerebral cortex. The putative KTP receptor has not been identified yet. As many other neuropeptides, KTP clearance is mediated by extracellular peptidases and peptide transporters. From the wide spectrum of biological activity of KTP, analgesia was by far the most studied. The mechanism of action is still unclear, but researchers agree that KTP induces Met-enkephalins release. More recently, KTP was proposed as biomarker of Alzheimer disease. Despite all that, KTP limited pharmacological value prompted researchers to develop derivatives more lipophilic and therefore more prone to cross the blood–brain barrier (BBB), and also more resistant to enzymatic degradation. Conjugation of KTP with functional molecules, such as ibuprofen, generated a new class of compounds with additional biological properties. Moreover, the safety profile of these derivatives compared to opioids and their efficacy as neuroprotective agents greatly increases their pharmacological value.

Keywords: kyotorphin, blood–brain barrier, kyotorphin-derived peptides, drug candidates, biological effects, clinical application

OPEN ACCESS

Edited by:
Chris Bailey,
University of Bath, UK

Reviewed by:
Mariana Spetea,
University of Innsbruck, Austria
Hiroshi Ueda,
Nagasaki University, Japan

****Correspondence:***
Sónia Sá Santos
sonia.sa.santos@gmail.com

Specialty section:
This article was submitted to Neuropharmacology, a section of the journal Frontiers in Pharmacology

Received: *30 September 2016*
Accepted: *20 December 2016*
Published: *12 January 2017*

Citation:
Perazzo J, Castanho MARB and Sá Santos S (2017) Pharmacological Potential of the Endogenous Dipeptide Kyotorphin and Selected Derivatives. Front. Pharmacol. 7:530. doi: 10.3389/fphar.2016.00530

DISCOVERY, DISTRIBUTION, AND RECEPTORS

The endogenous dipeptide L-tyrosine-L-arginine (YR) was first isolated from bovine brain in 1979 and found later on in other mammals' brains and in human cerebrospinal fluid (CSF) (Takagi et al., 1979b; Ueda et al., 1980; Nishimura et al., 1991; Santos et al., 2013). The dipeptide with endorphin-like properties discovered in Kyoto was named kyotorphin (KTP) (Takagi et al., 1979a).

Kyotorphin can be formed in the brain by two pathways: (i) from precursor proteins degradation either by membrane-bound aminopeptidase or cytosolic Ca^{2+} activated protease (Ueda et al., 1985; Yoshihara et al., 1990; Akasaki et al., 1995); and/or (ii) from its precursor L-amino acids, tyrosine and arginine, in a reaction catalyzed by KTP synthetase dependent of ATP and Mg^{2+} (Ueda et al., 1987). This pathway produces three–fourfold more KTP than the one formed by precursor proteins degradation (Ueda et al., 1987).

KTP synthetase distribution correlates closely with KTP levels in the rat brain (Ueda et al., 1987). Its enzymatic activity was also detected in rat adrenal glands and spinal cord (Kawabata et al., 1996).

Abbreviations: 2VO, bilateral common carotid artery occlusion; AMPs, antimicrobial peptides; Ib, ibuprofen; IVM, intravital microscopy; KTP, kyotorphin; KTPr, KTP receptor; KTP-NH_2, KTP-amide; LPS, lipopolysaccharide; NO, nitric oxide; NOS, nitric oxide synthetase; PEPT2, peptide transporter 2; PLC, phospholipase C; P_R, relative permeability; SP, substance P.

KTP is unevenly distributed over the brain. Lower brain stem regions, such as midbrain, pons, medulla oblongata and dorsal part of spinal cord are KTP-rich regions. These regions are sensitive to morphine and/or electrical stimulation-induced analgesia. However, 50% of total KTP brain's content is concentrated in cerebral cortex, an area with low content of opioid receptors and enkephalinases (Ueda et al., 1980). Lower KTP contents can be found in striatum, hippocampus, hypothalamus, thalamus, and cerebellum (Ueda et al., 1980). The regional distribution of KTP supports the idea that KTP might have non-opioid actions.

Subcellular fractioning revealed KTP is enriched in synaptosomal fraction. Synaptosomes preloaded with KTP were able to release the dipeptide in a Ca^{2+} dependent manner upon depolarizing stimuli and it seems KTP can be recaptured again by synaptosomes in a Na^{+}, temperature and energy-dependent manner. These data support the idea that KTP plays a role as neurotransmitter/neuromodulator (Ueda et al., 1986a,b).

Specific binding-assays using radioactive KTP suggest the presence of high affinity and low affinity receptors in the brain. The mechanism triggered by the binding of KTP to KTPr is mediated through protein G_i and phospholipase C (PLC) system that induces Ca^{2+} influx (Ueda et al., 1989). Thus, a nerve impulse is generated, ultimately leading to analgesia. The synthetic dipeptide L-leucine-L-arginine (LR) also binds KTPr with a great affinity but no effect, thereby constituting a potent antagonist (Ueda et al., 1989).

Interestingly, extremely low doses of KTP (femtomolar range) and more stable analogs (atomolar range) administered peripherally elicit nociceptive responses due to the release of substance P (SP) by nociceptor endings of primary afferent neurons. The authors speculate that the mechanism involved in such opposite responses (antinociceptive vs. nociceptive) might be mediated by different G proteins depending on KTP dosage, having a differential effect on PLC activation (Inoue et al., 1999; Ueda and Inoue, 2000).

The putative KTPr has not been identified yet. Despite many papers refer to "the KTPr" (Ueda et al., 1980, 1986b, 1989, 2000; Ueda and Inoue, 2000), it is not clear whether the receptor is specific or formed by μ- and δ-opioid receptors oligomerization (Machuqueiro and Baptista, 2007). From previous studies it is known that KTPr binding pocket must be different from opioid receptors (Takagi et al., 1979b; Rackham et al., 1982; Ueda and Inoue, 2000), but conformational studies on KTP suggested they should be structurally similar (Machuqueiro and Baptista, 2007).

METABOLISM AND CLEARANCE

PEPT2 Transporter

Neuropeptides are released in the brain to exert their function and thereafter they are cleared either by extracellular peptidases and/or removed from extracellular fluid by specific transporters. Both processes have shown to be equally important in KTP clearance (Xiang et al., 2010).

Fujita et al. (1999) were the first to report an interaction between KTP and the high-affinity transporter PEPT2, albeit in an indirect way, evaluating competitive inhibition of glycylsarcosine (GlySar) in rat synaptosomes. Later, KTP uptake by PEPT2 was demonstrated in a more direct way, measuring the peptide-induced inward currents (Thakkar et al., 2008).

PEPT2 is high-affinity and low capacity transporter which rely on a pH gradient between extracellular and intracellular compartments to transport di- and tri-peptides. This transporter is expressed in kidney, retina and brain (Liu et al., 1995; Berger and Hediger, 1999). Hybridization studies showed PEPT2 is expressed in astrocytes and ependymal cells throughout the brain, and also in epithelial cells of choroid plexus (Berger and Hediger, 1999; Dieck et al., 1999). Astrocytes are essential in the control of neuronal activity and synaptic neurotransmission (Araque et al., 1999), and several peptidases are known to be expressed on their extracellular membrane (Berger and Hediger, 1999). Therefore, PEPT2 function in astrocytes might be linked to the removal of neuropeptide fragments and small biologically active peptides from extracellular fluid, such as KTP and carnosine (Berger and Hediger, 1999). In choroid plexus, the transporter is specifically located in the apical membrane, suggesting a role in the efflux of peptides from CSF (Shu et al., 2002). In addition, PEPT2 null mice showed enhanced antinociceptive response to intracerebroventricular (i.c.v.) administered KTP (Jiang et al., 2009). Transport of peptides from blood to CNS via PEPT2 is unlikely since this transporter is not present at blood–brain barrier (BBB) (Berger and Hediger, 1999).

KTP-Degrading Aminopeptidases

Kyotorphin-degrading aminopeptidase activity was reported in brain homogenate (Ueda et al., 1985), lung and skin from rats (Orawski and Simmons, 1992). KTPase activity was inhibited by bestatin, but not puromycin, a potent inhibitor of soluble aminopeptidases (Ueda et al., 1985). Akasaki and Tsuji (1991) and Akasaki et al. (1991) identified two distinct KTPases in soluble fraction of rat brain. KTPase I is responsible for 95% of KTP-degrading activity, while KTPase II, which showed to be an enkephalin aminopeptidase, contributes only to 5% of KTP degradation.

Moreover, other authors found two dipeptide-cleaving enzymes associated to synaptic membranes (Orawski and Simmons, 1992). Both enzymes are inhibited by bestatin, but they can be distinguished based on their differential sensitivity to amastatin (Orawski and Simmons, 1992). Although KTPase I, described in Akasaki et al. (1991) presents similar characteristics to the KTP-degrading enzyme found by Orawski and Simmons (1992), it is not clear if they are identical (Akasaki et al., 1995).

MECHANISM OF ACTION

The first experiments done by Takagi et al. (1979b) revealed an analgesic activity of KTP 4.2 fold more potent than met-enkephalins, when injected intracisternally; an effect that was reversed by naloxone. Although naloxone is an opioid antagonist, studies demonstrated KTP itself does not bind to opioid receptors, but has rather an indirect action mediated

by met-enkephalin and β-endorphin, which activate δ- and/or μ-opioid receptors (Takagi et al., 1979b; Rackham et al., 1982; Ribeiro et al., 2011a). Other authors confirmed KTP-induced met-enkephalin release from guinea pig and rat brain slices (Shiomi et al., 1981; Takagi et al., 1982; Janicki and Lipkowski, 1983). In addition, there are evidences that KTP can inhibit some enkephalinases. This implies that met-enkephalins would be more protected from enzymatic degradation resulting in a relatively long-lasting analgesia (Takagi et al., 1979b; Hazato et al., 1986).

In patients with persistent pain, L-Arg intravenously administered induced analgesia and this action was antagonized by naloxone (Takagi, 1990; Takagi et al., 1990; Harima et al., 1991). It has been postulated that L-Arg can facilitate KTP synthesis in the brain, enhancing met-enkephalin release, which in turn activate δ- and/or μ-opioid receptors resulting in antinociception (Kawabata et al., 1993).

Alternatively, L-Arg is a well-known substrate for NOS. NOS and soluble guanylyl cyclase inhibitors administered i.c.v. caused antinociception. These findings led Kawabata et al. (1992, 1993) to conclude that L-Arg plays a dual role in nociceptive processing. In this case, NO-cyclic guanosine monophosphate (cGMP) pathway seems to be involved in nociceptive promotion in the CNS.

Kyotorphin-synthetase activity was detected outside the central nervous system (CNS), in adrenal gland, suggesting that KTP might have a role in peripheral system (Kawabata et al., 1996). In accordance, a study conducted in brown fat cell culture system showed KTP inhibited cell proliferation induced by noradrenaline. This indicates that these cells and probably other tissues in the periphery contain receptors for KTP (Bronnikov et al., 1997). In order to evaluate if KTP analgesic effect in the periphery was mediated by opioid receptors, a peripheral pain reflex test was conducted in mouse. Results showed the mechanism was mediated via KTPr but independent of opioid receptors, since naloxone was unable to prevent KTP analgesic effect (Inoue et al., 1997). The mechanism of action of KTP still not clear and some data are contradictory. However, there seems to exist two distinct pathways leading to analgesia, one mediated by opioids and other opioid-independent.

KTP BEYOND ANALGESIA

Physiological Effects

In addition to the extensively studied analgesic effect, KTP gathers a wide spectrum of biological activities (Dzambazova, 2010). Published papers have explored KTP role as antiepileptic (Godlevsky et al., 1995), thermoregulator (Sakurada et al., 1983), anti-hibernation regulator (Ignat'ev et al., 1998) and stress (Summy-Long et al., 1998) and behavior (Kolaeva et al., 2000) modulators.

Kyotorphin is present at moderate concentrations in the hypothalamus (Ueda et al., 1980), a structure with an important role in thermoregulation and stress. Naloxone-irreversible hypothermia was induced in mice, at room temperature, after i.c.v. administration of KTP and a more stable analog. However, thyrotropin (TRH) prevented this effect, suggesting the mechanism of KTP thermoregulation in the brain might involve the TRH neuronal system instead of opioid receptors (Sakurada et al., 1983). Regarding stress, high doses of KTP injected i.c.v. presumably activates the sympathetic nervous system, inducing a release of oxytocin (OT), a stress-hormone in rodents, concomitantly with elevating blood pressure and glucose plasma levels, but not vasopressin (Summy-Long et al., 1998).

Behavioral studies in rats and goldfish showed KTP reduced exploratory behavior mediated probably by the monoaminergic brain systems (Kolaeva et al., 2000).

KTP as a Promising Biomarker in Alzheimer's Disease

Recent estimates indicate 35.6 million people worldwide affected by dementia, a number that is expected to nearly double every 20 years (WHO, 2012). Alzheimer's Disease (AD) is the most prevalent form of dementia in later life. It is clinically characterized by a progressive deterioration of memory, orientation, language, learning capacity, emotional stability, motor skills, and ultimately self-care, causing social and occupational disability. Unfortunately, no effective cure is available and current treatment strategies only provide symptomatic relief without halting nor reversing disease progression.

There is an increased need for AD biomarkers to improve early detection, accurate diagnosis, and accelerate drug development in this field (Flaten et al., 2006; Hampel et al., 2010). In medicine, a biomarker is generally defined as a molecule or any other tangible parameter that serves as an indicator of biological or pathogenic processes that can be used to evaluate disease risk or prognosis, and to monitor therapeutic interventions (Hampel et al., 2010). Decreased CSF levels of β-amyloid peptides ($A\beta_{40}$, $A\beta_{42}$) combined with increased levels of total tau and phosphorylated tau proteins, have diagnostic value in AD (Flaten et al., 2006; Hampel et al., 2010), for instance.

Although chronic pain is also highly prevalent in AD patients (Pieper et al., 2013), its proper evaluation and treatment is a clinical and ethical challenge. It may seem strange because AD patients consume fewer analgesics than other patient groups, making the false impression that they may feel less pain. However, processing and perception of pain are not diminished in AD (Cole et al., 2006). In those patients, pain underestimation relates with their limited capacity of verbally expressing their pain or discomfort, worsening as the dementia progresses (Pieper et al., 2013). Recent evidence suggest that chronic pain contributes to the course of neurodegenerative events as an additional injury to the nervous system (Borsook, 2012). Cognitive impairment and limited communication in AD patients leads to underreported pain, which in turn leads to undertreatment. By failing to receive adequate pain treatment, structural and irreversible changes may occur in the nervous system, aggravating AD pathophysiology which

in turn contributes to chronic pain, maintaining a vicious cycle.

The benefits of finding a particular AD biomarker involved in the overlapping mechanisms of nociception and neurodegeneration that can be used in the clinics alongside with the existing ones (Flaten et al., 2006; Hampel et al., 2010) are obvious: (a) possibility to evaluate pain, regardless the level of cognitive impairment of the patient; (b) a biomarker that is itself a promising strategy for pharmaceutical development.

Our recent clinical studies showed a link between pain, AD and KTP in humans. In fact, we observe that pain was underestimated in AD patients (Santos and Castanho, 2013) and KTP has decreased levels in the CSF of AD patients with moderate cognitive impairment (Santos et al., 2013). Several other neuropeptides have been identified as diminished in AD (Raskind et al., 1986; Albericio et al., 1990). Lower levels of an analgesic molecule such as KTP may probably explain why AD patients are believed to have a higher incidence of hidden chronic pain; in agreement, Nishimura et al. (1991) have shown that CSF KTP levels decrease in chronic pain conditions.

Owing to the estimated low concentration of KTP in the human CSF (10^{-9} M) (Nishimura et al., 1991) we had to resort to electrospray ionization tandem mass spectrometry (ESI – MS/MS) (Santos et al., 2013). The decreased levels of KTP in AD samples correlate with a disease-specific atrophy

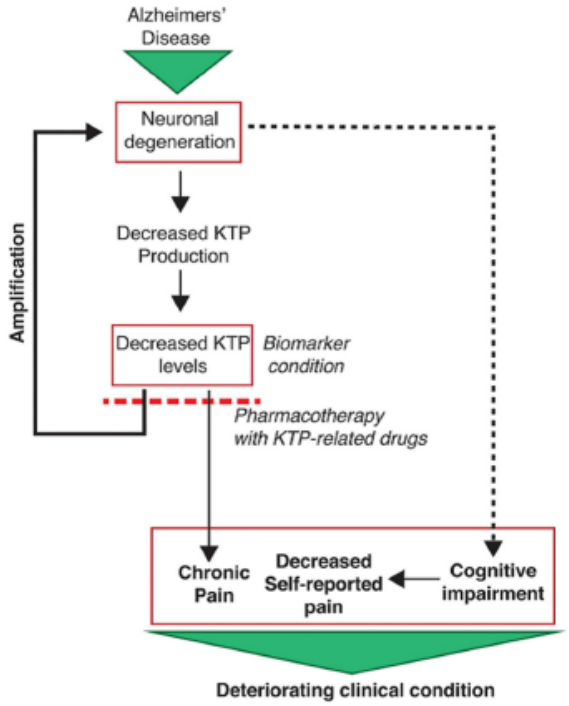

FIGURE 1 | Clinical implications of reduced KTP levels in cerebrospinal fluid (CSF) of Alzheimer disease (AD) patients (Santos et al., 2013).

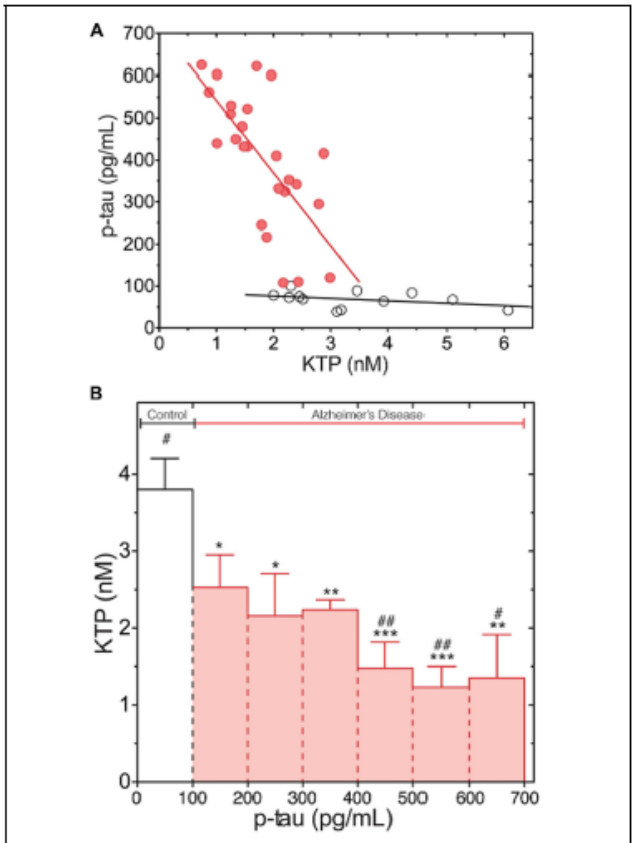

FIGURE 2 | Phosphorylated-tau (p-Tau) levels dependence on KTP concentration both in AD (red) and normal group (white). (A) Complete data set with individual values (linear regression line plotted as a guide to the eye). **(B)** The data set presented in **(A)** was clustered in classes according to regular intervals of amplitude of 100 pg/mL of p-tau concentration and averaged for KTP concentration (error bars: standard error). The average KTP value of all classes was compared to control (*$p < 0.04$, **$p < 0.0075$, ***$p < 0.0006$) or the 100- to 200-pg/mL p-tau class ($^{\#}p < 0.04$, $^{\#\#}p < 0.0046$) using the one-way ANOVA with Dunnett's post-test (Santos et al., 2013).

of some brain regions meaning damage and loss of neuronal cells, which possibly results in less KTP being produced and its CSF concentration naturally falling in those patients (**Figure 1**). Moreover, we also found an inverse correlation between levels of KTP and of phosphorylated-tau protein (p-tau) (**Figure 2**) (Santos et al., 2013). CSF p-tau reflects the phosphorylation state of tau and the formation of cortical neurofibrillary tangles in the brain (Flaten et al., 2006). As the disease progresses, more neuronal cells are destroyed, p-tau is released and KTP production is impaired (**Figure 1**). These decreased levels of KTP in the brain will probably contribute to a decreased NOS activity (see Mechanism of Action) causing a NO deficit to such a degree that will further promote the neurodegenerative events characteristic of AD. Disruption of NO homeostasis is known to hasten the development of AD (de la Torre and Stefano, 2000).

LIMITED PHARMACOLOGICAL POTENTIAL OF KTP

The majority of studies on KTP following its discovery aimed to unravel the mechanism of action and to evaluate the analgesic effect of this dipeptide. Although the mechanism of action remains an unsolved issue, direct administration of KTP and some analogs peptides into different parts of CNS showed very promising results regarding analgesia (Yajima et al., 1980; Sakurada et al., 1982; Vaught and Chipkin, 1982; Wang et al., 2001). Hereupon, several groups tested the effects following systemic administration (intraperitoneal i.p., intravenous i.v. and oral) but the results have been disappointing. KTP showed only a brief analgesic activity at a high dose of 200 mg/Kg when administered systemically to rodents (Chen et al., 1998).

Blood–brain barrier constitutes the major obstacle to systemically administered drugs to reach CNS due to the tight junctions that link endothelial cells in the brain capillaries and scarcity of receptors. Less than 2% of the drugs developed to treat CNS disorders cross BBB (Pardridge, 2002). Even some small lipophilic molecules that succeed to diffuse through BBB and penetrate into the brain can be exported back to blood stream by efflux pumps, such as *P*-glycoproteins. In addition, several lytic proteins located in the brain capillary endothelial cells surface form an enzymatic barrier to bioactive peptides from blood.

Obviously, some essential molecules, such as amino acids, hexoses and neuropeptides, which do not fulfill the criteria to diffuse passively through BBB need to reach the brain. Therefore there are specific carriers that mediate their transport. Larger molecules, such as proteins (e.g., insulin and transferrin) are transported by saturable transport systems. On the other hand, positively charged molecules (e.g., histones and cationized albumin) use an adsorptive-mediated endocytosis mechanism to enter the brain (Abbott et al., 2010).

At first it was thought KTP inability to cross BBB was related to low affinity of the peptide to lipid membrane (Chen et al., 1998). More recently the hypothesis that KTP can be pumped out by specific transporters has been raised (Jiang et al., 2009; Serrano et al., 2014a,b).

DEVELOPMENT OF NEW KTP DERIVATIVES

Kyotorphin pharmacological potential is limited probably due to its inability to cross BBB and/or susceptibility to enzymatic degradation. In order to overcome these issues while preserving effectiveness as analgesic, several groups including ours have worked in different strategies to modify the original peptide. Some of these strategies deal with (i) chirality (Rybal'chenko et al., 1999; Lopes et al., 2006a), (ii) use of unnatural amino acids and substitution of peptide bonds (Dzimbova et al., 2014; Serrano et al., 2014b), (iii) conjugation with lipophilic groups (Chen et al., 1998; Wang et al., 2001; Lopes et al., 2006b; Ribeiro et al., 2011b; Serrano et al., 2014b), (iv) cationicity improvement (Ribeiro et al., 2011a).

Interestingly, some liphophilic groups added to KTP have by themselves a biological action associated. For instance, Wang et al. (2001) synthesized two distinct KTP derivatives covalently linked to steroids, hydrocortisone (hydrocortisone-KTP) or estrone (estrone-KTP) (**Figure 3**). Unlike KTP, hydrocortisone-KTP and estrone-KTP exhibited good analgesia in the tail-flick test after i.p. administration. These derivatives showed improved pharmacokinetics and pharmacodynamics. Moreover, the researchers suggested that the steroids might be enhancing the KTP effect by increasing the number of its receptors (Wang et al., 2001).

We have extensively studied the analgesic effect of the derivative KTP-NH_2, which differs from the original peptide by substitution of the carboxylic acid for an amide (**Figure 3**). At physiological pH, this simple chemical modification causes an increase of the net charge of the peptide from +1 to +2. KTP-NH_2 was tested in acute, sustained and chronic inflammatory and neuropathic pain models following systemic administration (i.p. and oral). At a dosage of 32.3 $mg.kg^{-1}$, KTP-NH_2 (i.p.) showed an effect comparable to morphine at 5 $mg.kg^{-1}$ in acute pain animal models, meaning the equi-effective dose of KTP-NH_2 was about fivefold that of morphine. Oral administration required higher dosages to be effective. In chronic pain animal models antinociception induced by KTP-NH_2 was observed only after a week of daily treatment with 32.3 $mg.kg^{-1}$. In addition, KTP-NH_2 did not develop resistance unlike morphine, neither jeopardized blood pressure or motor capacity. Accordingly, the peptide showed low affinity to opioid receptors (Ribeiro et al., 2011a).

Other interesting derivatives are IbKTP and IbKTP-NH_2, which were designed by us to include in their structure a group corresponding to a lipophilic, analgesic and safe non-steroidal anti-inflammatory drug (NSAID), ibuprofen (Ib), covalently linked to the N-terminal of KTP or KTP-NH_2, respectively (**Figure 3**) (Ribeiro et al., 2011b). In the clinics, combination of different pain killers have been successfully used, e.g., Vicoprofen® (hydrocodone + Ib). Results in acute and chronic pain models showed that both IbKTP and IbKTP-NH_2, but mainly IbKTP-NH_2, improved analgesia after systemic administration (Ribeiro et al., 2011b).

Recently, eight novel derivatives from KTP and KTP-NH_2 were synthesized by addition of individual groups at the N-terminus, namely small carbon chains, tert-butyloxycarbonyl (Boc), aminobutyric acid (GABA) or by substitution of the tyrosil residue for an indole moiety. In some cases the peptide bond was substituted by a urea-like bond. The addition of Boc and indolyl groups, but not small carbon chains, increased significantly relative permeability (P_R) while the peptidomimetics which had the peptide bond substituted by an urea-like bond seemed more resistant to peptidases (Serrano et al., 2014b). Boc-uKTP-NH_2 and Ind-KTP-NH_2 (**Figure 3**) were the most promising derivatives, showing a prolonged analgesic effect correlated with higher membrane permeability (**Figure 4**). These two derivatives successfully combined lipophilicity and resistance to enzymatic degradation (Serrano et al., 2014b). Still, some derivatives with lower permeability, such as KTP-NH_2, have previously demonstrated good analgesic efficacy (Ribeiro et al.,

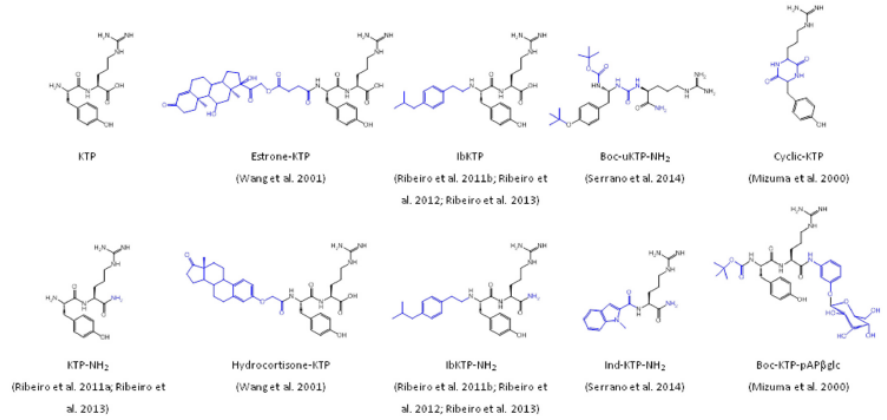

FIGURE 3 | Chemical structure of KTP derivatives.

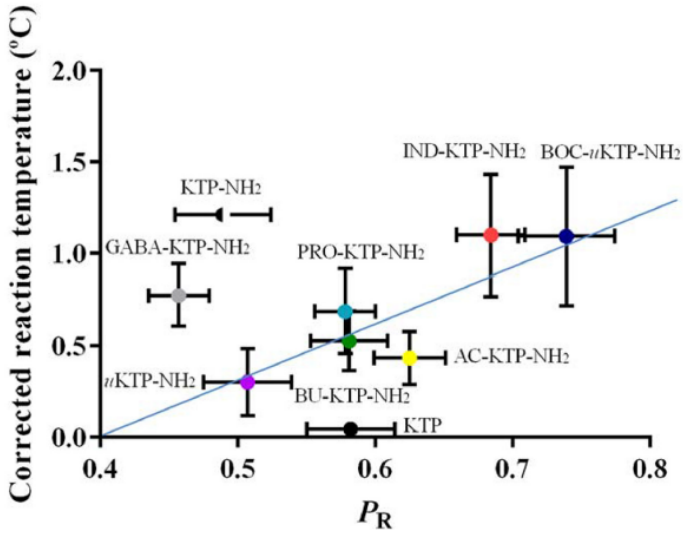

FIGURE 4 | Correlation between the analgesic efficacy and the relative permeability of KTP derivatives (Serrano et al., 2014b).

2011a). These results suggest that this particular derivative might have specific transporters to translocate BBB (Serrano et al., 2014b).

Other groups studied other interesting derivatives of KTP, namely a glucose-conjugated KTP and cyclic KTP (**Figure 3**) (Mizuma et al., 2000). Glucose-mediated drug delivery has been a strategy successfully applied to drugs whose final target is in the CNS [for review see (Serrano et al., 2012)]. N-terminal conjugation of p-amino phenyl β-glucoside and C-terminal conjugation of Boc to KTP (Boc-KTP-pAPβglc) (**Figure 3**) enhanced absorption and clearance in the rat intestine and cyclization protected the peptide from proteolytic attack, thereby enhancing enzymatic stability. Cyclic-KTP is suggested as a good analgesic drug candidate to be delivered orally (Mizuma et al., 2000).

Advantageous Alternatives over Current Opioids

Opium and its alkaloids (e.g., morphine) have been used for centuries as the most powerful centrally acting compounds for the relief of severe acute and chronic pain. However, they also trigger some side-effects such as nausea, constipation, respiratory depression, urinary retention, clouding of consciousness, motor disturbances, tolerance and addiction, which often hamper their widespread use in clinical practice (Fischer et al., 1992). Prolonged admininstration of opioids results in tolerance liability that leads to dose escalation, contributing to an increased incidence and severity of all side-effects. This can lead to discontinued use of the pain medication compromising the quality of life for patients. Thus, the discovery and/or development of potent analgesics that result in effective analgesia

with fewer side-effects is greatly needed; and this has long been the holy grail of opioid research (Solé and Barany, 1992; Corbett et al., 2006). In recent years, different approaches have been explored to design and synthesize analogs of naturally occurring opioid peptides (i.e., dermorphin, endomorphins, and enkephalins) as potential substitutes of exogenous opioids for pain relief (Gentilucci, 2004; Janecka et al., 2010; Ribeiro et al., 2011c; Piekielna et al., 2013). Other alternative strategies targeting opioid-receptor have been addressed (Solé and Barany, 1992; Ribeiro et al., 2011c).

KTP-NH_2 and IbKTP–NH_2 exhibited analgesic activity comparable to morphine and lower tolerance (Ribeiro et al., 2011a,b). Additionally, no evidences of *in vitro* cytotoxicity or hepatic lesions were detected at effective doses (Ribeiro et al., 2011a). Aiming to validate the pharmaceutical potential of these KTP derivatives as alternative to opioids, further *in vivo* studies were conducted. Hence, for a more detailed pharmacological profiling, both derivatives were studied regarding their side-effects and compared with two clinically relevant opioids, morphine and tramadol (Ribeiro et al., 2013). Particular attention was given to the common opioid-induced side-effects namely on locomotion, micturition, gastrointestinal, and cardiovascular functions (Benyamin et al., 2008). For comparison purposes, morphine and tramadol were selected because morphine remains the gold standard in analgesia (Ramage et al., 1991) while tramadol displays a safer side-effect profile than morphine (Dworkin et al., 2007). In the experimental paradigm, male rats were i.p. injected with a single dose of KTP-NH_2 (32.3 $mg.kg^{-1}$) or IbKTP-NH_2 (24.2 $mg.kg^{-1}$) or morphine (5 $mg.kg^{-1}$) or tramadol (10 $mg.kg^{-1}$) before the behavioral/metabolic testing. Doses of KTP derivatives, morphine and tramadol were chosen for inducing comparable analgesia levels in rats (Ribeiro et al., 2013).

Our findings clearly showed that both KTP-derivatives do not cause constipation, in contrast to morphine, and do not induce changes in blood pressure, or in water and food intake, in contrast to tramadol. Despite the fact that KTP–NH_2 (like tramadol) lowered urine volume this seems to be a minor physiological effect caused by this derivative as no major urinary retention occurred (i.e., increased blood pressure was not observed), and may be exploited as a positive effect in cases of micturition disturbances, i.e., detrusor overactivity. IbKTP-NH_2 only caused a mild motor impairment that was, however, less harmful than all the severe side-effects induced by tramadol and morphine (Ribeiro et al., 2013).

Overall, KTP derivatives do not trigger the major side-effects intrinsically associated with opioid receptor activation. This correlates with previous findings as direct binding of KTP amidated derivatives to opioid receptors is nearly absent (Ribeiro et al., 2011a,b) similarly to the original KTP molecule (Rackham et al., 1982). Taken together, our data indicates that KTP peptides and opioid drugs exhibit distinct mechanism of action. However, opioid pathways are indirectly involved in KTP peptides mode of action since naloxone decreases the analgesic efficacy of IbKTP-NH_2 and completely abolishes KTP-NH_2 analgesic activity (Ribeiro et al., 2011a,b).

Therefore, the strong analgesic activity coupled with the absence of the major side-effects associated to opioids renders both KTP–NH_2 and IbKTP–NH_2 as potential advantageous alternatives over current opioids.

KTP DERIVATIVES BEYOND ANALGESIA

As Antimicrobial Agents

Antimicrobial peptides represent a promising alternative to conventional antibiotics to fight resistant pathogens because development of resistance is not so effective. They are generally short amphiphilic cationic peptides with high affinity to negatively charged bacterial membranes. One possible mode of action, among others, is membrane disruption caused by peptide insertion into the bacterial membrane, short peptides having higher activity (Lopes-Ferreira et al., 2002; Catiau et al., 2011). Catiau et al. (2011) found that the tripeptide L-lysine-L-tyrosine-L-arginine (KYR) has antimicrobial activity. Since KTP (YR, net charge +1) does not have antimicrobial activity, the positive charge of lysine is of key importance. KTP (net charge: +1), KTP-NH_2 (+2), IbKTP-NH_2 (+1) and IbKTP (0) were tested against Gram-negative *Escherichia coli* (*E. coli*) and Gram-positive *Staphylococcus aureus* (*S. aureus*). (Ribeiro et al., 2012). All derivatives were inactive against *E. coli* up to 100 μM but they were active against *S. aureus*, with the exception of KTP. Details of surface structure alteration induced by KTP derivatives (10 μM) in *S. aureus* were obtained by atomic force microscopy (AFM). KTP-NH_2 and IbKTP-NH_2 induced shape alterations, unlike KTP and IbKTP. Membrane blebbing and disruption were more evident for KTP-NH_2. Ib-containing derivatives also interact with red blood cells (RBCs) outer monolayer changing the typical disk shape with uniform borders to spiky boundaries. This shape is known as echinocyte and is reversible. Regardless these changes all derivatives were virtually not toxic to RBCs (Ribeiro et al., 2012).

Neuroprotective Potential in Cerebral Hypoperfusion Rat Model

In the last two decades, intensive efforts to develop disease-modifying drugs were made to counteract the progression of AD (Flaten et al., 2006). Moreover, increasing attention has been dedicated to neuropeptides in the discovery of new drug targets for the treatment of nervous-system disorders (Hokfelt et al., 2003). Actually, some neuropeptides are densely localized in cognition-related brain regions and play an important role in dementia-associated pathophysiological mechanisms (Borbely et al., 2013).

Over the last decade, some authors hypothesized that KTP has neuromodulating and neuroprotective properties using animal models of cerebral resuscitation (after clinical death) (Nazarenko et al., 1999) and of epilepsy (i.e., picrotoxin- or pentylenetetrazole-induced seizures) (Godlevsky et al., 1995; Bocheva and Dzambazova-Maximova, 2004). In addition, there is consistent evidence about the protective role of NSAIDs,

particularly Ib, against neurodegeneration and to reduce the risk of developing AD or Parkinson's (Asanuma et al., 2001; Chen et al., 2005; Wilkinson et al., 2012). Hence, the potential of a drug candidate (namely KTP) comprising NSAID-based therapy to achieve a clinical benefit would be tremendous. In view of these facts and our recent clinical studies (see KTP as a Promising Biomarker in Alzheimer's Disease) the relevance of testing our improved KTP derivatives in dementia progression became obvious.

Therefore, KTP-NH_2 and IbKTP-NH_2 were recently studied for their ability in post-ischemia to ameliorate cognitive deficits induced by chronic brain hypoperfusion (Sá Santos et al., 2016). Cerebrovascular hypoperfusion is known to be a prominent risk in the development of neurological dysfunction and dementia. In rats, permanent 2VO produces a lasting and reliable reduction of cerebral blood flow, which leads to a progressive neuropathological damage in the hippocampus (particularly its CA1 subfield), learning and memory impairments as it occurs in AD (Farkas et al., 2007).

Our study included rats subjected to permanent global ischemia via 2VO-surgery (2VO-animals) and sham-operated animals (surgery without carotid artery ligation: control group). In the experimental paradigm, 2VO-animals were treated with KTP-NH_2 (32.3 $mg.kg^{-1}$) or IbKTP-NH_2 (24.2 $mg.kg^{-1}$) at weeks 2 and 5 post-surgery (single i.p. dose/day for 7 days) (Sá Santos et al., 2016). From a therapeutic perspective, it was of interest to assess their effectiveness after the onset of ischemic injury. Selected doses of KTP-derivatives were based on our previous studies (Ribeiro et al., 2011a,b, 2013).

Following treatment regimen, motor and spatial memory functions were evaluated using the open-field test and two-trial recognition Y-maze task, respectively. Evidences support a direct correlation between cerebral hypoperfusion-induced memory impairments and damage in CA1 pyramidal neurons (De Jong et al., 1999; Farkas et al., 2007; Cechetti et al., 2012). So, we also evaluated hippocampal CA1 integrity through immunohistochemistry protocols (Sá Santos et al., 2016).

Albeit ischemic injury can affect brain regions linked to motor function (i.e., cortex and neocortex), in our study there was no obvious signs of locomotion deficits in 2VO-operated animals (Sá Santos et al., 2016), similar to what has been reported for this experimental model (Farkas et al., 2007; Cechetti et al., 2012). Our findings clearly showed that both KTP-derivatives improved memory deficits of 2VO-animals and prevented CA1 neuronal injury (Sá Santos et al., 2016). Detailed mechanisms underlying their neuroprotective properties are still unknown. However, IbKTP-NH_2 was the more effective derivative in restoring normal memory function; the presence of NSAID ibuprofen may mitigate some neuroinflammatory events in 2VO-ischemic brain.

As Anti-Inflammatory Agents

Pain and inflammation are distinct physiological processes but they are frequently associated. Thus, the development of a single drug that could target pain and inflammation simultaneously would be ideal. We used an IVM approach to evaluate the pro- or anti-inflammatory effect of a topical application of KTP (96 μM), KTP-NH_2 (96 μM), IbKTP (96 μM) and IbKTP-NH_2 (96 μM) on the cremaster muscle using a rodent model of LPS-induced inflammation (Conceição et al., 2016). We have previously shown that Ib moiety is a enhancer of KTP analgesic action (Ribeiro et al., 2011b). Accordingly, we expected that KTP could also be an enhancer of Ib anti-inflammatory action.

Our data showed that KTP and its analogs did not cause damage on microcirculation. In addition they decreased the number of rolling and adherent leukocytes induced by LPS. This result might be explained by the ability of KTP analogs to bind/perturb LPS micelles, as shown by isothermal titration calorimetry studies, probably contributing to LPS aggregation and subsequent elimination (Conceição et al., 2016). Since KTP did not bind to LPS, the production of NO is the proposed anti-inflammatory mechanism. This is supported by the already discussed mechanism for KTP-induced analgesia that originates L-Arg, a well-known substrate for NOS that ultimately originates NO as product (see Mechanism of Action).

More recently, D-Tyr-L-Arg-NH_2 (KTP-NH_2-DL, 96 μM) also decreased the number of rolling leukocytes in a murine model of inflammation induced by LPS, but did not reveal a significant analgesic activity in the hot plate test (Perazzo et al., 2016). This KTP analog and others analyzed in the same study seem to have an action on the endothelium.

CONCLUDING REMARKS

Pain is a huge social and economic problem. In the half last century, innovation in the field of analgesic drug has been scarce. An increased interest has been directed toward peptides as future pain-killers. KTP gathers an interesting and wide set of biological activities; among them, analgesia is by far the most studied. In order to make this peptide more attractive from a pharmacological perspective, several chemical modifications have been made to the original molecule. This strategy has been successful so far and new advantageous properties have emerged from these derivatives, creating a new class of molecules with an increased pharmacological value.

AUTHOR CONTRIBUTIONS

JP, MC, and SS listed, have made substantial contribution to the writing and critical revision of the manuscript, and approved it for publication.

FUNDING

Funding was provided by the Portuguese Agency Fundação para a Ciência e a Tecnologia (SFRH/BPD/79542/2011 fellowship to SS and SFRH/BD/52225/2013 fellowship to JP), and by Marie Skłodowska-Curie Research and Innovation Staff Exchange (RISE): call H2020-MSCA-RISE-2014, Grant agreement 644167, 2015-2019.

REFERENCES

Abbott, N. J., Patabendige, A. A. K., Dolman, D. E. M., Yusof, S. R., and Begley, D. J. (2010). Structure and function of the blood-brain barrier. *Neurobiol. Dis.* 37, 13–25. doi: 10.1016/j.nbd.2009.07.030

Akasaki, K., Nakamura, A., Shiomi, H., and Tsuji, H. (1991). Identification and characterization of two distinct kyotorphin-hydrolyzing enzymes in rat brain. *Neuropeptides* 20, 103–107. doi: 10.1016/0143-4179(91)90059-R

Akasaki, K., and Tsuji, H. (1991). An enkephalin-degrading aminopeptidase from rat brain catalyzes the hydrolysis of a neuropeptide, kyotorphin (L-Tyr-L-Arg). *Chem. Pharm. Bull. (Tokyo)* 39, 1883–1885. doi: 10.1248/cpb.39.1883

Akasaki, K., Yoshimoto, H., Nakamura, A., Shiomi, H., and Tsuji, H. (1995). Purification and characterization of a major kyotorphin-hydrolyzing peptidase of rat brain. *J. Biochem.* 117, 897–902.

Albericio, F., Kneib-Cordonier, N., Biancalana, S., Gera, L., Masada, R. I., Hudson, D., et al. (1990). Preparation and application of the 5-(4-(9-fluorenylmethyloxycarbonyl)aminomethyl-3,5-dimethoxyphenoxy)-valeric acid (PAL) handle for the solid-phase synthesis of C-terminal peptide amides under mild conditions. *J. Org. Chem.* 55, 3730–3743. doi: 10.1021/jo00299a011

Araque, A., Parpura, V., Sanzgiri, R. P., and Haydon, P. G. (1999). Tripartite synapses: glia, the unacknowledged partner. *Trends Neurosci.* 22, 208–215. doi: 10.1016/s0166-2236(98)01349-6

Asanuma, M., Nishibayashi-Asanuma, S., Miyazaki, I., Kohno, M., and Ogawa, N. (2001). Neuroprotective effects of non-steroidal anti-inflammatory drugs by direct scavenging of nitric oxide radicals. *J. Neurochem.* 76, 1895–1904. doi: 10.1046/j.1471-4159.2001.00205.x

Benyamin, R., Trescot, A. M., Datta, S., Buenaventura, R., Adlaka, R., Sehgal, N., et al. (2008). Opioid complications and side effects. *Pain Physician* 11 2(Suppl.), S105–S120.

Berger, U. V., and Hediger, M. A. (1999). Distribution of peptide transporter PEPT2 mRNA in the rat nervous system. *Anat. Embryol. (Berl)* 199, 439–449. doi: 10.1007/s004290050242

Bocheva, A. I., and Dzambazova-Maximova, E. B. (2004). Effects of kyotorphin and analogues on nociception and pentylenetetrazole seizures. *Folia Med. (Plovdiv)* 46, 40–44.

Borbely, E., Scheich, B., and Helyes, Z. (2013). Neuropeptides in learning and memory. *Neuropeptides* 47, 439–450. doi: 10.1016/j.npep.2013.10.012

Borsook, D. (2012). Neurological diseases and pain. *Brain* 135(Pt 2), 320–344. doi: 10.1093/brain/awr271

Bronnikov, G., Dolgacheva, L., Zhang, S. J., Galitovskaya, E., Kramarova, L., and Zinchenko, V. (1997). The effect of neuropeptides kyotorphin and neokyotorphin on proliferation of cultured brown preadipocytes. *FEBS Lett.* 407, 73–77. doi: 10.1016/S0014-5793(97)00298-6

Catiau, L., Traisnel, J., Delval-Dubois, V. R., Chihib, N.-E., Guillochon, D., and Nedjar-Arroume, N. M. (2011). Minimal antimicrobial peptidic sequence from hemoglobin alpha-chain: KYR. *Peptides* 32, 633–638. doi: 10.1016/j.peptides.2010.12.016

Cechetti, F., Pagnussat, A. S., Worm, P. V., Elsner, V. R., Ben, J., da Costa, M. S., et al. (2012). Chronic brain hypoperfusion causes early glial activation and neuronal death, and subsequent long-term memory impairment. *Brain Res. Bull.* 87, 109–116. doi: 10.1016/j.brainresbull.2011.10.006

Chen, H., Jacobs, E., Schwarzschild, M. A., McCullough, M. L., Calle, E. E., Thun, M. J., et al. (2005). Nonsteroidal antiinflammatory drug use and the risk for Parkinson's disease. *Ann. Neurol.* 58, 963–967. doi: 10.1002/ana.20682

Chen, P., Bodor, N., Wu, W. M., and Prokai, L. (1998). Strategies to target kyotorphin analogues to the brain. *J. Med. Chem.* 41, 3773–3781. doi: 10.1021/jm970715l

Cole, L. J., Farrell, M. J., Duff, E. P., Barber, J. B., Egan, G. F., and Gibson, S. J. (2006). Pain sensitivity and fMRI pain-related brain activity in Alzheimer's disease. *Brain* 129(Pt 11), 2957–2965. doi: 10.1093/brain/awl228

Conceição, K., Magalhães, P. R., Campos, S. R. R., Domingues, M. M., Ramu, V. G., Michalek, M., et al. (2016). The anti-inflammatory action of the analgesic kyotorphin neuropeptide derivatives: insights of a lipid-mediated mechanism. *Amino Acids* 48, 307–318. doi: 10.1007/s00726-015-2088-9

Corbett, A. D., Henderson, G., McKnight, A. T., and Paterson, S. J. (2006). 75 years of opioid research: the exciting but vain quest for the Holy Grail. *Br. J. Pharmacol.* 147(Suppl. 1), S153–S162. doi: 10.1038/sj.bjp.0706435

De Jong, G. I., Farkas, E., Stienstra, C. M., Plass, J. R., Keijser, J. N., de la Torre, J. C., et al. (1999). Cerebral hypoperfusion yields capillary damage in the hippocampal CA1 area that correlates with spatial memory impairment. *Neuroscience* 91, 203–210. doi: 10.1016/S0306-4522(98)00659-9

de la Torre, J. C., and Stefano, G. B. (2000). Evidence that Alzheimer's disease is a microvascular disorder: the role of constitutive nitric oxide. *Brain Res. Brain Res. Rev* 34, 119–136. doi: 10.1016/S0165-0173(00)00043-6

Dieck, S. T., Heuer, H., Ehrchen, J., Otto, C., and Bauer, K. (1999). The peptide transporter PepT2 is expressed in rat brain and mediates the accumulation of the fluorescent dipeptide derivative beta-Ala-Lys-Nepsilon-AMCA in astrocytes. *Glia* 25, 10–20. doi: 10.1002/(SICI)1098-1136(19990101)25:1<10::AID-GLIA2>3.0.CO;2-Y

Dworkin, R. H., O'Connor, A. B., Backonja, M., Farrar, J. T., Finnerup, N. B., Jensen, T. S., et al. (2007). Pharmacologic management of neuropathic pain: evidence-based recommendations. *Pain* 132, 237–251. doi: 10.1016/j.pain.2007.08.033

Dzambazova, E. B. (2010). The unique brain dipeptide kyotorphin - from discovery to nowadays. *J. Biomed. Clin. Res.* 3, 3–11.

Dzimbova, T., Bocheva, A., and Pajpanova, T. (2014). Kyotorphin analogues containing unnatural amino acids: synthesis, analgesic activity and computer modeling of their interactions with m-receptor. *Med. Chem. Res.* 23, 3694–3704. doi: 10.1007/s00044-014-0953-9

Farkas, E., Luiten, P. G., and Bari, F. (2007). Permanent, bilateral common carotid artery occlusion in the rat: a model for chronic cerebral hypoperfusion-related neurodegenerative diseases. *Brain Res. Rev.* 54, 162–180. doi: 10.1016/j.brainresrev.2007.01.003

Fischer, P. M., Retson, K. V., Tyler, M. I., and Howden, M. E. (1992). Application of arylsulphonyl side-chain protected arginines in solid-phase peptide synthesis based on 9-fluorenylmethoxycarbonyl amino protecting strategy. *Int. J. Pept. Protein Res.* 40, 19–24. doi: 10.1111/j.1399-3011.1992.tb00100.x

Flaten, G. E., Dhanikula, A. B., Luthman, K., and Brandl, M. (2006). Drug permeability across a phospholipid vesicle based barrier: a novel approach for studying passive diffusion. *Eur. J. Pharm. Sci.* 27, 80–90. doi: 10.1016/j.ejps.2005.08.007

Fujita, T., Kishida, T., Okada, N., Ganapathy, V., Leibach, F. H., and Yamamoto, A. (1999). Interaction of kyotorphin and brain peptide transporter in synaptosomes prepared from rat cerebellum: implication of high affinity type H+/peptide transporter PEPT2 mediated transport system. *Neurosci. Lett.* 271, 117–120. doi: 10.1016/S0304-3940(99)00540-6

Gentilucci, L. (2004). New trends in the development of opioid peptide analogues as advanced remedies for pain relief. *Curr. Top. Med. Chem.* 4, 19–38. doi: 10.2174/1568026043451663

Godlevsky, L. S., Shandra, A. A., Mikhaleva, I. I., Vastyanov, R. S., and Mazarati, A. M. (1995). Seizure-protecting effects of kyotorphin and related peptides in an animal model of epilepsy. *Brain Res. Bull.* 37, 223–226. doi: 10.1016/0361-9230(94)00274-5

Hampel, H., Frank, R., Broich, K., Teipel, S. J., Katz, R. G., Hardy, J., et al. (2010). Biomarkers for Alzheimer's disease: academic, industry and regulatory perspectives. *Nat. Rev. Drug Discov.* 9, 560–574. doi: 10.1038/nrd3115

Harima, A., Shimizu, H., and Takagi, H. (1991). Analgesic effect of L-arginine in patients with persistent pain. *Eur. Neuropsychopharmacol.* 1, 529–533. doi: 10.1016/0924-977X(91)90006-G

Hazato, T., Kase, R., Ueda, H., Takagi, H., and Katayama, T. (1986). Inhibitory effects of the analgesic neuropeptides kyotorphin and neo-kyotorphin on enkephalin-degrading enzymes from monkey brain. *Biochem. Int.* 12, 379–383.

Hokfelt, T., Bartfai, T., and Bloom, F. (2003). Neuropeptides: opportunities for drug discovery. *Lancet Neurol.* 2, 463–472. doi: 10.1016/S1474-4422(03)00482-4

Ignat'ev, D. A., Vorob'ev, V. V., and Ziganshin, R. (1998). Effects of a number of short peptides isolated from the brain of the hibernating ground squirrel on the EEG and behavior in rats. *Neurosci. Behav. Physiol.* 28, 158–166. doi: 10.1007/BF02461962

Inoue, M., Nakayamada, H., Tokuyama, S., and Ueda, H. (1997). Peripheral non-opioid analgesic effects of kyotorphin in mice. *Neurosci. Lett.* 236, 60–62. doi: 10.1016/S0304-3940(97)00760-X

Inoue, M., Yamada, T., and Ueda, H. (1999). Low dose of kyotorphin (tyrosine-arginine) induces nociceptive responses through a substance P release from

nociceptor endings. *Brain Res. Mol. Brain Res.* 69, 302–305. doi: 10.1016/S0169-328X(99)00133-3

Janecka, A., Perlikowska, R., Gach, K., Wyrebska, A., and Fichna, J. (2010). Development of opioid peptide analogs for pain relief. *Curr. Pharm. Des.* 16, 1126–1135. doi: 10.2174/138161210790963869

Janicki, P. K., and Lipkowski, A. W. (1983). Kyotorphin and D-kyotorphin stimulate Met-enkephalin release from rat striatum in vitro. *Neurosci. Lett.* 43, 73–77. doi: 10.1016/0304-3940(83)90131-3

Jiang, H., Hu, Y., Keep, R. F., and Smith, D. E. (2009). Enhanced antinociceptive response to intracerebroventricular kyotorphin in Pept2 null mice. *J. Neurochem.* 109, 1536–1543. doi: 10.1111/j.1471-4159.2009.06090.x

Kawabata, A., Muguruma, H., Tanaka, M., and Takagi, H. (1996). Kyotorphin synthetase activity in rat adrenal glands and spinal cord. *Peptides* 17, 407–411. doi: 10.1016/0196-9781(96)00026-5

Kawabata, A., Nishimura, Y., and Takagi, H. (1992). l-Leucyl-l-arginine, naltrindole and d-arginine block antinociception elicited by l-arginine in mice with carrageenin-induced hyperalgesia. *Br. J. Pharmacol.* 107, 1096–1101. doi: 10.1111/j.1476-5381.1992.tb13413.x

Kawabata, A., Umeda, N., and Takagi, H. (1993). L-arginine exerts a dual role in nociceptive processing in the brain: involvement of the kyotorphin-Met-enkephalin pathway and NO-cyclic GMP pathway. *Br. J. Pharmacol.* 109, 73–79. doi: 10.1111/j.1476-5381.1993.tb13533.x

Kolaeva, S. G., Semenova, T. P., Santalova, I. M., Moshkov, D. A., Anoshkina, I. A., and Golozubova, V. (2000). Effects of L-thyrosyl - L-arginine (kyotorphin) on the behavior of rats and goldfish. *Peptides* 21, 1331–1336. doi: 10.1016/S0196-9781(00)00275-8

Liu, W., Liang, R., Ramamoorthy, S., Fei, Y. J., Ganapathy, M. E., Hediger, M. A., et al. (1995). Molecular cloning of PEPT 2, a new member of the H+/peptide cotransporter family, from human kidney. *Biochim. Biophys. Acta* 1235, 461–466. doi: 10.1016/0005-2736(95)80036-F

Lopes, S. C., Fedorov, A., and Castanho, M. A. (2006a). Chiral recognition of D-kyotorphin by lipidic membranes: relevance toward improved analgesic efficiency. *Chem. Med. Chem.* 1, 723–728. doi: 10.1002/cmdc.200600096

Lopes, S. C., Soares, C. M., Baptista, A. M., Goormaghtigh, E., Cabral, B. J., and Castanho, M. A. (2006b). Conformational and orientational guidance of the analgesic dipeptide kyotorphin induced by lipidic membranes: putative correlation toward receptor docking. *J. Phys. Chem. B* 110, 3385–3394. doi: 10.1021/jp053651w

Lopes-Ferreira, M., Moura-da-Silva, A. M., Piran-Soares, A. A., Angulo, Y., Lomonte, B., Gutierrez, J. M., et al. (2002). Hemostatic effects induced by *Thalassophryne nattereri* fish venom: a model of endothelium-mediated blood flow impairment. *Toxicon* 40, 1141–1147. doi: 10.1016/S0041-0101(02)00114-9

Machuqueiro, M., and Baptista, A. M. (2007). The pH-dependent conformational states of kyotorphin: a constant-pH molecular dynamics study. *Biophys. J.* 92, 1836–1845. doi: 10.1529/biophysj.106.092445

Mizuma, T., Koyanagi, A., and Awazu, S. (2000). Intestinal transport and metabolism of glucose-conjugated kyotorphin and cyclic kyotorphin: metabolic degradation is crucial to intestinal absorption of peptide drugs. *Biochim. Biophys. Acta* 1475, 90–98. doi: 10.1016/S0304-4165(00)00051-9

Nazarenko, I. V., Zvrushchenko, M., Volkov, A. V., Kamenskii, A. A., and Zaganshin, R. (1999). Functional-morphologic evaluation of the effect of the regulatory peptide kyotorphin on the status of the CNS in the post-resuscitation period. *Patol. Fiziol. Eksp. Ter.* 2, 31–33.

Nishimura, K., Kaya, K., Hazato, T., Ueda, H., Satoh, M., and Takagi, H. (1991). Kyotorphin like substance in human cerebrospinal fluid of patients with persistent pain. *Masui* 40, 1686–1690.

Orawski, A., and Simmons, W. (1992). Dipeptidase activities in rat brain synaptosomes can be distinguished on the basis of inhibition by bestatin and amastatin: identification of a kyotorphin (Tyr-Arg)-degrading enzyme. *Neurochem. Res.* 17, 817–820. doi: 10.1007/bf00969018

Pardridge, W. M. (2002). Why is the global CNS pharmaceutical market so under-penetrated? *Drug Discov. Today* 7, 5–7. doi: 10.1016/S1359-6446(01)02082-7

Perazzo, J., Lopes-Ferreira, M., Sá Santos, S., Serrano, I., Pinto, A., Lima, C., et al. (2016). Endothelium-mediated action of analogues of the endogenous neuropeptide kyotorphin (tyrosil-arginine): mechanistic insights from permeation and effects on microcirculation. *ACS Chem. Neurosci.* 7, 1130–1140. doi: 10.1021/acschemneuro.6b00099

Piekielna, J., Perlikowska, R., Gach, K., and Janecka, A. (2013). Cyclization in opioid peptides. *Curr. Drug Targets* 14, 798–816. doi: 10.2174/1389450111314070008

Pieper, M. J., van Dalen-Kok, A. H., Francke, A. L., van der Steen, J. T., Scherder, E. J., Husebo, B. S., et al. (2013). Interventions targeting pain or behaviour in dementia: a systematic review. *Ageing Res. Rev.* 12, 1042–1055. doi: 10.1016/j.arr.2013.05.002

Rackham, A., Wood, P. L., and Hudgin, R. L. (1982). Kyotorphin (tyrosine-arginine): further evidence for indirect opiate receptor activation. *Life Sci.* 30, 1337–1342. doi: 10.1016/0024-3205(82)90017-0

Ramage, R., Green, J., and Blake, A. J. (1991). An acid labile arginine derivative for peptide synthesis: NG-2,2,5,7,8-pentamethylchroman-6-sulphonyl-L-arginine. *Tetrahedron* 47, 6353–6370. doi: 10.1016/S0040-4020(01)86564-9

Raskind, M. A., Peskind, E. R., Lampe, T. H., Risse, S. C., Taborsky, G. J. Jr., and Dorsa, D. (1986). Cerebrospinal fluid vasopressin, oxytocin, somatostatin, and beta-endorphin in Alzheimer's disease. *Arch. Gen. Psychiatry* 43, 382–388. doi: 10.1001/archpsyc.1986.01800040092013

Ribeiro, M. M., Pinto, A., Pinto, M., Heras, M., Martins, I., Correia, A., et al. (2011a). Inhibition of nociceptive responses after systemic administration of amidated kyotorphin. *Br. J. Pharmacol.* 163, 964–973. doi: 10.1111/j.1476-5381.2011.01290.x

Ribeiro, M. M., Pinto, A. R., Domingues, M. M., Serrano, I., Heras, M., Bardaji, E. R., et al. (2011b). Chemical conjugation of the neuropeptide kyotorphin and ibuprofen enhances brain targeting and analgesia. *Mol. Pharm.* 8, 1929–1940. doi: 10.1021/mp2003016

Ribeiro, M. M. B., Serrano, I. D., and Sá Santos, S. (2011c). "Turning Endogenous Peptides Into New Analgesics: The Example of Kyotorphin Derivatives," in *Peptide Drug Discovery and Development: Translational Research in Academia and Industry*, 1st Edn, eds M. Castanho and N. Santos (Weinheim: WILEY-VCH Verlag GmbH & Co. KGaA), 171–188.

Ribeiro, M. M., Sá Santos, S., Sousa, D. S., Oliveira, M., Santos, S. M., Heras, M., et al. (2013). Side-effects of analgesic kyotorphin derivatives: advantages over clinical opioid drugs. *Amino Acids* 45, 171–178. doi: 10.1007/s00726-013-1484-2

Ribeiro, M. M. B., Franquelim, H. G., Torcato, I. S. M., Ramu, V. G., Heras, M., Bardaji, E. R., et al. (2012). Antimicrobial properties of analgesic kyotorphin peptides unraveled through atomic force microscopy. *Biochem. Biophys. Res. Commun.* 420, 676–679. doi: 10.1016/j.bbrc.2012.03.065

Rybal'chenko, V. K., Ostrovskaya, G. V., Poralo, I. V., Rybal'chenko, T. V., and Mel'nik, Y. M. (1999). Membranotropic activity of optical isomers of the neuropeptide kyotorphin and a cardiotonic agent, suphan. *Neurophysiology* 31, 223–225. doi: 10.1007/bf02515077

Sá Santos, S., Santos, S. M., Pinto, A. R., Ramu, V. G., Heras, M., Bardaji, E., et al. (2016). Amidated and ibuprofen-conjugated kyotorphins promote neuronal rescue and memory recovery in cerebral hypoperfusion dementia model. *Front. Aging Neurosci.* 8:1. doi: 10.3389/fnagi.2016.00001

Sakurada, S., Sakurada, T., Jin, H., Sato, T., Kisara, K., Sasaki, Y., et al. (1982). Antinociceptive activities of synthetic dipeptides in mice. *J. Pharm. Pharmacol.* 34, 750–751. doi: 10.1111/j.2042-7158.1982.tb06218.x

Sakurada, T., Sakurada, S., Watanabe, S., Matsumura, H., Kisara, K., Akutsu, Y., et al. (1983). Actions of intracerebroventricular administration of kyotorphin and an analog on thermoregulation in the mouse. *Peptides* 4, 859–863. doi: 10.1016/0196-9781(83)90081-5

Santos, S., and Castanho, M. (2013). The use of visual analog scales to compare pain between patients with Alzheimer's disease and patients without any known neurodegenerative disease and their caregivers. *Am. J. Alzheimers Dis. Other Demen.* 29, 320–325. doi: 10.1177/1533317513517046

Santos, S. M., Garcia-Nimo, L., Sá Santos, S., Tavares, I., Cocho, J. A., and Castanho, M. A. (2013). Neuropeptide kyotorphin (tyrosyl-arginine) has decreased levels in the cerebro-spinal fluid of Alzheimer's disease patients: potential diagnostic and pharmacological implications. *Front. Aging Neurosci.* 5:68. doi: 10.3389/fnagi.2013.00068

Serrano, I. D., Freire, J. M., Carvalho, M. V., Neves, M., Melo, M. N., and Castanho, M. A. R. B. (2014a). The Mechanisms and quantification of the selective permeability in transport across biological barriers: the example of kyotorphin.

Mini Rev. Med. Chem. 14, 99–110. doi: 10.2174/1389557514666140123130058

Serrano, I. D., Ramu, V. G., Pinto, A. R. T., Freire, J. M., Tavares, I., Heras, M., et al. (2014b). Correlation between membrane translocation and analgesic efficacy in kyotorphin derivatives. *Peptide Sci.* 104, 1–10. doi: 10.1002/bip.22580

Serrano, I. D., Ribeiro, M. M., and Castanho, M. A. (2012). A focus on glucose-mediated drug delivery to the central nervous system. *Mini Rev. Med. Chem.* 12, 301–312. doi: 10.2174/138955712799829302

Shiomi, H., Kuraishi, Y., Ueda, H., Harada, Y., Amano, H., and Takagi, H. (1981). Mechanism of kyotorphin-induced release of Met-enkephalin from guinea pig striatum and spinal cord. *Brain Res.* 221, 161–169. doi: 10.1016/0006-8993(81)91070-2

Shu, C., Shen, H., Teuscher, N. S., Lorenzi, P. J., Keep, R. F., and Smith, D. E. (2002). Role of PEPT2 in peptide/mimetic trafficking at the blood-cerebrospinal fluid barrier: studies in rat choroid plexus epithelial cells in primary culture. *J. Pharmacol. Exp. Ther.* 301, 820–829. doi: 10.1124/jpet.301.3.820

Solé, N. A., and Barany, G. (1992). Optimization of solid-phase synthesis of [Ala8]-dynorphin-A. *J. Org. Chem.* 57, 5399–5403. doi: 10.1021/Jo00046a022

Summy-Long, J. Y., Bui, V., Gestl, S., Koehler-Stec, E., Liu, H., Terrell, M. L., et al. (1998). Effects of central injection of kyotorphin and L-arginine on oxytocin and vasopressin release and blood pressure in conscious rats. *Brain Res. Bull.* 45, 395–403. doi: 10.1016/S0361-9230(97)00341-9

Takagi, H. (1990). [Physiological and pharmacological actions of a neuroactive dipeptide, kyotorphin, and its precursor, L-arginine, and clinical application]. *Nihon Yakurigaku Zasshi* 96, 85–96. doi: 10.1254/fpj.96.3_85

Takagi, H., Harima, A., and Shimizu, H. (1990). A novel clinical treatment of persistent pain with L-arginine. *Eur. J. Pharmacol.* 183: 1443. doi: 10.1016/0014-2999(90)94580-Q

Takagi, H., Shiomi, H., Kuraishi, Y., and Ueda, H. (1982). Analgesic dipeptide, L-Tyr-D-Arg (D-kyotorphin) induces Met-enkephalin release from guinea-pig striatal slices. *Experientia* 38, 1344–1345. doi: 10.1007/bf01954941

Takagi, H., Shiomi, H., Ueda, H., and Amano, H. (1979a). Morphine-like analgesia by a new dipeptide, L-tyrosyl-L-arginine (Kyotorphin) and its analogue. *Eur. J. Pharmacol.* 55, 109–111. doi: 10.1016/0014-2999(79)90154-7

Takagi, H., Shiomi, H., Ueda, H., and Amano, H. (1979b). A novel analgesic dipeptide from bovine brain is a possible Met-enkephalin releaser. *Nature* 282, 410–412. doi: 10.1038/282410a0

Thakkar, S. V., Miyauchi, S., Prasad, P. D., and Ganapathy, V. (2008). Stimulation of Na+/Cl–coupled opioid peptide transport system in SK-N-SH cells by L-kyotorphin, an endogenous substrate for H+-coupled peptide transporter PEPT2. *Drug Metab. Pharmacokinet.* 23, 254–262. doi: 10.2133/dmpk.23.254

Ueda, H., and Inoue, M. (2000). In vivo signal transduction of nociceptive response by kyotorphin (tyrosine-arginine) through Gai- and inositol trisphosphate-mediated Ca^{2+} influx. *Mol. Pharm.* 57, 108–115.

Ueda, H., Inoue, M., Weltrowska, G., and Schiller, P. W. (2000). An enzymatically stable kyotorphin analog induces pain in subattomol doses. *Peptides* 21, 717–722. doi: 10.1016/S0196-9781(00)00190-X

Ueda, H., Matsumoto, S., Yoshihara, Y., Fukushima, N., and Takagi, H. (1986a). Uptake and release of kyotorphin in rat brain synaptosomes. *Life Sci.* 38, 2405–2411. doi: 10.1016/0024-3205(86)90609-0

Ueda, H., Ming, G., Hazato, T., Katayama, T., and Takagi, H. (1985). Degradation of kyotoprhin by a purified membrane-bound-aminopeptidase from monkey brain: potentiation of kyotorphin-induced analgesia by a highly effective inhibitor, bestatin. *Life Sci.* 36, 1865–1871. doi: 10.1016/0024-3205(85)90160-2

Ueda, H., Shiomi, H., and Takagi, H. (1980). Regional distribution of a novel analgesic dipeptide kyotorphin (Tyr-Arg) in the rat brain and spinal cord. *Brain Res.* 198, 460–464. doi: 10.1016/0006-8993(80)90761-1

Ueda, H., Yoshihara, Y., Fukushima, N., Shiomi, H., Nakamura, A., and Takagi, H. (1987). Kyotorphin (tyrosine-arginine) synthetase in rat brain synaptosomes. *J. Biol. Chem.* 262, 8165–8173.

Ueda, H., Yoshihara, Y., Misawa, H., Fukushima, N., Katada, T., Ui, M., et al. (1989). The kyotorphin (tyrosine-arginine) receptor and a selective reconstitution with purified Gi, measured with GTPase and phospholipase C assays. *J. Biol. Chem.* 264, 3732–3741.

Ueda, H., Yoshihara, Y., and Takagi, H. (1986b). A putative met-enkephalin releaser, kyotorphin enhances intracellular Ca^{2+} in the synaptosomes. *Biochem. Biophys. Res. Commun.* 137, 897–902. doi: 10.1016/0006-291X(86)91164-2

Vaught, J. L., and Chipkin, R. E. (1982). A characterization of kyotorphin (Tyr-Arg)-induced antinociception. *Eur. J. Pharmacol.* 79, 167–173. doi: 10.1016/0014-2999(82)90622-7

Wang, C., Zhao, M., Yang, J., and Peng, S. (2001). Synthesis and analgesic effects of kyotorphin-steroid linkers. *Steroids* 66, 811–815. doi: 10.1016/S0039-128X(01)00112-X

WHO (2012). *Dementia: A Public Health Priority. WHO Library Cataloguing-in-Publication Data*. Geveva: WHO.

Wilkinson, B. L., Cramer, P. E., Varvel, N. H., Reed-Geaghan, E., Jiang, Q., Szabo, A., et al. (2012). Ibuprofen attenuates oxidative damage through NOX2 inhibition in Alzheimer's disease. *Neurobiol. Aging* 33, e121–e132. doi: 10.1016/j.neurobiolaging.2010.06.014

Xiang, J., Jiang, H., Hu, Y., Smith, D. E., and Keep, R. F. (2010). Kyotorphin transport and metabolism in rat and mouse neonatal astrocytes. *Brain Res.* 1347, 11–18. doi: 10.1016/j.brainres.2010.05.094

Yajima, H., Ogawa, H., Ueda, H., and Takagi, H. (1980). Studies on peptides. XCIV. Synthesis and activity of kyotorphin and its analogs. *Chem. Pharm. Bull. (Tokyo)* 28, 1935–1938. doi: 10.1248/cpb.28.1935

Yoshihara, Y., Ueda, H., Fujii, N., Shide, A., Yajima, H., and Satoh, M. (1990). Purification of a novel type of calcium-activated neutral protease from rat brain. Possible involvement in production of the neuropeptide kyotorphin from calpastatin fragments. *J. Biol. Chem.* 265, 5809–5815.

Conflict of Interest Statement: The authors declare that the research was conducted in the absence of any commercial or financial relationships that could be construed as a potential conflict of interest.

Aims

KTP-NH_2 is a very interesting candidate for pharmacological development due to its biological activity, but the pharmacodynamics of the peptide still needs improvement. We first aim to introduce minor changes in the chemical structure of KTP-NH_2 to optimize pharmacological action. Hopefully, these small chemical modifications will allow us to establish structure-activity relationships to understand how pharmacophores impact the stability and activity of the peptide. The stability of the analogues will be assayed in human serum and the ability to translocate the BBB will be evaluated *in vitro* using lipid membranes. We will focus on the analgesic and anti-inflammatory activities of the peptides that will be quantified through the hot plate test and IVM parameters, respectively. In addition, IVM will allow the observation of potential damage caused by the peptides on microcirculatory environment.

The mechanism of action of KTP-NH_2 is an extremely important issue to be addressed. We hypothesize that the anti-inflammatory activity of KTP-NH_2 could be the key to link analgesia and neuroprotection. We will resort to IVM again to explore the anti-inflammatory mechanism of KTP-NH_2. We will conjugate this technique with the use of pharmacological inhibitors of potential targets.

It has been proposed that KTP could act as an inhibitor of enkephalinases, therefore extending the half-life of endogenous opioid peptides and inducing analgesia. KTP-NH_2 differs from KTP by amidation only. We will test the hypothesis that KTP-NH_2 could also act as an inhibitor of enkephalinases using canonic enzymatic assays.

Section 2

Structure-activity relationship

ARTICLE 2

Endothelium-mediated action of analogues of the endogenous neuropeptide kyotorphin (tyrosil-arginine): Mechanistic insights from permeation and effects on microcirculation

ACS Chemical Neuroscience, 2016

I declare that the experimental design, data collection and data analysis regarding the hot-plate test and IVM, as well as the discussion were carried on by me under supervision of Prof. Miguel A.R.B. Castanho. The manuscript was written by me under guidance of my supervisor Prof. Miguel A.R.B. Castanho.

KTP-NH_2 has given proof of its diversified biological activities as analgesic (Ribeiro et al. 2011), anti-inflammatory (Conceição et al. 2016), antimicrobial (Ribeiro et al. 2012) and neuroprotector peptide (Sá Santos et al. 2016). However, the pharmacodynamics and pharmacokinetics of the dipeptide are not optimal and must be improved envisioning its pharmacological development (see appendix 1). In the work to be presented in this section, we designed KTP-NH_2 derivatives introducing minor changes in the chemical structure, such as N-terminal methylation and/or use o D-amino acid residues to improve lipophilicity and resistance to enzymatic degradation. For the sake of 3R's policy, only the most stable derivatives, with less than 10% conversion into free amino acids after 60 min by high performance liquid chromatography (HPLC) in human serum, were selected to be tested *in vivo*.

Our approach consisted in first to analyze the impact of these derivatives on microcirculation using IVM. This technique brings the advantage of allowing observation and registration of the microcirculation *in vivo* and in real time in a simple and fast way. This technique is commonly used to evaluate the effects of substances such as peptides and proteins in microcirculation and muscle fibers. Different events can be observed at the same time, such as bleeding, thrombus formation, arteriolar contraction/expansion, leukocyte rolling, adhesion and transmigration, etc. For these reasons, this tool is very adequate to study the inflammatory processes.

We have also tested the analgesic potential of these derivatives using the hot plate test and compared this data with the P_R of these compounds. Our group had previously established a correlation between P_R and analgesia, which applies to the majority of KTP derivatives tested (Serrano et al. 2015). However, KTP-NH_2 is one of the exceptions. This peptide is not very efficient in translocating lipid membranes (Serrano et al. 2015). In fact, its P_R is comparable to KTP, nevertheless KTP-NH_2 presents a remarkable analgesic activity after systemic administration in several pain models (Ribeiro et al. 2011).

Interestingly, KTP-NH_2 isomer, KTP-NH_2-DL (D-Tyr-L-Arg-NH_2) did not present a significant analgesic activity in the hot plate test. This data support the hypothesis that KTP-NH_2 uses a specific transporter to cross BBB, unable to transport other KTP-NH_2

derivatives. Methylated derivatives are very permeable through lipid membranes and may diffuse passively across BBB. This is in accordance with the prolonged analgesic effect observed, which contrasts with KTP-NH_2: maximal effect at 15 min and then decay over time (Ribeiro et al. 2011).

KTP-NH_2-DL has a pronounced anti-inflammatory action, similar to KTP-NH_2, while methylation at the N-terminus results in a pro-inflammatory activity. The mechanisms of these drugs are not totally clear, but they clearly target the endothelium.

In appendix 2 the reader can find supplementary material related to article that follows.

ACS Chemical Neuroscience

Research Article

pubs.acs.org/chemneuro

Endothelium-Mediated Action of Analogues of the Endogenous Neuropeptide Kyotorphin (Tyrosil-Arginine): Mechanistic Insights from Permeation and Effects on Microcirculation

Juliana Perazzo,[†] Mônica Lopes-Ferreira,[‡] Sónia Sá Santos,[†] Isa Serrano,[†] Antónia Pinto,[†] Carla Lima,[‡] Eduard Bardaji,[§] Isaura Tavares,[∥,⊥] Montserrat Heras,[§] Katia Conceição,[*,#] and Miguel A. R. B. Castanho[*,†]

[†]Instituto de Medicina Molecular, Faculdade de Medicina da Universidade de Lisboa, Av. Professor Egas Moniz, 1649-028 Lisboa, Portugal

[‡]Unidade de Imunorregulação, Laboratório Especial de Toxinologia Aplicada, Instituto Butantan, Av. Vital Brasil, 1500 São Paulo, Brazil

[§]Laboratori d'Innovació en processos i Productes de Síntesi Orgànica (LIPPSO), Department de Química, Universitat de Girona, Campus Montilivi, 17071 Girona, Spain

[∥]Instituto de Biologia Molecular e Celular, Rua do Campo Alegre, 4150-180 Porto, Portugal

[⊥]i3S - Instituto de Inovação e Investigação em Saúde, and Departamento de Biologia Experimental, Faculdade de Medicina, Universidade do Porto, 4099-002 Porto, Portugal

[#]Departamento de Ciência e Tecnologia, Universidade Federal de São Paulo, UNIFESP, Rua Talim, 330, 04021-001 São José dos Campos, Brazil

Supporting Information

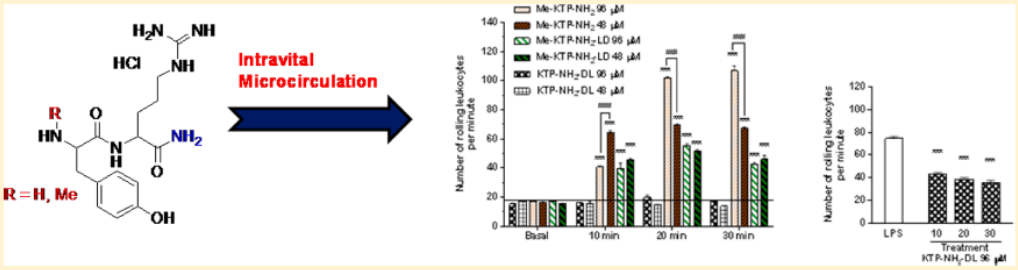

ABSTRACT: Kyotorphin (KTP) is an endogenous peptide with analgesic properties when administered into the central nervous system (CNS). Its amidated form (L-Tyr-L-Arg-NH_2; KTP-NH_2) has improved analgesic efficacy after systemic administration, suggesting blood-brain barrier (BBB) crossing. KTP-NH_2 also has anti-inflammatory action impacting on microcirculation. In this work, selected derivatives of KTP-NH_2 were synthesized to improve lipophilicity and resistance to enzymatic degradation while introducing only minor changes in the chemical structure: N-terminal methylation and/or use of D amino acid residues. Intravital microscopy data show that KTP-NH_2 having a D-Tyr residue, KTP-NH_2-DL, efficiently decreases the number of leukocyte rolling in a murine model of inflammation induced by bacterial lipopolysaccharide (LPS): down to 46% after 30 min with 96 μM KTP-NH_2-DL. The same molecule has lower ability to permeate membranes (relative permeability of 0.38) and no significant activity in a behavioral test which evaluates thermal nociception (hot-plate test). On the contrary, methylated isomers at 96 μM increase leukocyte rolling up to nearly 5-fold after 30 min, suggesting a proinflammatory activity. They have maximal ability to permeate membranes (relative permeability of 0.8) and induce long-lasting antinociception.

KEYWORDS: *Kyotophin, analgesia, microcirculation, permeability, pain, blood-brain barrier*

1. INTRODUCTION

Kyotorphin is a small endogenous dipeptide, L-Tyr-L-Arg (KTP), first isolated from a bovine brain in 1979[1,2] and afterward localized in the brain synaptosomes of mammals.[3] KTP is a powerful neuropeptide being 4-fold more potent than endogenous opioids;[1] however, the remarkable antinociceptive action of KTP in animal models was observed only when the molecule was administered directly into the central nervous system (CNS).[4] The reduced ability of KTP to cross the blood-brain barrier (BBB) is the most accepted explanation.[5] The

Received: April 5, 2016
Accepted: May 31, 2016
Published: May 31, 2016

DOI: 10.1021/acschemneuro.6b00099
ACS Chem. Neurosci. 2016, 7, 1130−1140

Scheme 1. General Synthetic Route for Solid Phase Synthesis of Kyotorphin Derivatives

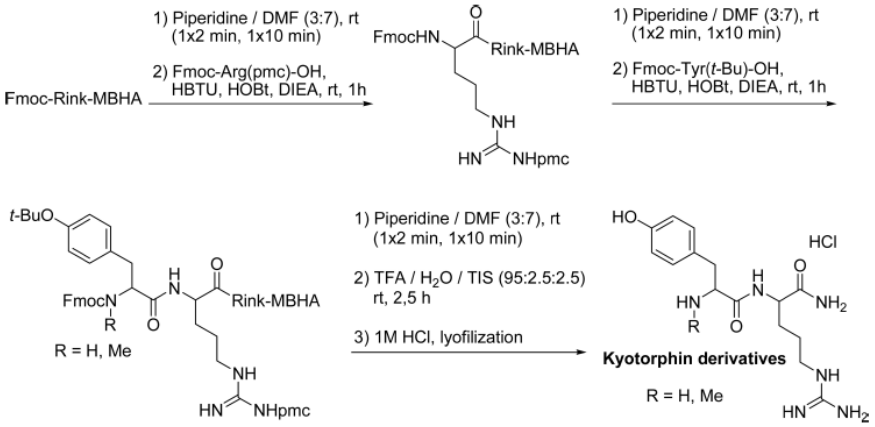

analgesia induced by KTP appears to be opioid-mediated via the release of the opioid Met-enkephalin involved in pain control.[1,6,7] It is suggested that KTP also mediates nonopioid activity without the release of enkephalins.[8,9]

Recently we have found that amidated KTP (KTP-NH_2) causes analgesia after systemic administration, which suggests KTP-NH_2 is able to cross the BBB,[10] in spite of modest permeation through lipid membranes.[11] In addition, KTP levels in cerebrospinal fluid correlate negatively with the progression of neurodegeneration in Alzheimer's disease patients[12] and KTP-NH_2 has neuroprotective effects in an animal model of dementia.[13] Because recent evidence shows that Alzheimer's disease is primarily a vascular disease with neurodegenerative consequences, rather than a neurodegenerative disorder with vascular consequences,[14] and the activity of KTP-NH_2 at BBB level, we have raised the hypothesis that the endothelium is a key element in the pharmacological action of KTP-NH_2. In addition to its hypothetical endothelial targeting, KTP-NH_2 is also an appealing drug lead because it does not cause damage on microcirculation,[15] has no significant cytotoxic effects[10] and does not induce the side effects associated with opioid drugs.[16]

When covalently associated with ibuprofen, KTP-NH_2 enhances the anti-inflammatory action of ibuprofen[15] and the ibuprofen moiety enhances the analgesic action of KTP-NH_2.[17] Chemical manipulation of KTP-NH_2 is a strategy to modulate its action. The key elements of KTP-NH_2 chemical nature that interfere with its biological action are the cationic charge,[18] lipophilicity,[19] and resistance to enzymatic degradation.[10,17] In this study, we have pursued the goal of finding simple and inexpensive KTP-NH_2 derivatives having endothelium-mediated action both as analgesic and anti-inflammatory drugs. The strategy was to explore enantiomers of KTP-NH_2 by using D-Tyr and/or D-Arg residues and/or methylation capping at the N-terminus. All the derivatives are thus analogues of KTP-NH_2 with minimal differences in structure, while exploring variation in charge, lipophilicity, and resistance to peptidases. An integrated approach using in vivo data from intravital microscopy (IVM) and evaluation of thermal nociceptive responses in rodents, combined with mechanistic permeation data in vitro, was used to unravel new drug leads targeted to endothelium-mediated action with impact both in inflammation and analgesia.

2. RESULTS

2.1. Synthesis of Kyotorphin Derivatives. First, amidated kyotorphin derivatives H-D-Tyr-Arg-NH_2 (KTP-NH_2-DL), H-Tyr-D-Arg-NH_2 (KTP-NH_2-LD), H-D-Tyr-D-Arg-NH_2 (KTP-NH_2-DD), H-N-Me-Tyr-D-Arg (Me-KTP-NH_2-LD), and H-N-Me-Tyr-Arg (Me-KTP-NH_2) have been prepared in small scale through standard solid phase peptide synthesis using a 9-fluorenylmethoxycarbonyl (Fmoc)/*tert*-butyl (*t*-Bu) strategy as illustrated in Scheme 1. Key elements of this solid-phase peptide synthesis are, employment of *t*-Bu group and 2,2,5,7,8-pentamethyl-chroman-6-sulfonyl (pmc) group as masks for the side chains of tyrosine and arginine, respectively; removal of Fmoc groups by treatment with 30% piperidine in dimethylformamide (DMF) and amide couplings mediated by *O*-(benzotriazol-1-yl)-*N*,*N*,*N*′,*N*′-tetramethyluronium hexafluorophosphate (HBTU) in the presence of *N*-hydroxybenzotriazole (HOBt) as racemization suppressant and diisopropylethylamine (DIEA) as base.

The side chain protection of arginine is an unsolved problem in solid phase peptide synthesis because the usually employed arylsulfonyl-based protecting groups (e.g., pmc)[20] are too stable to TFA and need extended cleavage to complete removal during the release step of the peptide from the support.[21] In addition, sometimes they are also difficult to scavenge and have a tendency to reattach or alkylate sensitive residues. Knowing this, the release step of KTP-NH_2-DL peptide was first examined using three different cleavage cocktails (Table 1). Reagents R[22] and B[23] are the most recommended cleavage cocktails for those peptides containing, among others amino acids residues, Arg(pmc). Nevertheless, under these conditions KTP-NH_2-DL was obtained in poor purity together with a significant amount of peptide with arginine residue still pmc-protected KTP-NH_2-DL(pmc) and several no identified impurities (Table 1, entries 1 and 2). The standard mixture of cleavage with TFA, water and triisopropylsilane (TIS) was tested at different cleavage times (Table 1, entries 3−6). After 2:20 h treatment, acceptable results of 80% purity of KTP-NH_2-DL and only a 2% of KTP-NH_2-DL(pmc) were obtained (Table 1, entry 5). Increasing cleavage time provided worse results (Table 1, entry 6). The best cleavage conditions were applied to the others kyotorphin derivatives which were obtained in a range of purities of 72−87%.

Next, the crude kyotorphin derivatives were purified manually by reverse-phase flash chromatography and the pure

DOI: 10.1021/acschemneuro.6b00099
ACS Chem. Neurosci. 2016, 7, 1130−1140

Table 1. KTP-NH_2-DL Peptide Submitted to Different Cleavage Conditions

entry	cleavage cocktail	time (h)	KTP-NH_2-DL (%)[c]	KTP-NH_2-DL(pmc) (%)[c]
1	TFA/thioanisole/EDT/anisole[a] (90:5:3:2)	2:00	55	3
2	TFA/phenol/H_2O/TIS[b] (88:5:5:2)	3:00	35	50
3	TFA/TIS/H_2O (95:2.5:2.5)	2:00	50	11
4	TFA/TIS/H_2O (95:2.5:2.5)	2:15	67	13
5	TFA/TIS/H_2O (95:2.5:2.5)	2:25	80	2
6	TFA/TIS/H_2O (95:2.5:2.5)	4:00	42	25

[a]Reagent R. [b]Reagent B. [c]Percentage determined by HPLC at 220 nm from the crude peptide.

peptides obtained were dissolved in 1 M aqueous HCl and lyophilized for three times to afford kyotorphin derivatives as a hydrochloride salts, with final yields and purities shown in Table 2.

Lead kyotorphin derivatives KTP-NH_2-DL, Me-KTP-NH_2-LD and Me-KTP-NH_2 have been prepared in large scale through standard solution phase peptide synthesis as illustrated in Scheme 2. Boc-tyrosine building blocks are commercially available protected with benzyl (Bzl) group in the side chain. Amide coupling between tyrosine and arginine building blocks was mediated by benzotriazole-1-yl-oxy-tris(dimethylamino)-phosphonium hexafluorophosphate (BOP) in the presence of *N*-methylmorpholine (NMM) at room temperature. Under these conditions, all protected kyotorphin derivatives were obtained in moderate to good yields and in excellent purities (Scheme 2).

In the case of methylated derivatives, although a single peak by HPLC analysis was observed, its ^{1}H NMR spectra showed some protons split specially for the α-carbonylic protons. In order to distinguish between a conformational equilibrium and a possible epimerization occurred during coupling reaction, a variable-temperature ^{1}H NMR study was undertaken. At 20 °C, the α-carboxylic protons of Me-KTP-NH_2-LD (protected) exhibit two separate and broad singlet signals, which coalesce between 40 and 60 °C (Figure 1), and sharpen even more at higher temperatures. These results are unequivocal evidence that the methylated kyotorphin derivatives present a slow conformational equilibrium which can be observed on the NMR time scale, and that epimerization process does not take place during coupling reaction.

Next, Bzl and Boc protecting groups of the kyotorphin derivatives, were removed by catalytic hydrogenation and treatment with a 4 M solution of HCl in dioxane, respectively. Thus, the final kyotorphin derivatives were obtained as hydrochloride salt in good yields (Scheme 2).

2.2. Selection of Lead Compounds Based on Lipid Interaction and Serum Stability. KTP-NH_2 is unstable in human serum (90% conversion in free amino acids after 60 min by HPLC), KTP-NH_2-LD is relatively stable (20% conversion), and the other derivatives are very stable (less than 10% conversion). Lipid interaction studies[24] using anionic lipids to better mimic brain endothelium surface[18] has shown a stronger interaction of the derivatives KTP-NH_2-DL, Me-KTP-NH_2-LD, and Me-KTP-NH_2 with lipid membranes (Figure 2), indicative of an increased potential to translocate membranes as insertion on lipid bilayers is the first key event in diffusion across membranes or receptor targeting.[24] Compounds KTP-NH_2-DL, Me-KTP-NH_2-LD, and Me-KTP-NH_2 are the most promising both in terms of pharmacokinetics (stability in serum) and efficacy (potential to translocate the blood-brain barrier) and were therefore selected as lead compounds in this study.

2.3. Intravital Microscopy Studies. Changes in the dynamics of microcirculation were evaluated by intravital microscopy following topical application of 20 μL of KTP derivatives 48 or 96 μM to mice cremaster muscle. Despite structural similarities, KTP derivatives presented distinct alterations in microcirculation. The peptide Me-KTP-NH_2 increased hugely the number of rolling leukocytes in a concentration-dependent manner. Except that at 10 min, 48 μM of this peptide increased more leukocyte rolling than 96 μM ($p < 0.001$). These values remained high, statistically unchanged, at 20 and 30 min (Figure 3A). The increase of rolling leukocytes caused by 48 μM of Me-KTP-NH_2 was about 4-fold compared to basal values ($p < 0.001$). At the highest concentration tested of 96 μM, Me-KTP-NH_2 increased approximately 6-fold the leukocyte rolling compared to control and reached a plateau at 20 min (Figure 3A). Moreover, a transient arteriolar contraction was observed 10 min after topical application of 96 μM Me-KTP-NH_2 (Figure 3C), while lower concentration caused an arteriolar contraction in only 25% of tested animals. No adherent leukocytes were observed over the experiment (data not shown).

The peptide Me-KTP-NH_2-LD did not show a concentration-dependent behavior, but also increased leukocyte rolling, by approximately 3-fold (Figure 3A). Furthermore, Me-KTP-NH_2-LD isomer did not induce arteriolar contraction nor increased the number of adherent leukocytes (data not shown). However, both Me-KTP-NH_2-LD and Me-KTP-NH_2 showed proinflammatory properties.

In contrast, KTP-NH_2-DL did not increase leukocyte rolling (Figure 3A). Consequently, we decided to study its effects on LPS-induced inflammation model. Mice injected ip with 0.05 μg/kg LPS present an average of 75 rolling leukocytes per min

Table 2. Yields and Purities of Kyototphin Derivatives Synthesized in Solid Phase

reference	sequence	yield (%)[a]	purity (%)[b]	HPLC t_R (min)
KTP-NH_2-DL	H-D-Tyr-Arg-NH_2	52	99.9	2.35
KTP-NH_2-LD	H-Tyr-D-Arg-NH_2	70	98.2	2.41
KTP-NH_2-DD	H-D-Tyr-D-Arg-NH_2	80	99.9	1.52
Me-KTP-NH_2-LD	H-N-Me-Tyr-D-Arg-NH_2	60	97.7	2.28
Me-KTP-NH_2	H-N-Me-Tyr-Arg-NH_2	58	98.7	1.66

[a]Yields were calculated from isolated product after reverse-phase flash chromatography. [b]Percentage determined by HPLC at 220 nm from the crude peptide.

DOI: 10.1021/acschemneuro.6b00099
ACS Chem. Neurosci. 2016, 7, 1130−1140

Scheme 2. Solution Phase Synthesis of Kyotorphin Derivatives

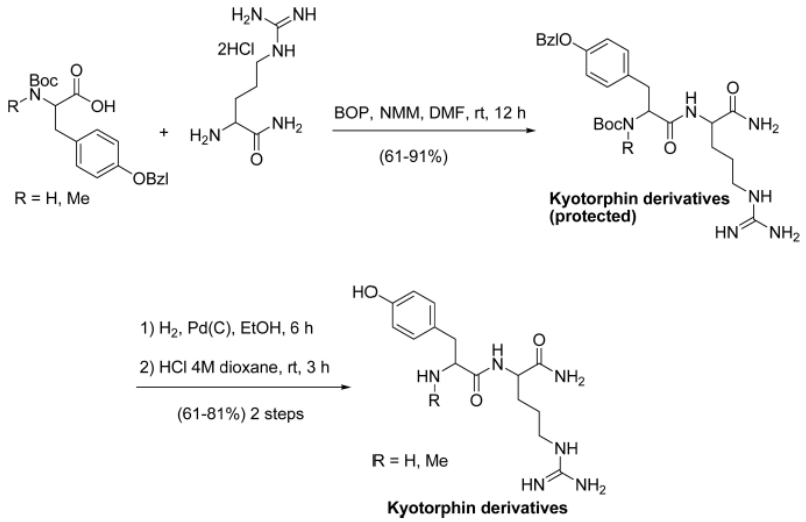

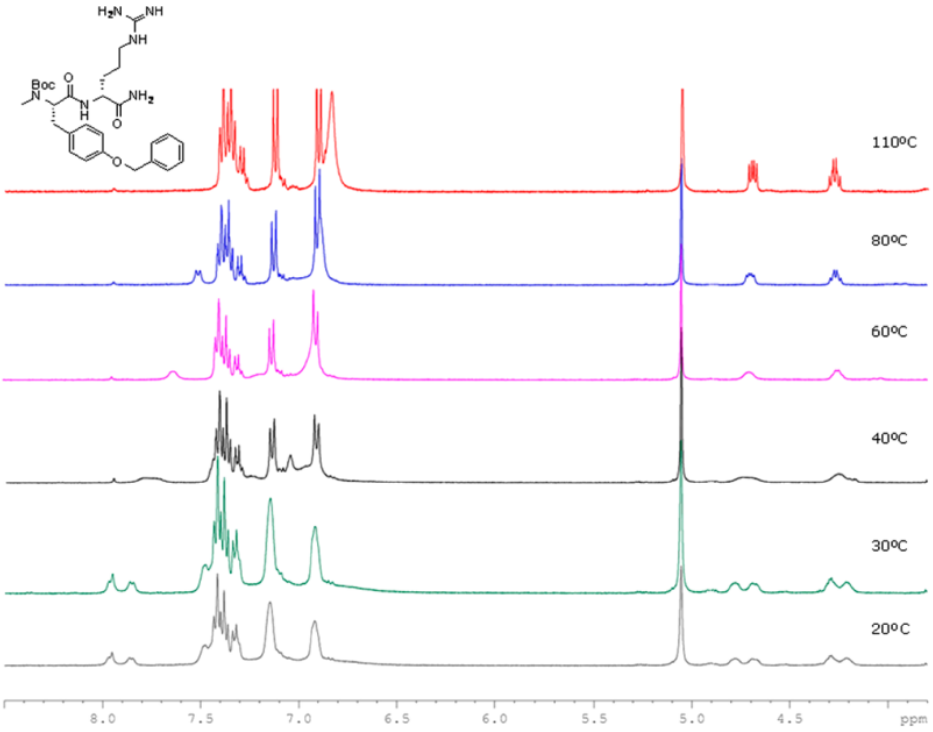

Figure 1. ^{1}H NMR spectra (region 4−8.5 ppm) of Me-KTP-NH_2-DL (protected) recorded in DMSO-d_6 from 20 to 110 °C.

along the vessel wall. Topical treatment with KTP-NH_2-DL reduced that number to approximately 39 rolling leukocytes/min. This result evidence a potential role of this isomer as an anti-inflammatory compound.

2.4. Evaluation of Thermal Nociceptive Responses. The analgesic effects of Me-KTP-NH_2-LD and Me-KTP-NH_2 were evaluated after ip administration to male Wistar rats. Both peptides induced a dose- and time-independent increased response threshold (average variation of 2−2.6 °C in relation to the respective baseline levels). In fact, after injection of Me-KTP-NH_2-LD at either 50 μmol/kg or 96 μmol/kg increases in threshold were detected at all time points, except at 75 min ($p < 0.05$ at 30 and 90 min and $p < 0.01$ at 15, 45, and 60 min for the dose 50 μmol/kg; $p < 0.05$ at 90 min, $p < 0.01$ at 30 and 60 min and $p < 0.001$ at 15 and 45 min for the dose 96 μmol/kg; Figure 4). Regarding the injection of Me-KTP-NH_2 at 50 μmol/kg, an increase in threshold was detected 15 ($p < 0.01$) and 45 min postinjection ($p < 0.05$). With the 96 μmol/kg the increases were detected at all the time points, except at 75 min ($p < 0.05$ at 30, 60, and 90 min and $p < 0.01$ at 15 and 45 min; Figure 4). After injection with saline, the variations in relation to the respective baseline levels along the time were negligible

DOI: 10.1021/acschemneuro.6b00099
ACS Chem. Neurosci. 2016, 7, 1130−1140

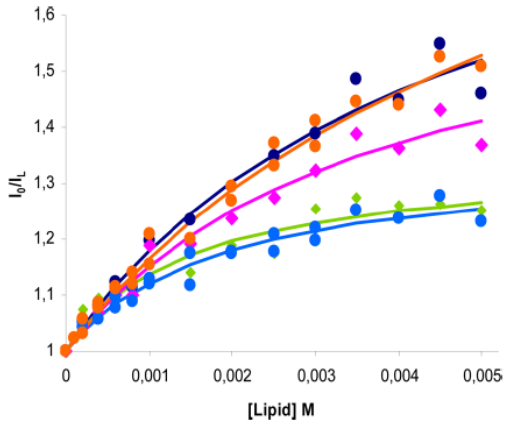

Figure 2. Normalized Tyr residue fluorescence emission upon titration of the KTP derivatives with lipid vesicles of POPG [1-hexadecanoyl-2-(9Z-octadecenoyl)-*sn*-glycero-3-phospho-(1′-*rac*-glycerol)], as described in refs 24 and 17. Maximal deviation from the initial value of fluorescence intensity reflects how strongly the fluorescence quantum yield of Tyr residue is affected by contact with the lipid. KTP-NH_2-LD, light blue; KTP-NH_2-DL, pink; KTP-NH_2-DD, green; Me-KTP-NH_2-LD, dark blue; and Me-KTP-NH_2, orange.

or nil (Figure 4). Regarding the effects of the peptide KTP-NH_2-DL, statistically significant increases were only detected at 45 min with the dose of 50 μmol/kg (Figure 4). Overall, the results indicate an analgesic effect of both LL and LD Me-KTP-NH_2 isomers, whereas the peptide KTP-NH_2-DL did not show a relevant analgesic effect.

2.5. Permeation Studies with Drug Candidates. The time-dependence of the normalized fluorescence emission intensity of the drugs in covered and blank filters versus time is presented in Supporting Information (Figure S1). The relative permeability was calculated for each drug candidate (Figure 5). The P_R of the five peptides ranged from 0.38 to 0.81, the highest value being attained by Me-KTP-NH_2. The P_R of KTP-NH_2-DL was significantly inferior to the one of KTP.

3. DISCUSSION

A new series of KTP-NH_2 derivatives have been designed in order to improve endothelial targeting both at peripheral and BBB level and were evaluated for their impact on microcirculation and analgesic efficacy in vivo. The potential to transpose lipid membranes in vitro was also evaluated. Modifications consisted in N-terminal methylation and/or L to D amino acid change.

The evaluation of the microcirculatory environment was assessed through IVM. This technique has been used for decades to help scientists understand the biophysical conditions under which leukocytes are exposed to in microvessels.[25−27] IVM provides a tool to acquire quantitative, qualitative, and dynamic insights into cell biology and endothelial−leukocyte interactions relevant to understanding the pathophysiology of inflammation in different disease states.[28]

After KTP derivatives application, the microcirculatory environment did not reveal toxic effects such as thrombi formation or contraction of myofibrils; however, Me-KTP-NH_2 and Me-KTP-NH_2-LD increased 6- and 3-fold, respectively, the number of rolling leukocytes relative to control (Figure 3), revealing a potential proinflammatory effect. However, vasodilatation, one of the earliest events of acute inflammation, was not detected. On the contrary, KTP-NH_2-DL did not increase leukocyte rolling nor induced cellular recruitment. In addition, it decreased leukocyte rolling induced by LPS (Figure 3B). This endotoxin is found in the outer membrane of Gram-negative bacteria and once LPS reaches the blood flow, it activates the CD14/toll-like receptor 4 (TLR4)/myeloid differentiation protein 2 (MD2) complex on the surface of immune cells consequently promoting the secretion of proinflammatory cytokines, nitric oxide, and eicosanoids, and inducing neutrophils recruitment.

KTP-NH_2-DL has low permeation across lipid membranes as P_R = 0.4 (Figure 5), a value at which no significant analgesic effect is expected among KTP derivatives that diffuse across lipid bilayers.[19] Consistently, KTP-NH_2-DL has the lowest analgesic effect among the three lead drugs tested (Figure 4). KTP-NH_2 is more effective than expected from simple inference based on P_R,[19] but KTP-NH_2-DL does not retain this property. As previously suggested,[19] KTP-NH_2 probably uses an active transporter like peptide transporter 2 (PEPT2) to translocate the BBB. Data in Figure 3 corroborates this hypothesis as KTP-NH_2-DL is an diastereoisomer of KTP-NH_2 and completely loses efficacy. The data suggest that KTP-NH_2 derivatives having high P_R permeate through the BBB passively and cause analgesia while KTP-NH_2 uses a selective transporter. This hypothesis also explains why KTP-NH_2 has a fast transient effect while methylated (Figure 5) and other derivatives have prolonged effects:[10,17] derivatization in both endings such as amidation at C terminus and methylation at N terminus, protects the peptides from the action of peptidases and proteases, improving pharmacokinetics.

Me-KTP-NH_2 is highly permeable having P_R = 0.8. The addition of a neutral, hydrophobic methyl group to KTP-NH_2 was a significant step to improve the interaction with lipid and confer increased membrane permeation. We have previously described a direct correlation between membrane permeation and analgesic activity.[19] The data obtained in the hot-plate test corroborate this hypothesis. The analogues with higher P_R, Me-KTP-NH_2 and Me-KTP-NH_2-LD, are the most effective in analgesia (Figure 4).

In this study, we have discovered KTP-NH_2-DL, an anti-inflammatory drug lead, and Me-KTP-NH_2, a very effective membrane-translocator analgesic drug lead. The parent molecule KTP-NH_2 combines anti-inflammatory properties with analgesic efficacy. Isomerization of the Tyr residue (D-Tyr) decreases permeation through membranes and abrogates analgesic action. Methylation at the N terminus increases permeation and improves analgesic efficacy but abrogates anti-inflammatory action, probably a consequence of cell-penetration at the endothelium and/or blood cells. Since the hot-plate is a behavioral test that evaluates acute responses to thermal nociceptive stimulation and in which the inflammatory reaction is nil,[29] future studies will evaluate the effects of those analogues in inflammatory pain models, such as articular inflammation.

The mechanism of action of KTP-NH_2 is still not totally clarified but the dual effect of KTP-NH_2[15] in pain and inflammation might shed light on this matter. Ueda and coworkers suggested that KTP receptor is coupled to G_i protein and mediates calcium influx via phospholipase C (PLC).[30] PLC also plays an important role in the inflammation pathway catalyzing the release of arachidonic acid that subsequently promotes the release of prostaglandins and leukotrienes. It is reasonable to speculate that KTP-NH_2 might interact with G

DOI: 10.1021/acschemneuro.6b00099
ACS Chem. Neurosci. 2016, 7, 1130−1140

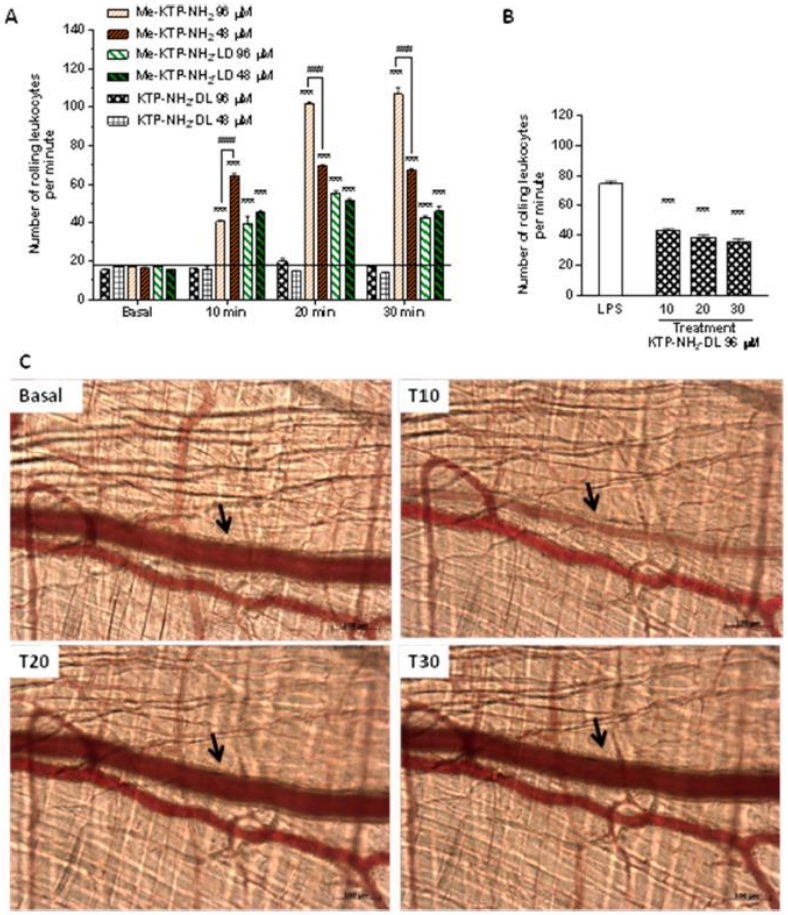

Figure 3. Effects of KTP-NH_2 derivatives on microcirculation. (A) Number of rolling leukocytes/min after topical application of 48 or 96 μM of the KTP-NH_2-DL, Me-KTP-NH_2, and Me-KTP-NH_2-LD peptides on the mice cremaster muscle ($n \geq 4$) at different time points. Bars represent mean ± SEM. Basal values correspond to number of rolling leukocytes per minute before peptide application. The horizontal line represents the average number of rolling leukocytes over time after PBS application. $^{***}p < 0.001$ compared to PBS using two-way ANOVA followed by Tukey's post test, $^{\#\#\#}p < 0.001$. (B) Number of rolling leukocytes per minute after challenge with LPS (0.05 μg/kg, ip) and following topical treatment with 96 μM of KTP-NH_2-DL. Determinations were performed each 10 min up to 30 min after peptide topical application on the mice cremaster muscle ($n = 4$). Each point represents mean ± SEM; $^{***}p < 0.001$ compared with LPS (control group: topical application of PBS) using two-way ANOVA followed by Tukey's post test. (C) Transient arteriolar contraction at 10 min after Me-KTP-NH2 (96 μM) topical application.

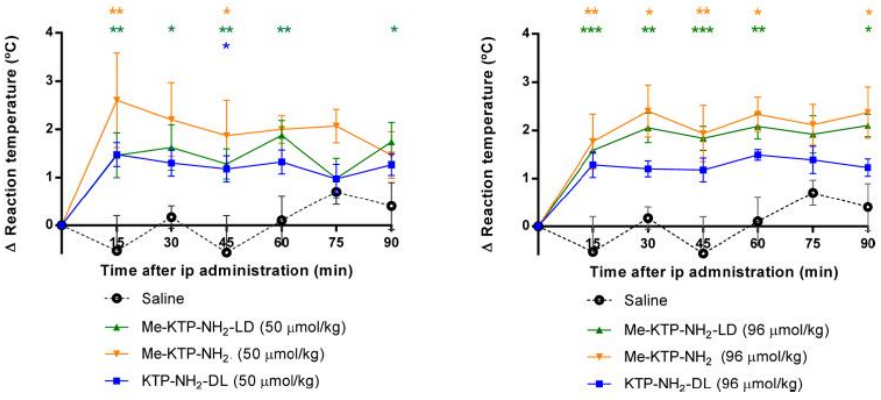

Figure 4. Effect of KTP-NH_2 derivatives on the nociceptive threshold of rats in the hot-plate test. Results shown as the difference between responses at each time point relative to basal values (time zero, i.e., immediately before injection). Compounds were ip administered at 50 μmol/kg (left panel) or 96 μmol/kg (right panel). Each point represents mean ± SEM ($n \geq 5$). $^{***}p < 0.001$, $^{**}p < 0.01$, and $^{*}p < 0.05$ versus saline-treated animals using two-way ANOVA followed by Tukey's post test.

DOI: 10.1021/acschemneuro.6b00099
ACS Chem. Neurosci. 2016, 7, 1130−1140

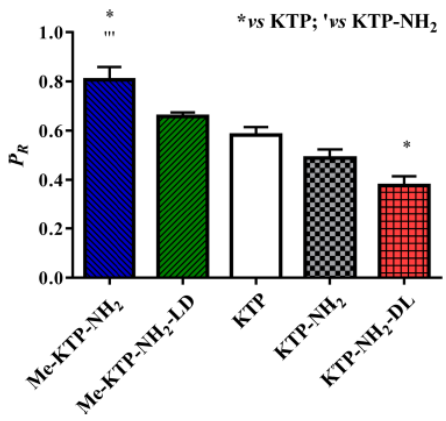

Figure 5. Relative permeability of Me-KTP-NH_2, Me-KTP-NH_2-LD, KTP-NH_2-DL, KTP, and KTP-NH_2. Data showed as mean ± SEM; each group is an average of three independent measures. *$P < 0.05$ versus KTP; '''$P < 0.001$ versus KTP-NH_2. One-way ANOVA, followed by Tukey's post test.

protein coupled receptors that play a role simultaneously in pain and inflammation. A good hypothetic target would be the protease-activated receptors (PARs). They are widely distributed in a variety of tissues and can be activated by small peptides, triggering different intracellular pathway depending on the cell type. "PARs are in essence peptides receptors that carry their own ligand, which remain silent until unmasked by site-specific receptor cleavage."[31] Four PAR isoforms have been identified so far. PAR1 and PAR4 agonists are able to induce analgesia and inflammation, while PAR2 antagonist cause analgesia and are anti-inflammatory. The interaction of KTP-NH_2 with PARs could be the key to explain how KTP-NH_2 and its derivatives impact on inflammation and analgesia.

4. CONCLUSIONS

(1) KTP-NH_2 is anti-inflammatory in mice as revealed by IVM and analgesic in rats as revealed by the hot plate test. Methylation at the N-terminus enhances analgesic efficacy through increased permeation across lipid membranes but abrogates anti-inflammatory action. Isomerization of the L-Tyr residue has the opposite effect.

(2) Globally, the results support the hypothesis that KTP-NH_2 uses a specific transporter across the BBB, not fitted to transport KTP-NH_2 derivatives. Methylated derivatives permeate membranes passively and may diffuse across the BBB, thus compensating for the lack of activity of the transporter.

(3) KTP-NH_2-DL has a pronounced anti-inflammatory action but low permeation through lipid membranes and decreased analgesic action.

In addition, the study opens new perspectives by casting the hypothesis that the interference of KTP-NH_2 and its derivatives with PAR may be the key to understand the dual action of these drugs in inflammation and nociception. PARs are expressed in endothelial cells and neurons, besides platelets and myocytes.

5. METHODS

5.1. Peptide Synthesis. *5.1.1. General Synthetic Procedures.* KTP and KTP-NH_2 were synthesized as described before.[10] All chemicals used for peptide synthesis were purchased from Sigma-Aldrich, Fluka, Bachem, or Iris-Biotech and used without further purification. The peptides synthesized in solid-phase were analyzed for purity on high performance liquid chromatography (HPLC) and characterized by mass spectra under electrospray ionization (ESI-MS) and proton nuclear magnetic resonance (^{1}H NMR). The peptides synthesized in solution phase were analyzed for purity on HPLC and characterized by ^{1}H NMR, ^{13}C NMR, and high resolution mass spectra under electrospray ionization (HRMS-ESI). HPLC analyses were carried out using a Dionex instrument composed of an UV/vis Dionex UVD170U detector, a P680 Dionex bomb, an ASI-100 Dionex automatic injector, and CHROMELEON 6.60 software. Separations were achieved on an analytical 100-C_{18} Kromasil reversed phase column (4.6 mm × 40 mm; 3.5 μm particle size). The compounds were eluted using a linear gradient of 0−100% CH_3CN in 0.1% TFA at flow rate of 1.0 mL/min. The absorbance was measured at 220 nm. The HPLC retention time of each compound was determined when the peak was at its maximum height. NMR spectra were recorded at 400 MHz on a Bruker DPX Advance spectrometer. Spectra recorded in DMSO-d_6 were referenced to residual DMSO-d_6 at 2.50 ppm for ^{1}H or 39.5 ppm for ^{13}C. Spectra recorded in D_2O were referenced to 4,4-dimethyl-4-silapentane-1-sulfonic acid (DDS = 0.0 ppm) as an internal standard. Coupling constants (J) are given in Hertz (Hz). The following abbreviations were used for spin multiplicity: s = singlet, d = doblet, t = triplet, q = quarter, m = multiplet, dd = double doublet, bs = broad singlet. ESI-MS analyses were performed with an Esquire 6000 ESI ion Trap LC/MS (Bruker Daltonics) instrument equipped with an electrospray ion source. The instrument was operated in the positive ESI(+) ion mode. Samples (5 μL) were introduced into the mass spectrometer ion source directly through an HPLC autosampler. The mobile phase (80:20 CH_3CN/H_2O at a flow rate of 100 μL min^{-1}) was delivered by a 1100 Series HPLC pump (Agilent). Nitrogen was employed as both the drying and nebulizing gas. HRMS were recorded under conditions of ESI with a Bruker MicroTof-Q instrument using a hybrid quadrupole time-of-flight mass spectrometer (University of Zaragoza). Samples were introduced into the mass spectrometer ion source directly through a 1100 Series Agilent HPLC autosampler and were externally calibrated using sodium formate. The instrument was operated in the positive ESI(+) ion mode. Reverse-phase flash chromatography (RF-FC) purifications were performed manually on C_{18}-reverse-phase silica gel 100 (400 mesh, Fluka).

5.1.2. Solid Phase Synthesis of Peptides KTP-NH_2-DL, KTP-NH_2-LD, KTP-NH_2-DD, Me-KTP-NH_2-LD and Me-KTP-NH_2. General Procedure. Peptides were prepared manually by the solid-phase method using Fmoc-type chemistry, Fmoc-Rink-MBHA resin (0.56 mmol/g) as solid support, *tert*-butyl side chain protection for tyrosine, and pmc for arginine. Coupling of amino acids was mediated by a mixture of HBTU (3.8 equiv), HOBt (4 equiv), and DIEA (3 equiv) in DMF at room temperature for 1 h. The completion of the reactions was monitored by the Kaiser test. Fmoc group was removed by treating the resin with 30% piperidine in DMF (2 + 8 min). After each coupling and deprotection step, the resin was washed with DMF (6 × 1 min) and air-dried. A mixture of TFA, water and TIS was used as cleavage cocktail.

The Fmoc-Rink-MBHA resin (450 mg) was placed into a plastic syringe fitted with a polypropylene frit to remove the Fmoc group and subsequently couple with arginine amino acid (4 equiv). After Fmoc group removal, the resin was treated with tyrosine derivative (4 equiv). The resulting dipeptides were deprotected with piperidine and released from the solid support by treatment with TFA/H_2O/TIS (95:2.5:2.5) with stirring for 2.25 h at room temperature. Following TFA evaporation and diethyl ether extraction, the crude peptides were purified by reverse-phase flash chromatography (H_2O/MeOH/TFA 90:10:0.01%). The resulting white solid was dissolved in 1 M aqueous HCl and lyophilized. This process was repeated three times to afford kyotorphin derivatives as a hydrochloride salt.

KTP-NH_2-DL. By the general procedure, Fmoc-Arg(pmc)−OH (4 equiv) and Fmoc-D-Tyr(*t*Bu)−OH (4 equiv) provided H-D-Tyr-Arg-NH_2 (48 mg, 52%) as a colorless solid. HPLC (water/acetonitrile, 0.1% TFA, 2−100%, 17 min): retention time, 2.36 min; 99.9% pure. ^{1}H NMR (D_2O, 400 MHz): δ 1.02−1.22 (m, 2H, $CH_2CH_2NH_{arginine}$),

DOI: 10.1021/acschemneuro.6b00099
ACS Chem. Neurosci. 2016, 7, 1130−1140

1.42−1.52 (m, 1H of the $CH_2CH_{arginine}$), 1.59−1.69 (m, 1H of the $CH_2CH_{arginine}$), 2.99 (dd, J = 13.4 Hz, J' = 10.3 Hz, 1H of the CH_2-$\beta_{tyrosine}$), 3.02−3.05 (m, 2H, CH_2-$\beta_{arginine}$), 3.22 (dd, J = 13.4 Hz, J' = 5.8 Hz, 1H of the CH_2-$\beta_{tyrosine}$), 4.08 (dd, J = 9.6 Hz, J' = 4.5 Hz, 1H, CH-$\alpha_{arginine}$), 4.18 (dd, J = 10.3 Hz, J' = 5.8 Hz, 1H, CH-$\alpha_{tyrosine}$), 6.88 (d, J = 8.5 Hz, 2H, CH_{aryl}), 7.15 (d, J = 8.5 Hz, 2H, CH_{aryl}). MS (ESI) m/z = 337.1 $[M + H]^+$, 169.0 $[M + 2H]^{2+}$.

KTP-NH$_2$-LD. By the general procedure, Fmoc-D-Arg(pmc)−OH (4 equiv) and Fmoc-Tyr(*t*Bu)−OH (4 equiv) provided H-Tyr-D-Arg-NH_2 (66 mg, 70%) as a colorless solid. HPLC (water/acetonitrile, 0.1% TFA, 2−100%, 17 min): retention time, 2.41 min; 99% pure. ^{1}H NMR (D_2O, 400 MHz): δ 1.00−1.19 (m, 2H, $CH_2CH_2NH_{arginine}$), 1.42−1.52 (m, 1H of the $CH_2CH_{arginine}$), 1.59−1.68 (m, 1H of the $CH_2CH_{arginine}$), 2.96 (dd, J = 13.3 Hz, J' = 10.3 Hz, 1H of the CH_2-$\beta_{tyrosine}$), 3.01−3.04 (m, 2H, CH_2-$\beta_{arginine}$), 3.21 (dd, J = 13.3 Hz, J' = 5.8 Hz, 1H of the CH_2-$\beta_{tyrosine}$), 4.06 (dd, J = 9.6 Hz, J' = 4.5 Hz, 1H, CH-$\alpha_{arginine}$), 4.17 (dd, J = 10.3 Hz, J' = 5.8 Hz, 1H, CH-$\alpha_{tyrosine}$), 6.87 (d, J = 8.5 Hz, 2H, CH_{aryl}), 7.14 (d, J = 8.5 Hz, 2H, CH_{aryl}). MS (ESI) m/z = 337.1 $[M + H]^+$, 169.0 $[M + 2H]^{2+}$.

KTP-NH$_2$-DD. By the general procedure, Fmoc-D-Arg(pmc)−OH (4 equiv) and Fmoc-D-Tyr(*t*Bu)−OH (4 equiv) provided H-D-Tyr-D-Arg-NH_2 (75 mg, 80%) as a colorless solid. HPLC (water/acetonitrile, 0.1% TFA, 2−100%, 17 min): retention time, 1.52 min; 99.9% pure. ^{1}H NMR (D_2O, 400 MHz): δ 1.49−1.62 (m, 2H, $CH_2CH_2NH_{arginine}$), 1.65−1.86 (m, 2H, $CH_2CH_{arginine}$), 3.10−3.17 (m, 4H, CH_2-$\beta_{arginine}$ and CH_2-$\beta_{tyrosine}$), 4.20−4.26 (m, 2H, CH-$\alpha_{tyrosine}$ and CH-$\alpha_{arginine}$), 6.85 (d, J = 8.4 Hz, 2H, CH_{aryl}), 7.13 (d, J = 8.4 Hz, 2H, CH_{aryl}). MS (ESI) m/z = 337.1 $[M + H]^+$, 169.0 $[M + 2H]^{2+}$.

Me-KTP-NH$_2$-LD. By the general procedure, Fmoc-D-Arg(pmc)−OH (4 equiv) and Fmoc-N-Me-Tyr(*t*Bu)−OH (4 equiv) provided *N*-Me-Tyr-D-Arg-NH_2 (58 mg, 60%) as a colorless solid. HPLC (water/acetonitrile, 0.1% TFA, 2−100%, 17 min): retention time, 2.29 min; 97.7% pure. ^{1}H NMR (D_2O, 400 MHz): δ 0.98−1.18 (m, 2H, $CH_2CH_2NH_{arginine}$), 1.39−1.49 (m, 1H of the $CH_2CH_{arginine}$), 1.56−1.65 (m, 1H of the $CH_2CH_{arginine}$), 2.73 (s, 3H, NCH_3), 2.94 (dd, J = 13.1 Hz, J' = 11.0 Hz, 1H of the CH_2-$\beta_{tyrosine}$), 2.99−3.04 (m, 2H, CH_2-$\beta_{arginine}$), 3.30 (dd, J = 13.1 Hz, J' = 5.3 Hz, 1H of the CH_2-$\beta_{tyrosine}$), 4.04 (dd, J = 9.8 Hz, J' = 4.6 Hz, 1H, CH-$\alpha_{arginine}$), 4.07 (dd, J = 11.0 Hz, J' = 5.3 Hz, 1H, CH-$\alpha_{tyrosine}$), 6.87 (d, J = 8.5 Hz, 2H, CH_{aryl}), 7.13 (d, J = 8.5 Hz, 2H, CH_{aryl}). MS (ESI) m/z = 351.1 $[M + H]^+$, 176.0 $[M + 2H]^{2+}$.

Me-KTP-NH$_2$. By the general procedure, Fmoc-Arg(pmc)−OH (4 equiv) and Fmoc-N-Me-Tyr(*t*Bu)−OH (4 equiv) provided *N*-Me-Tyr-Arg-NH_2 (56 mg, 58%) as a colorless solid. HPLC (water/acetonitrile, 0.1% TFA, 2−100%, 17 min): retention time, 1.66 min; 98.7% pure. ^{1}H NMR (D_2O, 400 MHz): δ 1.50−1.58 (m, 2H, $CH_2CH_2NH_{arginine}$), 1.63−1.70 (m, 1H of the $CH_2CH_{arginine}$), 1.72−1.80 (m, 1H of the $CH_2CH_{arginine}$), 2.71 (s, 3H, NCH_3), 3.06 (dd, J = 13.8 Hz, J' = 9.0 Hz, 1H of the CH_2-$\beta_{tyrosine}$), 3.17 (t, 2H, J = 6.9 Hz, CH_2-$\beta_{arginine}$), 3.20 (dd, J = 13.8 Hz, J' = 5.7 Hz, 1H of the CH_2-$\beta_{tyrosine}$), 4.12 (dd, J = 9.0 Hz, J' = 5.7 Hz, 1H, CH-$\alpha_{tyrosine}$), 4.42 (dd, J = 7.8 Hz, J' = 6.8 Hz, 1H, CH-$\alpha_{arginine}$), 6.86 (d, J = 8.5 Hz, 2H, CH_{aryl}), 7.12 (d, J = 8.5 Hz, 2H, CH_{aryl}). MS (ESI) m/z = 351.1 $[M + H]^+$, 176.0 $[M + 2H]^{2+}$.

5.1.3. Solution Phase Synthesis of Peptides KTP-NH$_2$-DL, Me-KTP-NH$_2$-LD, and Me-KTP-NH$_2$. General Procedure for the Coupling Reaction between Tyrosine and Arginine Derivatives. NMM (3 equiv, 30 mmol) was added to a solution of tyrosine derivative (1 equiv, 10 mmol) in DMF (40 mL), and the resulting mixture was stirred at room temperature for 1 h. Then, BOP (1 equiv, 10 mmol) and arginine derivative (1.05 equiv, 10.5 mmol) were added. The resulting reaction mixture was stirred overnight at room temperature. Upon completion of the reaction (HPLC monitoring), the reaction mixture was filtered. The resulting solution was diluted with ethyl acetate (100 mL), washed with saturated sodium bicarbonate (3 × 50 mL), water (100 mL), 1 M aqueous potassium hydrogensulfate (3 × 50 mL), and brine (50 mL). The organic layer was dried over magnesium sulfate, filtered, and concentrated under reduced pressure. The crude material was triturated with *n*-pentane, filtered, washed with *n*-pentane, and dried to obtain the expected peptides which were used in the next step without further purification.

Synthesis of Boc-D-Tyr(Bzl)-Arg-NH$_2$. By the general procedure, Boc-D-Tyr(Bzl)−OH (3.71 g, 10 mmol) and H-D-Arg-NH_2 2HCl (2.58 g, 10 mmol) provided Boc-D-Tyr(Bzl)-Arg-NH_2 (3.15 g, 60%) as a colorless solid. ^{1}H NMR (DMSO-d_6 + a drop D_2O, 400 MHz): δ 1.19−1.28 (m, 2H of the $CH_2CH_2NH_{arginine}$), 1.28 (s, 9H, $(CCH_3)_3$), 1.37−1.43 (m, 1H of the $CH_2CH_{arginine}$), 1.68−1.70 (m, 1H of the $CH_2CH_{arginine}$), 2.68 (dd, J = 13.6 Hz, J' = 9.2 Hz, 1H of the CH_2-$\beta_{tyrosine}$), 2.82 (dd, J = 13.6 Hz, J' = 5.2 Hz, 1H of the CH_2-$\beta_{tyrosine}$), 2.99 ($t_{apparent}$, J = 6.8 Hz, 2H, CH_2-$\beta_{arginine}$), 4.06−4.11 (m, 2H, CH-$\alpha_{tyrosine}$ and CH-$\alpha_{arginine}$), 5.01 (s, 2H, CH_2O), 6.87 (d, J = 8.4 Hz, 2H, CH_{aryl}), 7.00 (d, J = 7.2 Hz, 1H, NH), 7.12 (d, J = 8.4 Hz, 2H, CH_{aryl}), 7.17 (br, 1H, NH), 7.29−7.40 (m, 5H, CH_{aryl}), 8.12 (d, J = 8.0 Hz, 1H, NH). ^{13}C NMR (DMSO-d_6, 100 MHz): δ 24.8 (t), 28.2 (q, 3C), 28.9 (t), 36.3 (t), 40.3 (t), 51.8 (d), 56.3 (d), 69.1 (t), 78.2 (s), 114.3 (d, 2C), 127.6 (d, 2C), 127.7 (d), 128.4 (d, 2C), 130.0 (s), 130.2 (d, 2C), 137.2 (s), 155.6 (s), 156.7 (s), 156.9 (s), 171.8 (s), 173.3 (s). HRMS (ESI) m/z calcd. for $C_{27}H_{39}N_6O_5$ $[M + H]^+$ 527.2976, found 527.3005. HPLC (water/acetonitrile, 0.1% TFA, 2−100%, 17 min): retention time, 7.45 min; 99.9% pure.

Synthesis of Boc-N-Me-Tyr(Bzl)-D-Arg-NH$_2$. By the general procedure, Boc-N-Me-Tyr(Bzl)−OH (3.85 g, 10 mmol) and H-D-Arg-NH_2 2HCl (2.58 g, 10.5 mmol) provided Boc-N-Me-Tyr(Bzl)-D-Arg-NH_2 (4.86 g, 90%) as a colorless solid. ^{1}H NMR (DMSO-d_6, 400 MHz, 110 °C): δ 1.34 (s, 9H, $(CCH_3)_3$), 1.46−1.53 (m, 2H, $CH_2CH_2NH_{arginine}$), 1.55−1.63 (m, 1H of the $CH_2CH_{arginine}$), 1.72−1.81 (m, 1H of the $CH_2CH_{arginine}$), 2.69 (s, 3H, NCH_3), 2.83 (m, 1H of the CH_2-$\beta_{tyrosine}$), 3.10−3.14 (m, 3H, CH_2-$\beta_{arginine}$ and 1H of the CH_2-$\beta_{tyrosine}$), 4.25−4.30 (m, 1H, CH-$\alpha_{arginine}$), 4.69 (dd, J = 10.0 Hz, J' = 5.6 Hz, 1H, CH-$\alpha_{tyrosine}$), 5.05 (s, 2H, CH_2O), 6.83 (br, 4H, NH), 6.90 (d, J = 8.4 Hz, 2H, CH_{aryl}), 7.10 (d, J = 8.4 Hz, 2H, CH_{aryl}), 7.28−7.40 (m, 5H, CH_{aryl}). ^{13}C NMR (DMSO-d_6, 100 MHz, 80 °C): δ 24.5 (t), 27.5 (q, 3C), 28.7 (t), 30.6 (q), 33.2 (t), 40.1 (t), 51.5 (d), 59.7 (d), 69.2 (t), 78.7 (s), 114.4 (d, 2C), 126.9 (d, 2C), 127.1 (d), 127.8 (d, 2C), 129.4 (d, 2C), 129.9 (s), 136.9 (s), 154.6 (s), 156.7 (s), 156.9 (s), 169.7 (s), 172.6 (s). HRMS (ESI) m/z calcd. for $C_{28}H_{41}N_6O_5$ $[M + H]^+$ 541.3133, found 541.3151. HPLC (water/acetonitrile, 0.1% TFA, 2−100%, 17 min): retention time, 7.68 min; 99.9% pure.

Synthesis of Boc-N-Me-Tyr(Bzl)-Arg-NH$_2$. By the general procedure, Boc-N-Me-Tyr(Bzl)−OH (3.85 g, 10 mmol) and H-Arg-NH_2 2HCl (2.58 g, 10.5 mmol) provided Boc-N-Me-Tyr(Bzl)-D-Arg-NH_2 (4.91 g, 91%) as a colorless solid. ^{1}H NMR (DMSO-d_6, 400 MHz, 80 °C): δ 1.32 (s, 9H, $(CCH_3)_3$), 1.46−1.58 (m, 2H, $CH_2CH_2NH_{arginine}$), 1.60−1.64 (m, 1H of the $CH_2CH_{arginine}$), 1.75−1.83 (m, 1H of the $CH_2CH_{arginine}$), 2.70 (s, 3H, NCH_3), 2.85 (dd, J = 14.4 Hz, J' = 10.4 Hz, 1H of the CH_2-$\beta_{tyrosine}$), 3.11−3.17 (m, 4H, CH_2-$\beta_{arginine}$, 1H of the CH_2-$\beta_{tyrosine}$ and CH-$\alpha_{tyrosine}$), 4.25−4.30 (m, 1H, CH-$\alpha_{arginine}$), 5.07 (s, 2H, CH_2O), 6.91 (d, J = 8.6 Hz, 2H, CH_{aryl}), 6.85 (br, 5H, NH), 7.14 (d, J = 8.6 Hz, 2H, CH_{aryl}), 7.30−7.43 (m, 3H, CH_{aryl}), 7.49−7.51 (m, 2H, CH_{aryl}). ^{13}C NMR (DMSO-d_6, 100 MHz, 80 °C): δ 24.6 (t), 27.6 (q, 3C), 28.9 (t), 30.5 (q), 33.0 (t), 40.1 (t), 51.7 (d), 59.5 (d), 69.2 (t), 78.7 (s), 114.4 (d, 2C), 126.9 (d, 2C), 127.2 (d), 127.9 (d, 2C), 129.3 (d, 2C), 129.9 (s), 136.9 (s), 154.6 (s), 156.68 (s), 156.72 (s), 169.8 (s), 172.6 (s). HRMS (ESI) m/z calcd. for $C_{28}H_{41}N_6O_5$ $[M + H]^+$ 541.3133, found 541.3150. HPLC (water/acetonitrile, 0.1% TFA, 2−100%, 17 min): retention time, 7.62 min; 99.9% pure.

General Procedure for the Removal of OBzl and N-Boc Groups. The corresponding protected peptides (1 equiv) were dissolved in 50 mL of EtOH in a 100 mL two-neck round-bottom flask. Pd/C (10 mol %) was added to the solution and the mixture was degassed twice under vacuum (using a water pump) and was replacing each time the vacuum by hydrogen (H_2 balloon). Next, the reaction mixture was permitted to react at room temperature under a hydrogen flow (H_2 balloon). After completion of the reaction (HPLC monitoring), the mixture was filtered through a Celite bed to remove Pd/C, and the filtrate was evaporated in vacuo. The crude product was then dissolved in 50 mL of HCl 4 M in 1,4-dioxane and stirred at room temperature. After completion of the reaction (HPLC monitoring), the resulting precipitate was collected by filtration, washed with 1,4-dioxane (2 × 10

DOI: 10.1021/acschemneuro.6b00099
ACS Chem. Neurosci. 2016, 7, 1130−1140

mL), diethyl ether (2 × 10 mL), and *n*-pentane (2 × 10 mL), and dried in vacuo. The resulting white solid was dissolved in water and lyophylized to afford the corresponding deprotected dipeptides.

Synthesis of KTP-NH_2-DL. By the general procedure, Boc-D-Tyr(Bzl)-Arg-NH_2 (2.89 g, 5.5 mmol) provided H-D-Tyr-Arg-NH_2 (1.31 g, 71%) as a colorless solid. ^{1}H NMR (D_2O, 400 MHz): as described above. ^{13}C NMR (D_2O, 100 MHz): δ 27.2 (t), 30.9 (t), 39.0 (t), 43.3 (t), 56.2 (d), 57.5 (d), 118.7 (d, 2C), 128.6 (s), 133.6 (d, 2C), 158.1 (s), 159.6 (s), 172.3 (s), 178.8 (s). HRMS (ESI) *m*/*z* calcd. for $C_{15}H_{25}N_6O_3$ $[M + H]^+$ 337.1983, found 337.1988. HPLC (water/acetonitrile, 0.1% TFA, 2−100%, 17 min): retention time, 2.36 min; 99.9% pure.

Synthesis of Me-KTP-NH_2-LD. By the general procedure, Boc-N-Me-Tyr(Bzl)-D-Arg-NH_2 (4.32 g, 8.0 mmol) provided N-Me-Tyr-D-Arg-NH_2 (1.71 g, 61%) as a colorless solid. ^{1}H NMR (D_2O, 400 MHz): as describe above. ^{13}C NMR (D_2O, 100 MHz): δ 27.2 (t), 30.8 (t), 34.4 (q), 38.0 (t), 43.3 (t), 56.4 (d), 65.7 (d), 118.7 (d, 2C), 128.2 (s), 133.6 (d, 2C), 158.1 (s), 159.6 (s), 171.1 (s), 178.6 (s). HRMS (ESI) *m*/*z* calcd. for $C_{16}H_{26}N_6NaO_3$ $[M + Na]^+$ 373.1959, found 373.1961; calcd. for $C_{16}H_{27}N_6O_3$ $[M + H]^+$ 351.2139, found 351.2154. HPLC (water/acetonitrile, 0.1% TFA, 2−100%, 17 min): retention time, 2.29 min; 99.0% pure.

Synthesis of Me-KTP-NH_2. By the general procedure, Boc-N-Me-Tyr(Bzl)-Arg-NH_2 (4.32 g, 8.0 mmol) provided N-Me-Tyr-Arg-NH_2 (2.24 g, 81%) as a colorless solid. ^{1}H NMR (D_2O, 400 MHz): as describe above. ^{13}C NMR (D_2O, 100 MHz): δ 27.2 (t), 31.1 (t), 34.6 (q), 38.2 (t), 43.4 (t), 56.1 (d), 65.6 (d), 118.8 (d, 2C), 127.8 (s), 133.7 (d, 2C), 158.1 (s), 159.6 (s), 170.6 (s), 177.5 (s). HRMS (ESI) *m*/*z* calcd. for $C_{16}H_{27}N_6O_3$ $[M + H]^+$ 351.2139, found 351.2139. HPLC (water/acetonitrile, 0.1% TFA, 2−100%, 17 min): retention time, 1.66 min; 99.0% pure.

5.2. Animals. For the sake of the 3R's policy on animal experimentation, a preliminary screening test was performed to reduce the number of compounds to be tested. Given the number of tests and replicates, each drug lead to be withdrawn from the study impacts significantly on the number of animals to be manipulated and sacrificed. Three lead compounds were selected from in vitro determination of the affinity of the compounds to anionic lipid membranes: Me-KTP-NH_2, Me-KTP-NH_2-LD, and KTP-NH_2-DL; Me stands for methylation at the N terminus and D refers to the use of a D-Tyr residue (DL) or a D-Arg residue (LD). Data on KTP-NH_2 was published before[10,15] and used for comparison.

5.2.1. Mice. Male Swiss mice (4−6 weeks old) were obtained from a colony at Butantan Institute, São Paulo, Brazil. Animals were maintained in sterile microisolator cages with sterile rodent feed and acidified water ad libitum, and housed in positive-pressure air-conditioned units (25 °C, 50% relative humidity) on a 12 h light/dark cycle. All procedures were performed in accordance with the guidelines provided by the Brazilian College of Animal Experimentation.

5.2.2. Rats. Adult male Wistar rats (Charles River, L'Arbresle, France), weighing between 210 and 250 g, were housed in groups at temperature and light-controlled conditions (22 ± 2 °C; lights on between 7:00 a.m. and 7:00 p.m.), with free access to food and water. In order to induce habituation to the researcher and to minimize stress, the animals were gently handled daily in the test room and hot-plate device during 4 days prior to nociceptive evaluation. At the day of experiments, animals were brought to the same room for at least 2h before testing. All experiments were performed in accordance with the European Directive 2010/63/EU. The project was approved by the institutional Animal Welfare Body (ORBEA-IMM) and licensed by DGAV (Direcção Geral de Veterinária), the Portuguese competent authority for animal welfare.

5.3. Intravital Microscopy. The dynamics of alterations in the microcirculatory network were determined using IVM, a light microscopy-based approach that enables imaging subcellular structures in live animals. Endothelial cells can actively regulate the migration of leukocytes through the vessel wall by expressing adhesion molecules and chemokines on their luminal surface, allowing leukocytes to adhere and finally migrate into the tissue. The cremaster muscle was used as the principal tissue for analysis of leukocyte−vessel wall interactions because of its thin and transparent nature. IVM was conducted on an upright microscope (Axiolab, Carl Zeiss, Oberkochen, Germany) coupled to a digital camera for image acquisition (AxioCam Icc1, Carl Zeiss, Oberkochen, Germany).

5.3.1. Cremaster Muscle Preparation. Mice were injected ip with a muscle relaxant drug (0.4% xylazine) (Calmiun, Agner União, São Paulo, Brazil) and after 5 min anesthetized with 0.5 g/kg of ketamine (Holliday-Scott SA, Buenos Aires, Argentina) ip. Animals were placed on a 37 °C heating pad, and the microsurgery was performed as described previously.[32] Briefly, the scrotum was opened and the cremaster muscle exteriorized. A longitudinal incision on the muscle allowed its exposure to full access to the microcirculatory network. Postcapillary venules were measured with Axiovision program v 4.8.2.0, and one venule ranging between 25 and 40 μm of diameter in each animal was chosen to count the number of rolling leukocytes.

5.3.2. Leukocyte Recruitment Measurements.[33] After stabilization of the microcirculation, the number of rolling and adherent leukocytes in the postcapillary venules were counted every 10 min, up to 30 min, after peptide topical application. A leukocyte was considered to be adhering to the venular endothelium if it remained stationary for 60 s or longer at a preset distance of 100 μM. A rolling leukocyte was defined as a white cell that moved slower than the stream of flowing erythrocytes. The number of rolling leukocytes was quantified as the number of white cells that passed a fixed preset point during 1 min.

5.3.3. Experimental Protocol for IVM. Initially, cremaster muscles of mice were topically applied with 20 μL of KTP-NH_2-DL, Me-KTP-NH_2, or Me-KTP-NH_2-LD at 48 or 96 μM for visualization of their capacity to induce mobilization of leukocytes along the vessel wall. Sterile phosphate-buffered saline (PBS, pH 7.4) was used as control.

For investigation of the anti-inflammatory effect of KTP-NH_2-DL, mice were pretreated with an ip injection of LPS at 0.05 μg/kg (*E. coli* 055:B5, Sigma) dissolved in sterile saline. At 30 min after ip administration of LPS, cremaster muscles of mice were exposed to a topic application of 20 μL of KTP-NH_2-DL at 96 μM. Negative-control mice were pretreated with ip injection of sterile saline and submitted to topic application of sterile PBS. Positive-control mice were pretreated with ip injection of LPS and submitted to topic application of sterile PBS.

5.4. Evaluation of Thermal Nociceptive Responses in the Hot Plate Test.[29] The hot plate test consisted in evaluation of animal behavioral responses to noxious thermal stimulus, such as hind-paw withdrawal and/or shaking.[34] The hot plate test is frequently elected to evaluate behavioral responses to acute nociceptive stimulation and has the advantage over other acute behavioral tests of depending on central processing and not being a simple spinal reflex.[32] The hot plate test is frequently the only acute behavioral test used to predict the analgesic efficacy of new drugs.[35−38] Based on these reasons and in order to allow comparisons of the results of the present study with our previous reports with KTP derivatives,[10,17] the hot plate test was elected. Animals were placed inside a transparent glass box (20.5 × 10 cm; 20 cm height) on the metallic surface of the hot plate apparatus (IITC Incremental Hot/Cold plate, Series 8/Software, IITC Life San Fernando Valley, CA). The initial temperature was 35.2 °C, and an increasing rate temperature of 9 °C/min was defined (cutoff at 52,5 °C). The temperature to elicit a pain behavior was recorded. A cutoff temperature of 52.5 °C was defined. Animals ($n \geq 5$ per group) were evaluated before Me-KTP-NH_2, Me-KTP-NH_2-LD, KTP-NH_2-DL or saline injection (basal values) and 15, 30, 45, 60, 75, and 90 min after ip injections. The responses are shown as the difference between values at each time point after injection and the respective basal values (at time zero). This is a solid procedure which allows that the response of each animal is analyzed and compared with the respective baseline values along the time.[10,17,39] Data are represented as the group means ± SEM. The significance of differences in each group was analyzed with two-way ANOVA followed by Tukey's post hoc test (subection 5.6).

5.5. Permeation Studies. Permeation studies were performed in a 24-well transwell permeable supports. They were carried out for 18 h and were performed in triplicate. The basal compartment was filled

DOI: 10.1021/acschemneuro.6b00099
ACS Chem. Neurosci. 2016, 7, 1130−1140

with 800 μL of 4-(2-hydroxyethyl)-1-piperazineethanesulfonic acid (HEPES, pH 7.4) buffer and the apical compartment loaded with 200 μL of the drug solution. The apical compartment was placed on top of the base being separated by a filter with or without lipid (sample versus blank filter). The apparatus were then incubated at 25 °C in an orbital shaker at 100 rpm for different time intervals. After incubation, the apparatus was disassembled and the basal and apical solutions were kept at 4 °C until use. Samples were transferred to standard 10 mm path length quartz cuvettes and the fluorescence emission intensity was measured in a spectrofluorimeter (FS920, Edinburgh Instruments, Livingston, UK), at room temperature. The spectroscopic experiments were as described elsewhere.[17] After permeation assays, the samples were diluted to an absorbance bellow 0.1 at the excitation wavelength to minimize inner filter effects.[40] The dose tested was based on a previous study showing that the analgesic dose of KTP-NH_2, 32.3 mg·kg^{-1} = 96 μM, was efficient in all pain models tested.[10] Thus, stock solutions of KTP-NH_2 isomers and KTP were prepared by dissolving in HEPES buffer to a final apical concentration of 1.6 mM.

5.5.1. Relative Permeability Calculation. The fluorescence intensity of the drug at the apical compartment was plotted against time and the slope, m, of the linear part of the curves (approximate steady-state flux rate) at $t = 0$ was calculated for both samples (filter + lipid bilayers stack) and blank filters (i.e., in the absence of lipid). Sample permeability (P_s) and blank permeability (P_b) may be simply calculated according to[11]

$$P_x = m_x \frac{V}{A} \tag{2}$$

where x refers to sample (s) or blank (b), V is the basal volume, and A the area of the filter. Experimentally, the relative permeability (P_R) reads:

$$P_R = \frac{P_s}{P_b} = \frac{m_s}{m_b} \tag{3}$$

P_R was calculated considering the first 10 h, during which it was observed an approximate linear regime for the majority of drugs (Supporting Information).

5.5.2. Preparation of Lipid Barriers. The preparation of the lipid barrier was described elsewhere.[19] Shortly, small unilamellar vesicles (SUVs) of 1-palmitoyl-2-oleoyl-*sn*-glycero-3-phosphocholine (POPC) were prepared. The deposited lipid film was hydrated with HEPES buffer to a final concentration of 5 mM. The lipid was then homogenized by 8 cycles of freeze−thawing and dissolved with HEPES buffer to a final concentration of 1 mM. SUVs were obtained by sonication with a tip sonicator (Vibra cell, Sonics & Material Inc., Danbury, CT) operated in a continuous mode for 15 min with refrigeration, followed by centrifugation (Eppendorf centrifuge) at maximum speed for 30 min to remove titanium particles.

A volume of 100 μL of the vesicular suspension was deposited to each culture insert in the transwells (0.4 μm pore size, 0.33 cm^2 area), and 10 mM of $CaCl_2$ was added to promote the formation of fused vesicles. The inserts were placed into a 24-well culture plate, and centrifuged at 693*g* (2000 rpm) (Multifuge 1L-R, Heraeus, Germany) for 4 min, at room temperature. The inserts were then placed in fresh wells, and 100 μL of the vesicular suspension were again added to the filters followed by centrifugation at the same speed for 10 min. To improve lipid dispersion in the filter area, the plates were rotated 180 °C between centrifugations. The inserts were placed in a new plate and incubated at 50 °C for 25 min. After 5 min at room temperature, 100 μL of the liposomal suspension were added to the filters and centrifuged for 30 min. Few filters did not hold the lipid suspension and were excluded from the experiment.[41] The remaining filters were carefully inverted to discard the supernatant. Thereafter, the filters were freez/thawed at −80 °C for 1 h and 65 °C for 30 min, followed by incubation overnight at 4 °C until permeation studies.

5.6. Statistical Analyses. Data are represented as mean ± SEM. Statistical differences were analyzed by one-way or two-way ANOVA followed by Tukey's post test. Differences were considered significant when $p < 0.05$. $p < 0.01$ and $p < 0.001$ are also mentioned where applicable for the sake of completeness of the results. All statistical analyses were calculated with Prism 6 software (GraphPad Software, version 6.02).

■ ASSOCIATED CONTENT

Supporting Information

The Supporting Information is available free of charge on the ACS Publications website at DOI: 10.1021/acschemneuro.6b00099.

NMR (^{1}H, ^{13}C, COSY dept) and HRMS for all new compounds; HPLC of final compounds; measure of relative permeability in permeation studies (PDF)

■ AUTHOR INFORMATION

Corresponding Authors

*E-mail: katia.conceicao@unifesp.br.

*E-mail: macastanho@medicina.ulisboa.pt.

Author Contributions

K.C. and M.A.R.B.C. contributed equally to this work. J.P. and S.S.S. wrote the initial draft of the manuscript, was was later reviewed by all authors. J.P., S.S.S., I.S., A.P., M.H., and K.C. performed experiments. M.L.-F., E.B. I.T., M.H., K.C., and M.A.R.B.C. designed, supervised, and coordinated different parts of the study.

Funding

FCT-MCTES is acknowledged for PhD fellowship SFRH/BD/52225/2013 to J.P. Marie Skłodowska-Curie Research and Innovation Staff Exchange (RISE) is acknowledged for funding: call H2020-MSCA-RISE-2014, Grant agreement 644167, 2015-2019.

Notes

The authors declare no competing financial interest.

■ ACKNOWLEDGMENTS

The authors thank Dr. Marta Ribeiro for lipid affinity and plasma stability studies and Dr. Ricardo Pinheiro for participation in the chemical syntheses.

■ ABBREVIATIONS USED

BOP, benzotriazole-1-yl-oxy-tris(dimethylamino)-phosphonium hexafluorophosphate; Bzl, benzyl; DIEA, diisopropylethylamine; HBTU, *O*-(benzotriazol-1-yl)-*N*,*N*,*N*′,*N*′-tetramethyluronium hexafluorophosphate; HCl, hydrochloric acid; HEPES, 4-(2-hydroxyethyl)-1-piperazineethanesulfonic acid; HOBt, *N*-hydroxybenzotriazole; IVM, intravital microscopy; KTP, kyotorphin; KTP-NH_2, amidated KTP; LPS, lipopolysaccharide; MD2, myeloid differentiation protein 2; NMM, *N*-methylmorpholine; PEPT2, peptide transporter 2; PLC, phospholipase C; pmc, 2,2,5,7,8-pentamethyl-chroman-6-sulfonyl; P_R, relative permeability; SUVs, small unilamellar vesicles; TIS, triisopropylsilane

■ REFERENCES

(1) Takagi, H., Shiomi, H., Ueda, H., and Amano, H. (1979) A novel analgesic dipeptide from bovine brain is a possible Met-enkephalin releaser. *Nature 282* (5737), 410−412.

(2) Takagi, H., Shiomi, H., Ueda, H., and Amano, H. (1979) Morphine-like analgesia by a new dipeptide, L-tyrosyl-L-arginine (kyotorphin) and its analogue. *Eur. J. Pharmacol. 55* (1), 109−111.

(3) Ueda, H., Tatsumi, K., Shiomi, H., and Takagi, H. (1982) Analgesic dipeptide, kyotorphin (tyr-arg), is highly concentrated in the synaptosomal fraction of the rat brain. *Brain Res. 231* (1), 222−224.

DOI: 10.1021/acschemneuro.6b00099
ACS Chem. Neurosci. 2016, 7, 1130−1140

(4) Shiomi, H., Ueda, H., and Takagi, H. (1981) Isolation and identification of an analgesic opioid dipeptide kyotorphin (tyr-arg) from bovine brain. *Neuropharmacology 20* (7), 633−638.
(5) Chen, P., Bodor, N., Wu, W. M., and Prokai, L. (1998) Strategies to target kyotorphin analogues to the brain. *J. Med. Chem. 41* (20), 3773−3781.
(6) Kawabata, A., Umeda, N., and Takagi, H. (1993) L-arginine exerts a dual role in nociceptive processing in the brain: Involvement of the kyotorphin-Met-enkephalin pathway and NO-cyclic GMP pathway. *Br. J. Pharmacol. 109* (1), 73−79.
(7) Shiomi, H., Kuraishi, Y., Ueda, H., Harada, Y., Amano, H., and Takagi, H. (1981) Mechanism of kyotorphin-induced release of Met-enkephalin from guinea pig striatum and spinal cord. *Brain Res. 221* (1), 161−169.
(8) Kolaeva, S. G., Semenova, T. P., Santalova, I. M., Moshkov, D. A., Anoshkina, I. A., and Golozubova, V. (2000) Effects of L-thyrosyl-L-arginine (kyotorphin) on the behavior of rats and goldfish. *Peptides 21* (9), 1331−1336.
(9) Inoue, M., Nakayamada, H., Tokuyama, S., and Ueda, H. (1997) Peripheral non-opioid analgesic effects of kyotorphin in mice. *Neurosci. Lett. 236* (1), 60−62.
(10) Ribeiro, M. M., Pinto, A., Pinto, M., Heras, M., Martins, I., Correia, A., Bardaji, E., Tavares, I., and Castanho, M. (2011) Inhibition of nociceptive responses after systemic administration of amidated kyotorphin. *Br. J. Pharmacol. 163* (5), 964−973.
(11) Serrano, I., Freire, J., Carvalho, M., Neves, M., Melo, M., and Castanho, M. (2014) The mechanisms and quantification of the selective permeability in transport across biological barriers: The example of kyotorphin. *Mini-Rev. Med. Chem. 14* (2), 99−110.
(12) Santos, S. M., Garcia-Nimo, L., Sa Santos, S., Tavares, I., Cocho, J. A., and Castanho, M. A. (2013) Neuropeptide kyotorphin (tyrosyl-arginine) has decreased levels in the cerebro-spinal fluid of Alzheimer's disease patients: Potential diagnostic and pharmacological implications. *Front. Aging Neurosci. 5*, 68.
(13) Sá Santos, S., Santos, S. M., Pinto, A. R., Ramu, V. G., Heras, M., Bardaji, E., Tavares, I., and Castanho, M. (2016) Amidated and ibuprofen-conjugated kyotorphins promote neuronal rescue and memory recovery in cerebral hypoperfusion dementia model. *Front. Aging Neurosci. 8*, 1.
(14) de la Torre, J. C., and Stefano, G. B. (2000) Evidence that Alzheimer's disease is a microvascular disorder: The role of constitutive nitric oxide. *Brain Res. Rev. 34* (3), 119−136.
(15) Conceição, K., Magalhães, P. R., Campos, S. R., Domingues, M. M., Ramu, V. G., Michalek, M., Bertani, P., Baptista, A. M., Heras, M., Bardaji, E. R., Bechinger, B., Ferreira, M. L., and Castanho, M. A. (2016) The anti-inflammatory action of the analgesic kyotorphin neuropeptide derivatives: Insights of a lipid-mediated mechanism. *Amino Acids 48* (1), 307−318.
(16) Ribeiro, M. M., Santos, S. S., Sousa, D. S., Oliveira, M., Santos, S. M., Heras, M., Bardaji, E., Tavares, I., and Castanho, M. A. (2013) Side-effects of analgesic kyotorphin derivatives: Advantages over clinical opioid drugs. *Amino Acids 45* (1), 171−178.
(17) Ribeiro, M. M., Pinto, A. R., Domingues, M. M., Serrano, I., Heras, M., Bardaji, E. R., Tavares, I., and Castanho, M. A. (2011) Chemical conjugation of the neuropeptide kyotorphin and ibuprofen enhances brain targeting and analgesia. *Mol. Pharmaceutics 8* (5), 1929−1940.
(18) Ribeiro, M. M., Domingues, M. M., Freire, J. M., Santos, N. C., and Castanho, M. A. (2012) Translocating the blood-brain barrier using electrostatics. *Front. Cell. Neurosci. 6*, 44.
(19) Serrano, I. D., Ramu, V. G., Pinto, A. R., Freire, J. M., Tavares, I., Heras, M., Bardaji, E. R., and Castanho, M. A. (2015) Correlation between membrane translocation and analgesic efficacy in kyotorphin derivatives. *Biopolymers 104* (1), 1−10.
(20) Ramage, R., Green, J., and Blake, A. J. (1991) An acid labile arginine derivative for peptide synthesis: NG-2,2,5,7,8-pentamethyl-chroman-6-sulphonyl-l-arginine. *Tetrahedron 47*, 6353−6370.
(21) Fischer, P. M., Retson, K. V., Tyler, M. I., and Howden, M. E. (1992) Application of arylsulphonyl side-chain protected arginines in solid-phase peptide synthesis based on 9-fluorenylmethoxycarbonyl amino protecting strategy. *Int. J. Pept. Protein Res. 40* (1), 19−24.
(22) Albericio, F., Kneib-Cordonier, N., Biancalana, S., Gera, L., Masada, R. I., Hudson, D., and Barany, G. (1990) Preparation and application of the 5-(4-(9-fluorenylmethyloxycarbonyl)aminomethyl-3,5-dimethoxyphenoxy)-valeric acid (PAL) handle for the solid-phase synthesis of C-terminal peptide amides under mild conditions. *J. Org. Chem. 55* (12), 3730−3743.
(23) Solé, N. A., and Barany, G. (1992) Optimization of solid-phase synthesis of [Ala8]-dynorphin-A. *J. Org. Chem. 57* (20), 5399−5403.
(24) Ribeiro, M., Melo, M. N., Serrano, I. D., Santos, N. C., and Castanho, M. A. R. B. (2010) Drug-lipid interaction evaluation: why a 19th century solution? *Trends Pharmacol. Sci. 31*, 449−454.
(25) Atherton, A., and Born, G. V. R. (1972) Quantitative investigations of the adhesiveness of circulating polymorphonuclear leucocytes to blood vessel walls. *J. Physiol. 222* (2), 447−474.
(26) Masedunskas, A., Milberg, O., Porat-Shliom, N., Sramkova, M., Wigand, T., Amornphimoltham, P., and Weigert, R. (2012) Intravital microscopy: A practical guide on imaging intracellular structures in live animals. *Bioarchitecture 2* (5), 143−157.
(27) Weigert, R., Porat-Shliom, N., and Amornphimoltham, P. (2013) Imaging cell biology in live animals: Ready for prime time. *J. Cell Biol. 201* (7), 969−979.
(28) Gavins, F. N. (2012) Intravital microscopy: New insights into cellular interactions. *Curr. Opin. Pharmacol. 12* (5), 601−607.
(29) Le Bars, D., Gozariu, M., and Cadden, S. W. (2001) Animal models of nociception. *Pharmacol. Rev. 53* (4), 597−652.
(30) Ueda, H., Yoshihara, Y., Misawa, H., Fukushima, N., Katada, T., Ui, M., Takagi, H., and Satoh, M. (1989) The kyotorphin (tyrosine-arginine) receptor and a selective reconstitution with purified Gi, measured with GTPase and phospholipase C assays. *J. Biol. Chem. 264* (7), 3732−3741.
(31) Vergnolle, N. (2009) Protease-activated receptors as drug targets in inflammation and pain. *Pharmacol. Ther. 123* (3), 292−309.
(32) Lopes-Ferreira, M., Moura-da-Silva, A. M., Piran-Soares, A. A., Angulo, Y., Lomonte, B., Gutierrez, J. M., and Farsky, S. H. (2002) Hemostatic effects induced by thalassophryne nattereri fish venom: A model of endothelium-mediated blood flow impairment. *Toxicon 40* (8), 1141−147.
(33) Sperandio, M., Pickard, J., Unnikrishnan, S., Acton, S. T., and Ley, K. (2006) Analysis of leukocyte rolling in vivo and in vitro. *Methods Enzymol. 416*, 346−371.
(34) Carter, R. B. (1991) Differentiating analgesic and non-analgesic drug activities on rat hot plate: Effect of behavioral endpoint. *Pain 47* (2), 211−220.
(35) Craft, R. M., Ulibarri, C., Leitl, M. D., and Sumner, J. E. (2008) Dose- and time-dependent estradiol modulation of morphine antinociception in adult female rats. *Eur. J. Pain. 12* (4), 472−479.
(36) Kline, R. H. t., and Wiley, R. G. (2008) Spinal mu-opioid receptor-expressing dorsal horn neurons: Role in nociception and morphine antinociception. *J. Neurosci. 28* (4), 904−913.
(37) Li, X., Shi, X., Liang, D. Y., and Clark, J. D. (2005) Spinal CK2 regulates nociceptive signaling in models of inflammatory pain. *Pain 115* (1−2), 182−190.
(38) Ruskin, D. N., Kawamura, M., and Masino, S. A. (2009) Reduced pain and inflammation in juvenile and adult rats fed a ketogenic diet. *PLoS One 4* (12), e8349.
(39) Martins, I., Pinto, M., Wilson, S. P., Lima, D., and Tavares, I. (2008) Dynamic of migration of HSV-1 from a medullary pronociceptive centre: Antinociception by overexpression of the preproenkephalin transgene. *Eur. J. Neurosci. 28* (10), 2075−2083.
(40) Lakowicz, J. R. (1999) *Principles of fluorescence spectroscopy*, Kluwer Academic/Plenum Publishers, New York.
(41) Flaten, G. E., Dhanikula, A. B., Luthman, K., and Brandl, M. (2006) Drug permeability across a phospholipid vesicle based barrier: A novel approach for studying passive diffusion. *Eur. J. Pharm. Sci. 27* (1), 80−90.

DOI: 10.1021/acschemneuro.6b00099
ACS Chem. Neurosci. 2016, 7, 1130−1140

Section 3

Mechanism of Action

ARTICLE 3

Neuropeptide kyotorphin impacts on lipopolysaccharide-induced glucocorticoid-mediated anti-inflammatory response. A molecular link to nociception, neuroprotection, and anti-inflammatory action

ACS Chemical Neuroscience, 2017

I declare that the experimental design, data collection, data analysis and discussion were carried on by me under supervision of Prof. Miguel A.R.B. Castanho. I have not participated in peptide synthesis. The manuscript was written by me under guidance of my supervisor Prof. Miguel A.R.B. Castanho.

Article 2 demonstrated the endothelium-mediated action of the analogues of KTP. The methylated derivatives presented a prolonged analgesic effect, but they have a pro-inflammatory action; KTP-NH_2-DL was anti-inflammatory, but did not show a relevant analgesic activity. Despite KTP-NH_2 analogues were more stable in human serum, KTP-NH_2 was the only one that gathered analgesic and anti-inflammatory activities simultaneously. Therefore, we selected KTP-NH_2 to study further. The aim of the following paper was to shed light on the analgesic and anti-inflammatory mechanism of action of KTP-NH_2 and to find the molecular link that might explain these effects.

KTP-NH_2 differs from KTP by substitution of the carboxylic acid for an amide. It is known that KTP has a naloxone-reversible analgesic effect 4.2 times more potent than met-enkephalins when administered directly into the brain (Takagi et al. 1979) but does not bind to opioid receptors (Takagi et al. 1979; Rackham et al. 1982; Ribeiro et al. 2011). Although the mechanism of action of KTP is not completely understood and some data are controversial, it is believed that KTP has the ability to induce the release of a particular type of opioid peptides, met-enkephalins, and stabilize their effect by inhibiting enkephalinases (Takagi et al. 1979; Shiomi et al. 1981; Janicki and Lipkowski 1983; Hazato et al. 1986). Based on that, we raised the hypothesis that KTP-NH_2 might also act as inhibitor of enkephalinases.

Searching through the literature at least eight different human enkephalinases (Table 1) are identified, most of them present in the brain. In this work, we tested the ability of KTP-NH_2 to inhibit two enkephalinases, dypeptidyl-peptidase III (DPP3, EC 3.4.14.4) and angiotensin converting enzyme (ACE, EC 3.4.15.1) using fluorimetric and colorimetric enzyme assay kits, respectively. The peptide did not inhibit any of them up to 100 μmol/L. Still, we cannot totally exclude the possibility that the peptide may inhibit some of the untested enkephalinases.

Table 1. Compilation of the information about the enzymes that have the ability to degrade enkephalins. The information below was compiled from http://www.sigmaaldrich.com/technical-documents/articles/biology/rbi-handbook/peptide-receptors-and-peptide-metabolism/neuropeptidases.html and the databases IUBMB, BRENDA, EXPASY, MEROPS, Wikigenes and NCBI. Abbreviations: AI – Angiotensin I, AII – Angiotensin II, AIII – Angiotensin III, ANP – atrial natriuretic peptide, BK – bradykinin, CCK – cholecystokinin, EDTA – ethylenediaminetetraacetic acid, EGTA – ethylene glycol-bis(2-aminoethylether)-N,N,N',N'-tetraacetic acid, ET-1 – endothelin-1, ET-2 – endothelin-2, ET-3 – endothelin-3, GEMSA – guanidinoethylmercaptosuccinic acid, LTA4 – leukotriene A_4 hydrolase, MGTA – 2-mercaptomethyl-3-guanidinoethylthiopropanoic acid, NKA – neurokinin A, NKB – neurokinin B, NT – neurotensin, PC18 – 2-amino4-methylsulfonyl butane thiol, SP – substance P, SS – somatostatin.

	Membrane alanyl aminopeptidase EC 3.4.11.2	**Aminopeptidase B EC 3.4.11.6**	**Dipeptidyl-peptidase III EC 3.4.14.4**	**Peptidyl-dipeptidase A EC 3.4.15.1**	**Carboxyopeptidase A6 (Not yet included in IUBMB recommendations)**	**Lysine carboxypeptidase EC 3.4.17.3**	**Carboxypeptidase E EC 3.4.17.10**	**Neprilysin EC 3.4.24.11**
Alternative names	Amino-oligopeptidase, aminopeptidase M, aminopeptidase N, membrane alanine aminopeptidase, membrane aminopeptidase I, microsomal aminopeptidase, particle-bound aminopeptidase, peptidase E, CD13	Arylamidase II, arginine aminopeptidase, arginyl aminopeptidase, cytosol aminopeptidase IV, Cl^--activated arginine aminopeptidase	Dipeptidyl aminopeptidase III, dipeptidyl arylamidase III, enkephalinase B, red cell angiotensinase	Angiotensin-converting enzyme, kininase II, dipeptidyl carboxypeptidase I, peptidyl dipeptidase I, peptidyl-dipeptide hydrolase	CPA6	Carboxypeptidase N, arginine carboxypeptidase, kininase I, bradykinase, hyppuryllysine hydrolase, creatine kinase convertion fator, plasma carboxypeptidase B, Anaphylatoxin inactivator	Carboxypeptidase H, enkephalin convertase, membrane-bound carboxypeptidase, enkephalin-precursor endopeptidase, insulin-granule-associated carboxypeptidase	Endopeptidase-24.11, neutral endopeptidase, enkephalinase, CALLA (common acute lymphoblastic leukemia-associated) antigens, CD10, membrane metalloendopeptidase, neutral metalloendopeptidase
Typical substrates *in vitro*	Leu-enkephalin, Met-enkephalin, γ and β-endorphin, AIII	Leu-enkephalin, Met-enkephalin, BK, LTA4, SS	AII, AIII, Leu-enkephalin, prolactin, alpha-melanocyte-stimulating hormone	AI, BK, CCK, NT, bradykinin, Leu-enkephalin, Met-enkephalin, SP, gastrin	Leu-enkephalin, Met-enkephalin, AI, NT	Enkephalin hexapeptides, dynorphin, BK, Atriopeptin II	Enkephalin hexapeptides, dynorphin, BK, atriopeptin II	Leu-enkephalin, Met-enkephalin, ANP, ET-1, ET-2, ET-3, CCK, NT, SS, SP, NKA, NKB, amyloid β-peptide

Table continued…

	Membrane alanyl aminopeptidase EC 3.4.11.2	Aminopeptidase B EC 3.4.11.6	Dipeptidyl-peptidase III EC 3.4.14.4	Peptidyl-dipeptidase A EC 3.4.15.1	Carboxyopeptidase A6 (Not yet included in IUBMB recommendations)	Lysine carboxypeptidase EC 3.4.17.3	Carboxypeptidase E EC 3.4.17.10	Neprilysin EC 3.4.24.11
Typical inhibitors	Amastatin, bestatin, actinonin, PC18	Arphamenine A, arphamenine B, bestatin, lysine thiol	1,10-phenanthroline, EDTA, EGTA, dithiothreitol, 2-mercaptoethanol, fluostatins A and B, probestin, puromycin,	Captopril, lisinopril, enalaprilat	Potato carboxypeptidase inhibitor, benzylsuccinic acid	MGTA	GEMSA, MGTA, 1,10-phenanthroline	Phosphoramidon, thiorphan
Subcellular localization	Plasma membrane	Soluble, secreted, Golgi	Soluble, cytosolic	Plasma membrane, soluble (plasma)	Extracellular matrix	Soluble	Membrane, secretory vesicles	Plasma membrane
Tissue distribution	Abundant in kidney, intestine liver placenta, brain, lung, hematopoietic (myeloid) cells, vascular and endothelial cells	Widely distributed in kidney, intestine, lung, heart, brain, pituitary, pancreas, testis	Uterine tissues, prostate, brain, tongue, tumor tissue, lung, testis, pancreas, eye, blood	kidney, intestine, lung, testis, brain, endothelial cells, blood	Olfactory bulb, embryonic brain	Liver, blood, stomach, kidney, lung	Brain, pituitary, pancreas, neuroendocrine tissues	Kidney, intestine, lung, reproductive tissue, brain
Physiological effects	Pain regulation, T-cell development, angiogenesis, viral receptor (coronavirus 229E), glutathione metabolism	Inflammation	Pain	Cardiovascular regulation, fertility, water and salt balance, hematopoietic stem cell proliferation	food digestion, biosynthesis of neuroendocrine peptides	Protection against anaphylaxis	Neuroendocrine physiology, pancreatic physiology, muscle strength/co-ordination	Blood pressure, pain regulation, anti-inflammatory, antidiarrhoeic
Disease relevance	Cancer metastasis	Inflammatory disorders	Endometrial and ovarian cancers	Hypertension, congestive heart failure, diabetes, nephropathy, renal insufficiency	Duane syndrome	Angioedema	Obesity, diabetes, anxiety, depression	Cardiovascular, prostate cancer, Alzheimer's disease, hypertension, renal disease

The second part of this study intended to explore the anti-inflammatory mechanism of KTP-NH_2 and to find a molecular link that could explain the multiple biological activities of the peptide, such as anti-inflammatory, analgesic and neuroprotective activities. We worked with a murine model of inflammation induced by lipopolysaccharide (LPS) and by CXCL-1 to show that KTP-NH_2 has a very fast (10 minutes) and therefore nongenomic anti-inflammatory mechanism that probably blocks the activation/expression of adhesion molecules on the endothelium. We used an IVM approach combined with pharmacological inhibitors to demonstrate that KTP-NH_2 has dual action: a glucocorticoid (GC)-mediated action, which is dominant in full-fledged inflammation models, and a GC-independent mechanism, which is predominant in models in which leukocyte rolling is stimulated but inflammation is not totally developed. Overall, the results show that GCs might be the molecular link that explains the multiple biological activities of KTP-NH_2.

ACS Chemical Neuroscience

Letter

pubs.acs.org/chemneuro

Neuropeptide Kyotorphin Impacts on Lipopolysaccharide-Induced Glucocorticoid-Mediated Inflammatory Response. A Molecular Link to Nociception, Neuroprotection, and Anti-Inflammatory Action

Juliana Perazzo,[†] Carla Lima,[‡] Montserrat Heras,[§] Eduard Bardají,[§] Mônica Lopes-Ferreira,*[,‡] and Miguel Castanho*[,†]

[†]Faculdade de Medicina da Universidade de Lisboa, Instituto de Medicina Molecular, Av. Professor Egas Moniz, 1649-028 Lisboa, Portugal

[‡]Unidade de Imunorregulação, Laboratório Especial de Toxinologia Aplicada, Instituto Butantan, Av. Vital Brasil 1500, 05503-900 São Paulo, Brazil

[§]Laboratori d'Innovació en processos i Productes de Síntesi Orgànica (LIPPSO), Department de Química, Universitat de Girona, Maria Aurelia Capmany 69, 17003 Girona, Spain

ABSTRACT: Neuropeptide kyotorphin (KTP) is a potent analgesic if administered directly into the brain. In contrast, KTP-amide (KTP-NH_2) is analgesic, neuroprotective, and anti-inflammatory following systemic administration, albeit its mechanism of action is unknown. The aim of this study was to shed light on the mechanism of action of KTP-NH_2 at the molecular level. KTP-NH_2 does not inhibit the enkephalinases angiotensin-converting-enzyme and dipeptidyl-peptidase 3. Intravital microscopy showed that KTP-NH_2 decreased the number of rolling leukocytes in a mouse model of inflammation induced by lipopolysaccharide (LPS). Pretreatment with metyrapone abrogated the action of KTP-NH_2. Interestingly, stimulating rolling leukocytes using CXCL-1 is also counteracted by the KTP-NH_2, but this effect is not abrogated by metyrapone. We conclude that KTP-NH_2 has dual action: a glucocorticoid-mediated action, which is dominant in the full-fledged LPS-induced inflammation model, and a glucocorticoid-independent mechanism, which is predominant in models in which leukocyte rolling is stimulated but inflammation is not totally developed.

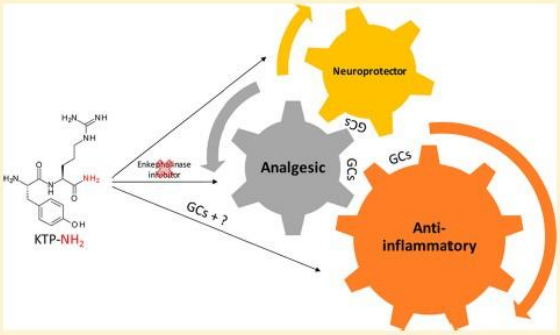

KEYWORDS: *Kyotorphin, kyotorphin-amide, intravital microscopy, glucocorticoids, mechanism of action, anti-inflammatory*

The dipeptide tyrosil-arginine (Tyr-Arg) was discovered in 1979 in Kyoto and because of its similar properties to morphine was named kyotorphin (KTP).[1,2] When injected directly into the brain, KTP induces the release of met-enkephalins, promoting a potent analgesia, up to 4.2-fold more than endogenous opioids.[1] It was also suggested that KTP is an inhibitor of enkephalinases, which would explain its analgesic properties.[1,3] However, KTP is not efficient after peripheral administration, probably due to its inability to cross the blood-brain barrier (BBB).[4] In order to overcome this limitation, biologically active KTP analogues have been developed to facilitate BBB crossing.[4−7] KTP-amide (KTP-NH_2) was designed to cause minimal changes in the chemical structure of the natural dipeptide.[5] Amidation of KTP increases the formal net charge of the peptide from +1 to +2 in physiological conditions and is also expected to increase the half-life of the peptide in vivo. We have shown that KTP-NH_2 is analgesic after systemic administration,[5] even though in vitro studies predict a low permeability across lipid membranes.[7] It has been suggested that a peptide transporter, such as PEPT2, might be responsible to translocate KTP-NH_2 into the brain.[7,8] In addition to analgesic activity, neuroprotective,[9] anti-inflammatory,[10] and antimicrobial[11] properties can be added to the list of biological effects of KTP-NH_2.

In contrast with the abundant data on the biological effects of KTP-NH_2, its mechanism of action is still poorly understood. Because the anti-inflammatory action may be the key to link analgesia and neuroprotection, in this work we attempted to unravel the anti-inflammatory mechanism of action at the molecular level. In addition, we tested the hypothesis that KTP-NH_2 could act as an inhibitor of the enkephalinases angiotensin-converting enzyme (ACE, EC 3.4.15.1) and dipeptidyl-peptidase III (DPP3, EC 3.4.14.4).

Received: January 7, 2017
Accepted: May 4, 2017
Published: May 4, 2017

DOI: 10.1021/acschemneuro.7b00007
ACS Chem. Neurosci. 2017, 8, 1663−1667

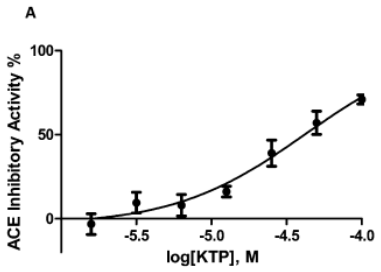

	ACE	DPP3
KTP	-4.37±0.44	> -4.00
KTP-NH_2	> -4.00	> -4.00

Figure 1. KTP modestly inhibits ACE, but not DPP3. KTP-NH_2 does not inhibit neither ACE or DPP3. (A) ACE inhibitory activity vs Log(molar KTP). Data are represented as mean ± standard error of the mean (SEM). (B) The table summarizes log(molar concentration) values of KTP and KTP-NH_2 for the enkephalinases ACE (EC 3.4.15.1) and DPP3 (EC 3.4.14.4) at IC_{50}. Triplicate tests were performed for each sample.

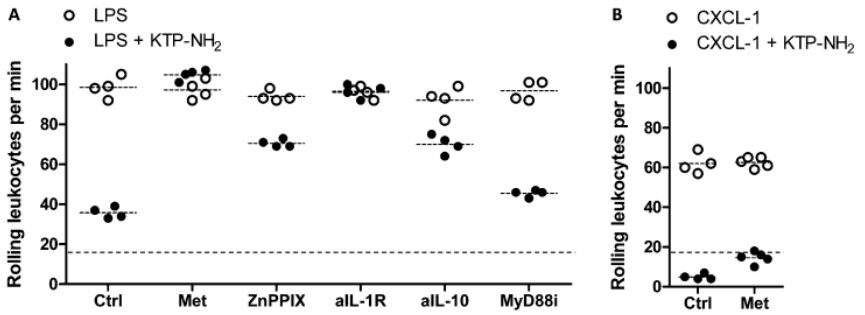

Figure 2. KTP-NH_2 anti-inflammatory mechanism depends on GC synthesis to decrease leukocyte rolling in a murine model of inflammation induced with LPS, but not with CXCL-1. (A) Swiss male mice were injected with LPS ip at 1 mg/kg; after 1 h animals were anesthetized and cremaster muscle was exposed to topical application of 30 μL of KTP-NH_2 96 μM. The number of rolling leukocytes per min was counted before (open circles) and 10 min after KTP-NH_2 application (closed circles). (B) Swiss male mice were injected with 50 μL of CXCL-1 intrascrotal at 0.05 μg/mL and concomitantly anesthetized via ip. Deeply anesthetized animals underwent surgery to allow the exposure of the cremaster muscle. The number of rolling leukocytes was counted before (open circles) and 10 min after (closed circles) the topical application of 30 μL of KTP-NH_2 96 μM. Drugs doses and routes of administration are summarized in Table 1. Dashed line represents the average number of rolling leukocytes over time after saline ip injection (baseline). Four animals were used in each group (one per data point).

RESULTS AND DISCUSSION

Action on Enkephalinases. The biological effect of KTP-NH_2 has been studied and established but its mechanism of action remains elusive. Moreover, since this peptide is multifunctional, the mechanism of action may reveal key relationships between pain, neuroprotection and endothelium-related anti-inflammatory action.

It has been previously suggested that KTP might inhibit enkephalinases,[1,3] therefore increasing the half-life of enkephalins and consequently inducing prolonged analgesia. We tested the hypothesis that KTP analogue, KTP-NH_2, could act as an enkephalinase inhibitor.

While KTP modestly inhibited ACE (IC_{50} = 41.5 μmol/L), in accordance with other authors,[12] KTP-NH_2 did not inhibit ACE or DPP3 up to 100 μmol/L (Figure 1B). A well-known inhibitor of ACE, lisinopril, was tested as a positive control and presented an IC_{50} = 1.68 nmol/L. Regarding inhibition of DPP3 activity, we were unable to calculate IC_{50} values for both KTP and KTP-NH_2 since for the maximal concentration tested, 100 μmol/L (Figure 1B), the peptides presented an inhibitory activity of approximately 30% and 18%, respectively (data not shown).

In 1986, Hazato and co-workers[3] reported that KTP inhibits DPP with IC_{50} = 18 μmol/L, which contrasts with data in Figure 1. They used enkephalinases isolated from monkey brain while in the present study, we used human recombinant DPP3 provided with the fluorogenic DPP3 assay kit.

Data in Figure 1 does not rule out completely the hypothesis that KTP-NH_2 might act as an inhibitor of untested enkephalinases, such as neprilysin (EC 3.4.24.11), aminopeptidase N (EC 3.4.11.2), aminopeptidase B (EC 3.4.11.6), carboxypeptidase H (EC 3.4.17.10), carboxypeptidase N (EC 3.4.17.3) and carboxypeptidase A6 (EC 3.4.17.1), but demonstrates that KTP-NH_2 is not an inhibitor of the standard reference enkephalinases ACE and DPP3, which are usual models consecrated in the literature.

KTP-NH_2 Triggers a Nongenomic GC-Dependent Anti-Inflammatory Mechanism. Subsequently, we used pharmacological interventions to explore KTP-NH_2 anti-inflammatory mechanisms through intravital microscopy (IVM). In control group, lipopolysaccharide (LPS) increased from 19 ± 1 to 99 ± 5 the number of rolling leukocytes compared to baseline (Figure 2A, dashed line vs ctrl group, open circles) and treatment with KTP-NH_2 decreased that number to 36 ± 3, which is about 3 fold less (Figure 2A, ctrl group, closed circles).

It has been previously shown that KTP-NH_2 decreases rolling and adhesion of leukocytes in a murine model of LPS-induced inflammation.[10] Isothermal titration calorimetry studies showed that KTP-NH_2 can bind to LPS,[10] probably hampering its binding to toll-like receptor 4 (TLR4) and jeopardizing signal transduction that triggers leukocyte rolling and recruitment to peripheral tissues. In this study, we demonstrated that KTP-NH_2 decreases leukocyte rolling not only in a mouse model of inflammation induced with LPS, but also induced with CXCL-1 (Figure 2B). This finding suggests

DOI: 10.1021/acschemneuro.7b00007
ACS Chem. Neurosci. 2017, 8, 1663−1667

Table 1. Summary of Experimental Protocol and Action of Drugs in Figure 2

model(s)	group	drug	dose and route of administration[a]	action
LPS and CXCL-1	Met	metyrapone	4.5 mg/kg ip	blocks cortisol synthesis by inhibiting reversibly 11-β-hydroxylase
LPS	ZnPPIX	zinc protoporphyrin IX	9 mg/kg ip	competitive inhibitor of heme-oxygenase-1 (HO-1)
LPS	aIL-1R	Rat antimouse CD121a antibody	0.1 mg/kg ip	binds to type I IL-1 receptor (IL-1R) blocking the binding of IL-1α, IL-1β, and IL-1Ra
LPS	aIL-10	monoclonal rat IgG_1 clone antimouse IL-10 antibody	0.25 mg/kg ip	blocks IL-10
LPS	MyD88i	Pepinh-MYD	0.4 mg/kg intrascrotal	blocks MyD88 signaling by inhibiting its homodimerization through binding

[a]See detailed information in Methods.

that KTP-NH_2 anti-inflammatory mechanism is not primarily dependent on its interaction with LPS neither with the TLR4 signaling pathway since the inhibitor MyD88 ($MyD88_i$) had a minor effect in the action of KTP-NH_2 (46 ± 2 vs 36 ± 3) (Figure 2A, $MyD88_i$ group, closed circles vs ctrl group, closed circles). It is reasonable to hypothesize that KTP-NH_2 decreases the expression and/or activation of adhesion molecules, such as selectins and integrins, either on endothelial surface or on neutrophil surface, therefore impairing rolling and adhesion of leukocytes to the endothelium.

Pretreatment with an inhibitor of glucocorticoid (GC) synthesis, metyrapone (Met), inhibited completely the ability of KTP-NH_2 to decrease leukocyte rolling induced by LPS (105 ± 3 vs 97 ± 5) (Figure 2A, Met group, closed vs open circles), suggesting the peptide is dependent on GCs to decrease inflammation. Although not totally consensual,[13] some studies associate the expression of endogenous GCs and administration of exogenous GCs to a decrease of adhesion molecules on the endothelium.[14,15] Leech and co-workers have demonstrated that endogenous GCs modulate P-selectin expression in the early phase of carrageenan arthritis.[15] After an inflammatory stimulus, the endothelium can rapidly express P-selectin, which is stored into Weibel-Palade bodies,[16] therefore being a possible target for KTP-NH_2 and other KTP derivatives, which have a very rapid effect (10 min). In addition, it is well established that endothelial activation by IL-1, among other pro-inflammatory cytokines, impacts in the adhesive properties of the endothelium.[17] Pretreatment with an inhibitor of IL-1R completely abrogated the effect of the topic treatment with KTP-NH_2 (97 ± 3 vs 96 ± 3) (Figure 2A, aIL-1R group, closed circles vs open circles) further reinforcing the hypothesis that the peptide interferes with adhesion through a nongenomic mechanism.

KTP-NH_2 reduced by 1.3-fold the number of rolling leukocytes in zinc protoporphyrin (ZnPPIX) (from 94 ± 3 to 71 ± 2) and anti-interleukin-10 (aIL-10) groups (92 ± 7 vs 70 ± 5) (Figure 2A, ZnPPIX and aIL-10 groups, from open to closed circles and aIL-10, open vs closed circles). However, after treatment, the total number of rolling leukocytes in ZnPPIX and aIL-10 groups are twice as much as the ctrl group (Figure 2A, ZnPPIX and aIL-10 groups, closed circles vs ctrl group, closed circles). These data suggest a partial requirement of heme-oxygenase-1 (HO-1) and IL-10 to enhance anti-inflammatory response. The expression of endogenous GCs in response to a stimulus correlates with an increase of IL-10[18] and in turn, IL-10 induces the production of HO-1.[19] These correlations might explain the putative role of HO-1 and IL-10 in the anti-inflammatory mechanism of KTP-NH_2.

3. A Multitarget Mechanism. The neutrophil chemotactic factor, CXCL-1, administered via intrascrotal increased from 19 ± 1 to 62 ± 5 the number of rolling leukocytes compared to baseline (Figure 2B, dashed line vs ctrl group, open circles). Treatment with KTP-NH_2 decreased the rolling to 5 ± 1 (Figure 2B, ctrl group, closed circles), which is approximately 12-fold less compared to the rolling before treatment (Figure 2B, ctrl group, open circles) and 4 fold less compared to baseline (Figure 2B, dashed line). This action is not reverted by metyrapone, showing that in this case leukocyte adhesion modulation by KTP-NH_2 is not mediated by GCs.

While CXCL-1 induces leukocyte rolling, it should be emphasized that it does not elicit a full scale multivariate inflammatory process. LPS triggers inflammation, activating the HPA axis, which leads to glucocorticoid production. GCs modulate immune and inflammatory responses. KTP-NH_2 is able to translocate the BBB thus being able to reach the HPA axis. Being a multifunctional neuropeptide is thus likely that KTP-NH_2 targets the HPA axis in the central nervous system, relative to targeting GC production directly in adrenal glands.

■ CONCLUSION

We have demonstrated that GCs play an important role in the anti-inflammatory mechanism of action in a mouse model of inflammation induced with LPS, but KTP-NH_2 is multifunctional as the peptide was able to decrease leukocyte rolling induced by CXCL-1 even in animals that were unable to produce GCs. Thus, we conclude that KTP-NH_2 has dual action: a nongenomic GC-mediated action, which is dominant in full-fledged inflammation models, and a nongenomic GC-independent mechanism, which is predominant in models in which leukocyte rolling is stimulated but inflammatory stress is not totally developed.

The endothelium is the common player between analgesic, anti-inflammatory and neuroprotective properties of KTP-NH_2. There is increasing evidence that Alzheimer's disease is a vascular disease with neurodegenerative consequences rather than a neurodegenerative disorder with vascular consequences. On the other hand, pain and inflammation are distinct physiological processes, but they are frequently associated. There is a clear overlapping between the pain system modulated by GCs and the pain system modulated by opioids.[20] Kesmati and co-workers demonstrated that inhibition of GC receptor prevents the analgesic action of morphine and GCs have naloxone-reversible analgesic effects.[20] It is known that KTP-NH_2 does not bind directly to opioid receptors, but its analgesic activity is reversed by naloxone, an antagonist of opioids.[5]

DOI: 10.1021/acschemneuro.7b00007
ACS Chem. Neurosci. 2017, 8, 1663−1667

In conclusion, GCs explain partially the anti-inflammatory action of KTP-NH_2 and it might be the molecular link between the analgesic, neuroprotective and anti-inflammatory activities of the peptide, which has remained elusive for decades.

METHODS

Peptide Synthesis. The hydrochloride salt of KTP and KTP-NH_2 was synthesized in solution chemistry, at gram scale, as previously described.[5]

Enkephalinases Inhibitory Activity. ACE inhibitory activity was determined using an ACE kit-WST (Dojindo Laboratories). The assay was carried out according to the manufacturer's instructions. Absorbances of the reactions were measured using a multimode microplate reader (Tecan, Infinity M200) at 450 nm. The ACE inhibitory activity of the samples was calculated using eq 1.

$$\text{ACE inhibitory activity (\%)} = \frac{A_{\text{blank1}} - A_{\text{sample}}}{A_{\text{blank1}} - A_{\text{blank2}}} \times 100 \quad (1)$$

where A_{blank1} is absorbance of the solution containing enzyme and substrate (positive control), A_{blank2} is absorbance of the solution containing substrate (reagent blank), and A_{sample} is absorbance of the solution containing enzyme, substrate and test inhibitor.

DPP3 inhibitory activity was determined using a fluorogenic DPP3 assay kit (BPS Bioscience). The assay was carried out according to the manufacturer's instructions. Samples were read in a multimode microplate reader (Tecan, Infinity M200). The excitation and emission wavelengths used were 365 and 450 nm, respectively. The DPP3 inhibitory activity of the samples was calculated using eq 2.

$$\text{DPP3 inhibitory activity (\%)} = \frac{F_{\text{E+S}} - F_{\text{A}}}{F_{\text{E+S}} - F_{\text{S}}} \times 100 \quad (2)$$

where $F_{\text{E+S}}$ is fluorescence intensity of the sample containing enzyme and substrate, F_{A} is fluorescence intensity of the sample containing enzyme, substrate, and peptide (test inhibitor), and F_{S} is fluorescence intensity of the sample containing substrate and peptide (test inhibitor).

Data in dose−response curves (activity vs log([inhibitor])) were fitted using eq 3. A is inhibitory activity obtained using eqs 1 or 2, m is the extrapolated minimal value of activity, M is the extrapolated maximal value of activity, and IC_{50} is the concentration of the inhibitor corresponding to half-height inhibitory action $[(M - m)/2]$. m is expected to be statistically nil, and M is expected to be statistically equivalent to 100%. IC_{50} values were calculated with GraphPad Prism 5.01 software.

$$A = m + \frac{M - m}{1 + 10^{\log IC_{50} - \log([\text{inhibitor}])}} \quad (3)$$

Animals. Male Swiss mice (4−6 weeks old) were obtained from a colony at Butantan Institute, São Paulo, Brazil. Animals were maintained in sterile microisolator cages with sterile rodent feed and acidified water ad libitum, and housed in positive-pressure air-conditioned units (25 °C, 50% relative humidity) on a 12 h light/dark cycle. All procedures were performed in accordance with the guidelines provided by the Brazilian College of Animal Experimentation and approved by the local Ethics Committee.

Intravital Microscopy. Intravital microscopy (IVM) is a light microscopy-based approach that enables imaging the microcirculatory network and cellular routes, such as rolling and migration, in vivo. The cremaster muscle was the tissue elected to analyze leukocyte rolling, as a measure of inflammation, because of its thin and transparent nature. IVM was conducted on an upright microscope (Axiolab, Carl Zeiss, Oberkochen, Germany) coupled to a digital camera for image acquisition (AxioCam Icc1, Carl Zeiss, Oberkochen, Germany).

Cremaster Muscle Preparation. Mice were injected ip with a cocktail of 120 mg/kg ketamine (Holliday-Scott SA, Buenos Aires, Argentina) and 16 mg/kg xylazine (Calmiun, Agner União, São Paulo, Brazil). Animals were placed on a 37 °C heating pad and the microsurgery was performed on deeply anesthetized animals. Briefly, the scrotum was opened and the cremaster muscle exteriorized. A longitudinal incision on the muscle allowed its exposure to full access to the microcirculatory network. One postcapillary venule ranging between 25 and 40 μm of diameter in each animal was chosen to count the number of rolling leukocytes.

A rolling leukocyte was defined as a white cell that moved slower than the stream of flowing erythrocytes. The number of rolling leukocytes was quantified as the number of white cells that passed a fixed preset point during 1 min.

Experimental Protocol for IVM. *LPS Model.* Control group (Figure 2A, ctrl group) was injected ip with LPS (*E. coli* 055:B5, Sigma) at 1 mg/kg and after 1h cremaster muscle of deeply anesthetized animals was exposed to count the number of rolling leukocytes (open circles). Treatment with KTP-NH_2 at 96 μM (30 μL) was topically applied on the cremaster muscle, and rolling leukocytes were counted again after 10 min (closed circles). Baseline mice were pretreated with ip injection of sterile saline and submitted to topic application of sterile saline (Figure 2A, dashed line). KTP-NH_2 dosage was chosen based on our previous study in which we have shown that 96 μM of this peptide could effectively decrease leukocyte rolling in a mouse model of inflammation induced by LPS.[10] LPS dosage has been optimized to cause a significant increase in leukocyte rolling within the established time frame of the experiment.

Independent groups of mice ($n = 4$ for each group) were pretreated as follows.

Met group: Metyrapone (Met, Sigma) at 4.5 mg/kg ip twice a day for 3 days before LPS injection.[21]

ZnPPIX group: Zinc protoporphyrin IX (ZnPPIX, Sigma) at 9 mg/kg ip twice a day for 1 day before LPS injection.[21]

aIL-1R group: Rat anti-mouse CD121a (aIL-1R, BD Pharmingen) at 0.1 mg/kg ip 30 min before LPS injection.[21]

aIL-10 group: Monoclonal rat IgG_1 clone anti-mouse IL-10 antibody (aIL-10, R&D systems) at 0.25 mg/kg ip 30 min before LPS injection.

$MyD88_i$ group: Pepinh-MYD ($MyD88_i$, Invivogen) at 0.4 mg/kg intrascrotal 30 min after LPS injection. For all groups pretreated with pharmacological inhibitors, the induction of inflammation and subsequent treatment with KTP-NH_2 was performed as previously described for ctrl group.

CXCL-1 Model. Control group (Figure 2B, ctrl group) was injected with 50 μL of the neutrophil chemotactic factor CXCL-1 (453-KC, R&D System) at 0.05 μg/mL, via intrascrotal. Concomitantly, animals were anesthetized as previously described.

The cremaster muscle of deeply anesthetized animals was exposed and the number of rolling leukocytes was counted. Treatment with KTP-NH_2 at 96 μM (30 μL) was topically applied on the cremaster muscle, and rolling leukocytes were counted again after 10 min.

Met group was pretreated with Metyrapone (Met, Sigma) at 4.5 mg/kg ip twice a day for 3 days before CXCL-1 injection. The induction of inflammation with CXCL-1 and treatment with KTP-NH_2 was performed as described above.

AUTHOR INFORMATION

Corresponding Authors

*E-mail: macastanho@medicina.ulisboa.pt.

*E-mail: monica.lopesferreira@butantan.gov.br.

ORCID

Miguel Castanho: 0000-0001-7891-7562

Author Contributions

M.H. and E.B. contributed to peptide synthesis; J.P. and M.C. contributed to enkephalinase inibitory activity assays; J.P., C.L., and M.L.-F. contributed to intravital microscopy studies. All authors contributed to data discussion and paper writing.

Funding

FCT-MCTES is acknowledged for Ph.D. fellowship SFRH/BD/52225/2013 to J.P. Marie Skłodowska-Curie Research and Innovation Staff Exchange (RISE) is acknowledged for funding:

DOI: 10.1021/acschemneuro.7b00007
ACS Chem. Neurosci. 2017, 8, 1663−1667

call H2020-MSCA-RISE-2014, Grant Agreement 644167, 2015-2019.

Notes

The authors declare no competing financial interest.

■ ABBREVIATIONS

ACE, angiotensin converting enzyme; BBB, blood-brain barrier; DPP3, dipeptidyl-peptidase 3; GC, glucocorticoid; HO-1, heme-oxygenase 1; IL, interleukin; IL-1R, interleukin-1 receptor; IVM, intravital microscopy; KTP, kyotorphin; KTP-NH_2, kyotorphin-amide; LPS, lipopolysaccharide; Met, metyrapone; MyD88$_i$, MyD88 inhibitor; TLR4, toll-like receptor 4; ZnPPIX, zinc protoporphyrin IX

■ REFERENCES

(1) Takagi, H., Shiomi, H., Ueda, H., and Amano, H. (1979) A novel analgesic dipeptide from bovine brain is a possible Met-enkephalin releaser. *Nature 282*, 410−412.

(2) Takagi, H., Shiomi, H., Ueda, H., and Amano, H. (1979) Morphine-like analgesia by a new dipeptide, L-tyrosyl-L-arginine (Kyotorphin) and its analogue. *Eur. J. Pharmacol. 55*, 109−111.

(3) Hazato, T., Kase, R., Ueda, H., Takagi, H., and Katayama, T. (1986) Inhibitory effects of the analgesic neuropeptides kyotorphin and neo-kyotorphin on enkephalin-degrading enzymes from monkey brain. *Biochem Int. 12*, 379−383.

(4) Chen, P., Bodor, N., Wu, W. M., and Prokai, L. (1998) Strategies to target kyotorphin analogues to the brain. *J. Med. Chem. 41*, 3773−3781.

(5) Ribeiro, M. M., Pinto, A., Pinto, M., Heras, M., Martins, I., Correia, A., Bardaji, E., Tavares, I., and Castanho, M. (2011) Inhibition of nociceptive responses after systemic administration of amidated kyotorphin. *Br. J. Pharmacol. 163*, 964−973.

(6) Ribeiro, M. M., Pinto, A. R., Domingues, M. M., Serrano, I., Heras, M., Bardaji, E. R., Tavares, I., and Castanho, M. A. (2011) Chemical conjugation of the neuropeptide kyotorphin and ibuprofen enhances brain targeting and analgesia. *Mol. Pharmaceutics 8*, 1929−1940.

(7) Serrano, I. D., Ramu, V. G., Pinto, A. R., Freire, J. M., Tavares, I., Heras, M., Bardaji, E. R., and Castanho, M. A. (2015) Correlation between membrane translocation and analgesic efficacy in kyotorphin derivatives. *Biopolymers 104*, 1−10.

(8) Perazzo, J., Lopes-Ferreira, M., Sa Santos, S., Serrano, I., Pinto, A., Lima, C., Bardaji, E., Tavares, I., Heras, M., Conceicao, K., and Castanho, M. A. (2016) Endothelium-Mediated Action of Analogues of the Endogenous Neuropeptide Kyotorphin (Tyrosil-Arginine): Mechanistic Insights from Permeation and Effects on Microcirculation. *ACS Chem. Neurosci. 7*, 1130−1140.

(9) Sá Santos, S., Santos, S. M., Pinto, A. R., Ramu, V. G., Heras, M., Bardaji, E., Tavares, I., and Castanho, M. (2016) Amidated and ibuprofen-conjugated kyotorphins promote neuronal rescue and memory recovery in cerebral hypoperfusion dementia model. *Front. Aging Neurosci. 8*, 1−11.

(10) Conceição, K., Magalhães, P. R., Campos, S. R. R., Domingues, M. M., Ramu, V. G., Michalek, M., Bertani, P., Baptista, A. M., Heras, M., Bardaji, E. R., Bechinger, B., Ferreira, M. L., and Castanho, M. A. R. B. (2016) The anti-inflammatory action of the analgesic kyotorphin neuropeptide derivatives: insights of a lipid-mediated mechanism. *Amino Acids 48*, 307−318.

(11) Ribeiro, M. M. B., Franquelim, H. G., Torcato, I. s. M., Ramu, V. G., Heras, M., Bardaji, E. R., and Castanho, M. A. R. B. (2012) Antimicrobial properties of analgesic kyotorphin peptides unraveled through atomic force microscopy. *Biochem. Biophys. Res. Commun. 420*, 676−679.

(12) Miguel, M., Manso, M., Aleixandre, A., Alonso, M. J., Salaices, M., and Lopez-Fandino, R. (2007) Vascular effects, angiotensin I-converting enzyme (ACE)-inhibitory activity, and antihypertensive properties of peptides derived from egg white. *J. Agric. Food Chem. 55*, 10615−10621.

(13) Forsyth, K. D., and Talbot, V. (1992) Role of glucocorticoids in neutrophil and endothelial adhesion molecule expression and function. *Mediators Inflamm. 1*, 101−106.

(14) Cronstein, B. N., Kimmel, S. C., Levin, R. I., Martiniuk, F., and Weissmann, G. (1992) A mechanism for the antiinflammatory effects of corticosteroids: the glucocorticoid receptor regulates leukocyte adhesion to endothelial cells and expression of endothelial-leukocyte adhesion molecule 1 and intercellular adhesion molecule 1. *Proc. Natl. Acad. Sci. U. S. A. 89*, 9991−9995.

(15) Leech, M., Hutchinson, P., Holdsworth, S. R., and Morand, E. F. (1998) Endogenous glucocorticoids modulate neutrophil migration and synovial P-selectin but not neutrophil phagocytic or oxidative function in experimental arthritis. *Clin. Exp. Immunol. 112*, 383−388.

(16) Abbas, A. K., Lichtman, A. H. H., and Pillai, S. (2011) *Cellular and Molecular Immunology*, Elsevier Health Sciences.

(17) Schleimer, R. P., Benenati, S. V., Friedman, B., and Bochner, B. S. (1991) Do cytokines play a role in leukocyte recruitment and activation in the lungs? *Am. Rev. Respir. Dis. 143*, 1169−1174 discussion 1175−1166.

(18) Swain, M. G., Appleyard, C., Wallace, J., Wong, H., and Le, T. (1999) Endogenous glucocorticoids released during acute toxic liver injury enhance hepatic IL-10 synthesis and release. *Am. J. Physiol. 276*, G199−205.

(19) Lee, T. S., and Chau, L. Y. (2002) Heme oxygenase-1 mediates the anti-inflammatory effect of interleukin-10 in mice. *Nat. Med. 8*, 240−246.

(20) Kesmati, M., Rezaie, M., and Fathi-Moghaddam, H. (2010) Interaction between glucocorticoids and opioids in nociception in young and adult rats. *Open Access Anim. Physiol. 2010*, 87−92.

(21) Ferreira, M. J., Lima, C., and Lopes-Ferreira, M. (2014) Anti-inflammatory effect of Natterins, the major toxins from the Thalassophryne nattereri fish venom is dependent on TLR4/MyD88/PI3K signaling pathway. *Toxicon 87*, 54−67.

DOI: 10.1021/acschemneuro.7b00007
ACS Chem. Neurosci. 2017, 8, 1663−1667

Section 4

Final Conclusion

Pain is a huge social and economic problem. The current analgesics available have the disadvantage of having side effects and/or not being always efficient. In addition, analgesics have not undergone significant changes over the last sixty years. Thus, an increased interest has been directed towards analgesic peptides. The dipeptide KTP gathers an interesting and wide set of biological activities; over the last years several KTP analogues have been improved to allow a peripheral administration with the analgesic effect of a central administration (4.2 fold more potent than endogenous opioids). The aim of this thesis was to better understand the mechanism of action and targets of KTP-NH_2, a peptide developed by us with an increased pharmacological value compared to KTP. However, since the pharmacodynamics and pharmacokinetics of KTP-NH_2 are not optimal (see appendix 1), we aimed to improve the peptide by introducing minor changes in the chemical structure.

In article 2, we designed several KTP-NH_2 analogues by introducing minor changes in the chemical structure of KTP-NH_2 such as D-amino acid residues and/or N-terminal methylation. By doing that, we aimed to improve the pharmacodynamics of KTP-NH_2. We accessed the efficacy of KTP-NH_2 analogues as analgesic and anti-inflammatory and correlated the data with their respective P_R. The results showed that the methylated analogues (Figure 2) have a prolonged analgesic effect probably due to its high P_R but is pro-inflammatory. On the other hand, KTP-NH_2-DL (Figure 2) has not a significant analgesic effect, which is in accordance with its low P_R, but is anti-inflammatory. These structure-activity correlations support the hypothesis that KTP-NH_2, which is analgesic and has a low P_R, might cross the BBB using transporters not fitted to translocate KTP-NH_2-DL. Methylated analogues, in turn, might cross the BBB by a non-saturable mechanism, such as passive diffusion. KTP-NH_2 analogues are more stable in human serum, but KTP-NH_2 still is a more interesting peptide from the drug development strategies perspective. Among the analogues tested, only KTP-NH_2 gathers analgesic and anti-inflammatory activities. Pain and inflammation frequently coexist. “Pain is a hallmark of inflammation and inflammatory pain is a major clinical problem in many disorders” (Conceição et al. 2016). The gold standard for pain treatment, the opioids, have deleterious side effects. Therefore, having a single dipeptide capable of targeting pain and inflammation, with none or few side effects is very much appealing.

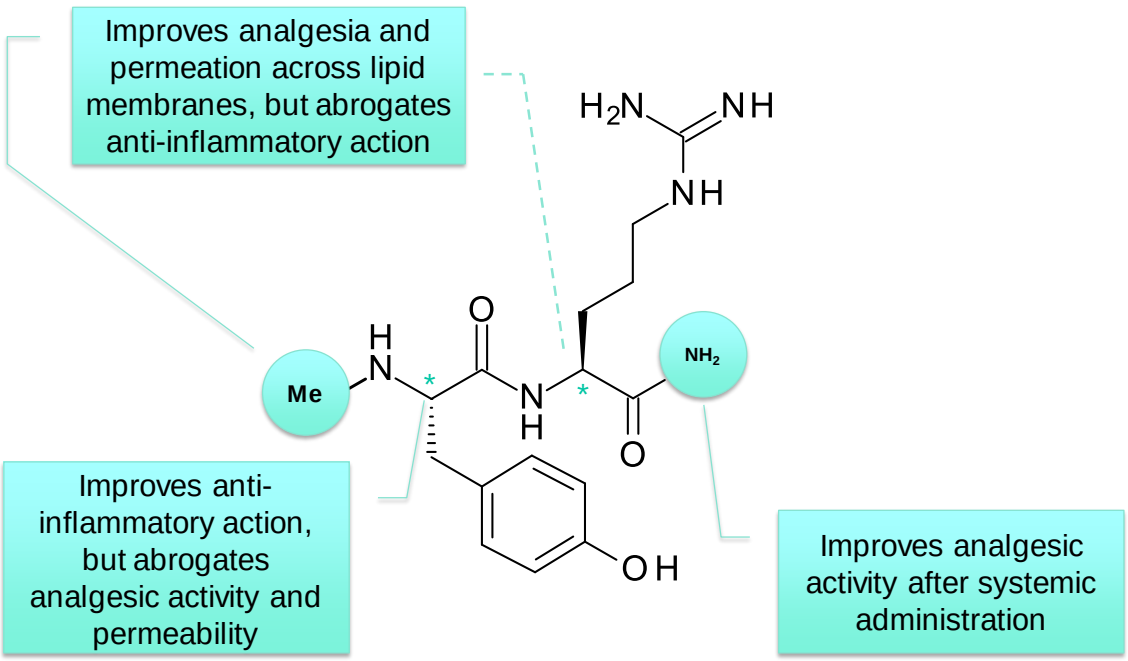

Figure 2. A schematic view of how minor chemical modifications impact the activity of the dipeptide KTP.

Previous studies carried by us have shown the antimicrobial (Ribeiro et al. 2012) and neuroprotective (Sa Santos et al. 2016) properties of KTP-NH_2. In addition, KTP-NH_2 is cheap to synthesize, is safe (Ribeiro et al. 2013) and its physiological effects are well characterized *in vivo*. But in contrast with the abundant data on the biological action of KTP-NH_2, its mechanism of action still is poorly understood. In article 3, we excluded the hypothesis that KTP-NH_2 could be a generic inhibitor of enkephalinases as two model enzymes, ACE and DPP3, are not inhibited at therapeutic doses. However, the central hypothesis in article 3 was that the anti-inflammatory action could be the key to link analgesia and neuroprotection. So, we attempted to unravel the anti-inflammatory mechanism of action of KTP-NH_2 at the molecular level using pharmacological inhibitors. Using two models of inflammation, one induced with LPS and other induced with CXCL-1, we demonstrated that KTP-NH_2 is able to decrease inflammation in both models in only ten minutes. In the full-fledge inflammation model induced with LPS, GCs were crucial to decrease inflammation and heme-oxygenase 1 (HO-1) and interleukin-10 (IL-10) seemed to play a partial role in this process. Interestingly, in the model where the recruitment of neutrophils is induced by CXCL-1, GCs do not participate in the anti-inflammatory mechanism of KTP-NH_2. Thus,

we concluded that KTP-NH_2 has dual action: a GC-mediated action, which is dominant in full-fledged inflammation models, and a GC-independent mechanism, which is predominant in models in which leukocyte rolling is stimulated but inflammation is not totally developed. Whichever the mechanism of action, it does not require *de novo* transcription.

We have shown that KTP-NH_2 and its analogues have an impact in the endothelium (section 2), which in turn play important roles in pain, inflammatory and neurodegenerative processes. For instance, there is increasing evidence that AD is a vascular disease with neurodegenerative consequences rather than a neurodegenerative disorder with vascular consequences.

GCs regulate different aspects of endothelial physiology, such as the expression of adhesion molecules, production of cytokines and chemokines and maintenance of endothelial barrier integrity (Zielińska et al. 2016). We believe that GCs might be the molecular link to explain the main biological activities of the peptide since they regulate numerous homeostatic functions. In clinical setting, GCs are widely used as anti-inflammatory agents. Similar to KTP-NH_2, GCs can also have naloxone-reversible analgesic effects (Kesmati et al. 2010). On the other hand, inhibition of GC receptor (GR) prevents the analgesic action of morphine, indicating a clear overlapping between the two pain modulation systems (Kesmati et al. 2010).

It was recently reported that KTP-NH_2 binds/perturbs LPS micelles, which would ultimately jeopardize signal transduction triggered by the binding of LPS to its receptor, TLR4. This was the mechanism proposed by Conceição and co-workers to explain the ability of KTP-NH_2 to decrease the number of rolling leukocytes in a murine model of inflammation induced by LPS (Conceição et al. 2016). However, our findings weaken this hypothesis and suggest that KTP-NH_2 anti-inflammatory mechanism is not primarily dependent of its interaction with LPS neither with TLR4 signaling pathway. It has rather a more general and unspecific mechanism such as blocking the activation/expression of adhesion molecules on the endothelium.

In conclusion, the data presented in this thesis reinforces that KTP-NH_2 is a multifunctional peptide with huge pharmacological potential. Even though the peptide

is quickly metabolized (see appendix 1), our data support the hypothesis that KTP-NH_2 crosses BBB mediated by a saturable transport mechanism. The fast action of the peptide, within 10-15 minutes, either at peripheral or central level, points towards a nongenomic mechanism and the involvement of GCs might be the molecular link to explain the analgesic and anti-inflammatory properties of the peptide. This finding opens avenues for future industrial drug development of KTP-NH_2.

Section 5

References

LIST OF REFERENCES USED IN TEXT (EXCLUDES REFERENCES IN PUBLISHED ARTICLES)

Berger, U. V. and M. A. Hediger (1999). "Distribution of peptide transporter PEPT2 mRNA in the rat nervous system." Anat Embryol (Berl) **199**(5): 439-449.

Chen, P., N. Bodor, et al. (1998). "Strategies to target kyotorphin analogues to the brain." J Med Chem **41**(20): 3773-3781.

Conceição, K., P. R. Magalhães, et al. (2016). "The anti-inflammatory action of the analgesic kyotorphin neuropeptide derivatives: insights of a lipid-mediated mechanism." Amino Acids **48**(1): 307-318.

Dieck, S. T., H. Heuer, et al. (1999). "The peptide transporter PepT2 is expressed in rat brain and mediates the accumulation of the fluorescent dipeptide derivative β-Ala-Lys-Nε-AMCA in astrocytes." Glia **25**(1): 10-20.

Fujita, T., T. Kishida, et al. (1999). "Interaction of kyotorphin and brain peptide transporter in synaptosomes prepared from rat cerebellum: implication of high affinity type H+/peptide transporter PEPT2 mediated transport system." Neurosci Lett **271**(2): 117-120.

Godlevsky, L. S., A. A. Shandra, et al. (1995). "Seizure-protecting effects of kyotorphin and related peptides in an animal model of epilepsy." Brain Res Bull **37**(3): 223-226.

Hazato, T., R. Kase, et al. (1986). "Inhibitory effects of the analgesic neuropeptides kyotorphin and neo-kyotorphin on enkephalin-degrading enzymes from monkey brain." Biochem Int **12**(3): 379-383.

Ignat'ev, D. A., V. V. Vorob'ev, et al. (1998). "Effects of a number of short peptides isolated from the brain of the hibernating ground squirrel on the EEG and behavior in rats." Neurosci Behav Physiol **28**(2): 158-166.

Inoue, M., H. Nakayamada, et al. (1997). "Peripheral non-opioid analgesic effects of kyotorphin in mice." Neurosci Lett **236**(1): 60-62.

Janicki, P. K. and A. W. Lipkowski (1983). "Kyotorphin and D-kyotorphin stimulate Met-enkephalin release from rat striatum in vitro." Neurosci Lett **43**(1): 73-77.

Jiang, H., Y. Hu, et al. (2009). "Enhanced antinociceptive response to intracerebroventricular kyotorphin in Pept2 null mice." J Neurochem **109**(5): 1536-1543.

Kawabata, A., S. Manabe, et al. (1994). "Comparison of antinociception induced by supraspinally administered L-arginine and kyotorphin." Br J Pharmacol **112**(3): 817-822.

Kawabata, A., H. Muguruma, et al. (1996). "Kyotorphin synthetase activity in rat adrenal glands and spinal cord." Peptides **17**(3): 407-411.

Kawabata, A., N. Umeda, et al. (1993). "L-arginine exerts a dual role in nociceptive processing in the brain: involvement of the kyotorphin-Met-enkephalin pathway and NO-cyclic GMP pathway." Br J Pharmacol **109**(1): 73-79.

Kesmati, M., M. Rezaie, et al. (2010). "Interaction between glucocorticoids and opioids in nociception in young and adult rats." Open Access Anim Physiol **2010**(2): 87-92.

Kolaeva, S. G., T. P. Semenova, et al. (2000). "Effects of L-thyrosyl - L-arginine (kyotorphin) on the behavior of rats and goldfish." Peptides **21**(9): 1331-1336.

Miguel, M., M. Manso, et al. (2007). "Vascular effects, angiotensin I-converting enzyme (ACE)-inhibitory activity, and antihypertensive properties of peptides derived from egg white." J Agric Food Chem **55**(26): 10615-10621.

Nishimura, K., K. Kaya, et al. (1991). "[Kyotorphin like substance in human cerebrospinal fluid of patients with persistent pain]." Masui **40**(11): 1686-1690.

Rackham, A., P. L. Wood, et al. (1982). "Kyotorphin (tyrosine-arginine): further evidence for indirect opiate receptor activation." Life Sci **30**(16): 1337-1342.

Ribeiro, M. M., A. Pinto, et al. (2011). "Inhibition of nociceptive responses after systemic administration of amidated kyotorphin." Br J Pharmacol **163**(5): 964-973.

Ribeiro, M. M., A. R. Pinto, et al. (2011). "Chemical conjugation of the neuropeptide kyotorphin and ibuprofen enhances brain targeting and analgesia." Mol Pharm **8**(5): 1929-1940.

Ribeiro, M. M., S. S. Santos, et al. (2013). "Side-effects of analgesic kyotorphin derivatives: advantages over clinical opioid drugs." Amino Acids **45**(1): 171-178.

Ribeiro, M. M. B., H. G. Franquelim, et al. (2012). "Antimicrobial properties of analgesic kyotorphin peptides unraveled through atomic force microscopy." Biochem Biophys Res Commun **420**(3): 676-679.

Sa Santos, S., S. M. Santos, et al. (2016). "Amidated and Ibuprofen-Conjugated Kyotorphins Promote Neuronal Rescue and Memory Recovery in Cerebral Hypoperfusion Dementia Model." Front Aging Neurosci **8**(1): 1-11.

Sakurada, T., S. Sakurada, et al. (1983). "Actions of intracerebroventricular administration of kyotorphin and an analog on thermoregulation in the mouse." Peptides **4**(6): 859-863.

Santos, S., L. Garcia-Nimo, et al. (2013). "Neuropeptide Kyotorphin (Tyrosyl-Arginine) has Decreased Levels in the Cerebro-Spinal Fluid of Alzheimer's Disease Patients: Potential Diagnostic and Pharmacological Implications." Front Aging Neurosci **5**(68): 1-6.

Serrano, I., J. M. Freire, et al. (2014). "The Mechanisms and Quantification of the Selective Permeability in Transport Across Biological Barriers: the Example of Kyotorphin." Mini Rev Med Chem **14**(2): 99-110.

Serrano, I. D., V. G. Ramu, et al. (2015). "Correlation between membrane translocation and analgesic efficacy in kyotorphin derivatives." Biopolymers **104**(1): 1-10.

Shiomi, H., Y. Kuraishi, et al. (1981). "Mechanism of kyotorphin-induced release of Met-enkephalin from guinea pig striatum and spinal cord." Brain Res **221**(1): 161-169.

Summy-Long, J. Y., V. Bui, et al. (1998). "Effects of central injection of kyotorphin and L-arginine on oxytocin and vasopressin release and blood pressure in conscious rats." Brain Res Bull **45**(4): 395-403.

Takagi, H., H. Shiomi, et al. (1982). "Analgesic dipeptide, L-Tyr-D-Arg (D-kyotorphin) induces Met-enkephalin release from guinea-pig striatal slices." Experientia **38**(11): 1344-1345.

Takagi, H., H. Shiomi, et al. (1979). "Morphine-like analgesia by a new dipeptide, L-tyrosyl-L-arginine (Kyotorphin) and its analogue." Eur J Pharmacol **55**(1): 109-111.

Takagi, H., H. Shiomi, et al. (1979). "A novel analgesic dipeptide from bovine brain is a possible Met-enkephalin releaser." Nature **282**(5737): 410-412.

Thakkar, S. V., S. Miyauchi, et al. (2008). "Stimulation of Na^+/Cl^--coupled opioid peptide transport system in SK-N-SH cells by L-kyotorphin, an endogenous substrate for H^+-coupled peptide transporter PEPT2." Drug Metab Pharmacokinet **23**(4): 254-262.

Ueda, H. and M. Inoue (2000). "In Vivo Signal Transduction of Nociceptive Response by Kyotorphin (Tyrosine-Arginine) through Gαi- and Inositol Trisphosphate-Mediated Ca^{2+} Influx." Mol Pharm **57**(1): 108-115.

Ueda, H., H. Shiomi, et al. (1980). "Regional distribution of a novel analgesic dipeptide kyotorphin (Tyr-Arg) in the rat brain and spinal cord." Brain Res **198**(2): 460-464.

Ueda, H., Y. Yoshihara, et al. (1989). "The kyotorphin (tyrosine-arginine) receptor and a selective reconstitution with purified Gi, measured with GTPase and phospholipase C assays." J Biol Chem **264**(7): 3732-3741.

Zielińska, K. A., L. Van Moortel, et al. (2016). "Endothelial Response to Glucocorticoids in Inflammatory Diseases." Front Immunol **7**(592): 1-20.

Appendix 1

ARTICLE 4

Improvement of the pharmacological properties of amidate kyotophin by means of iodination

MedChemComm, 2016

I declare that I have participated in the data discussion and writing of the manuscript under guidance of Prof. Miguel A.R.B. Castanho.

The limited potential of KTP to induce analgesia after systemic administration (Chen et al. 1998), probably due to its inability to cross the BBB and/or susceptibility to enzymatic degradation, has stimulated the development of more efficient analogues. We have successfully designed KTP analogues applying strategies of conjugation with lipophilic groups (Ribeiro et al. 2011; Ribeiro et al. 2011), improvement of cationicity (Ribeiro et al. 2011), use of D-amino acids and substitution of peptide bonds (Serrano et al. 2015). KTP-NH_2 is one of the successful analogues designed by us that retain the analgesic activity after systemic administration (Ribeiro et al. 2011). In 2011, KTP-NH_2 was patented (Ribeiro et al. 2009) for the treatment of pain recognizing its huge pharmacological potential. In addition, anti-inflammatory (Conceição et al. 2016) and neuroprotective (Sá Santos et al. 2016) properties have been described for KTP-NH_2.

As part of the pharmacological development of a drug, it is important to know its biodistribution/metabolism *in vivo*. In line with this context, in the following paper we have synthesized a radioioditanated KTP-NH_2 analogue ([I^{125}]MIK) as a tool to evaluate KTP-NH_2 biological fate *in vivo* and to assess its ability to cross BBB. It turned out the [I^{125}]MIK showed improved pharmacological properties over KTP-NH_2. While KTP-NH_2 is quickly metabolized by enzymes, [I^{125}]MIK is moderately stable in human serum at 37°C. Moreover, [I^{125}]MIK analgesic activity peaks later than KTP-NH_2 (30 vs. 15 min, respectively) but the overall effect lasts for a longer period. This analgesic activity shows a good correlation with ability of the peptide to translocate lipid membranes in vitro, but only a very low percentage of [I^{125}]MIK was found in the brain after systemic administration. Hereupon, we cannot exclude the peripheral effects of the radioiodinated peptide. The relative high levels of radioactivity found in the liver and intestines suggest that [I^{125}]MIK is mainly removed by the hepatobiliary tract and probably undergoes enzymatic dehalogenation in the liver. The resulting free radioiodade is probably captured by the thyroid which presents relevant levels of radioactivity. Low levels of radioactivity in the blood reflect the rapid radiopeptide clearance. Nevertheless 72.5% of the radioactivity of the plasma collected 5 min post-injection corresponded to [I^{125}]MIK.

Labeling of such a small peptide as KTP-NH_2 is challenging and the use of radioactivity seems to be the only approach that works in these cases. However, the strategy used in this article was not ideal since the designed radioiodinated analogue is not directly comparable to KTP-NH_2. Future studies using radioactive atoms incorporated in the backbone of the peptide, such as tritium, will certainly improve our technique to follow the dipeptide *in vivo*. Nevertheless, this

article have shown the pharmacokynetics of the peptide is not optimal and must be improved envisioning its clinical development.

MedChemComm

RESEARCH ARTICLE

Cite this: *Med. Chem. Commun.*, 2016, 7, 906

Improvement of the pharmacological properties of amidated kyotorphin by means of iodination†‡

Maria Cristina Oliveira,*[a] Lurdes Gano,[a] Isabel Santos,[a] João D. G. Correia,[a] Isa D. Serrano,[b] Sónia Sá Santos,[b] Marta Ribeiro,[b] Juliana Perazzo,[b] Isaura Tavares,[cd] Montserrat Heras,[e] Eduard Bardaji[e] and Miguel A. Castanho[b]

Received 14th January 2016,
Accepted 19th February 2016

DOI: 10.1039/c6md00028b

www.rsc.org/medchemcomm

Amidated kyotorphin (L-Tyr-L-Arg-NH_2; KTP-NH_2) shows analgesic properties following systemic administration. Although KTP-NH_2 does not have toxic effects in the liver, its biodistribution is unknown. KTP-NH_2 was radioiodinated to evaluate its biological fate *in vivo*. Mono-radioiodinated KTP-NH_2 ([^{125}I]MIK) was radiochemically stable *in vitro*, namely in saline at 4 °C up to 1 week, and moderately stable when incubated with human serum at 37 °C. Although the radioiodinated peptide could translocate a cellular model of the blood–brain barrier (BBB), the levels of radioactivity in the brain were minimal, 5 and 10 min after intraperitoneal injection (i.p.). Significant accumulation of ^{125}I was found in the thyroid probably reflecting the hydrolysis of the iodine–tyrosine bond by liver deiodinases. HPLC analysis of plasma samples collected 5 min post-injection showed that intact [^{125}I]MIK accounted for 72.5% of the total radioactivity, whereas the remaining radioactivity was associated with free radioiodide (I^-). These findings were subsequently confirmed by the low radioactivity found in the liver and kidney homogenates from rats sacrificed 10 min after i.p. administration. The analgesic activity of mono- and di-iodinated KTP-NH_2 was also evaluated by a hot plate assay showing a delayed peak of maximal efficacy compared to KTP-NH_2 (30 *vs.* 15 minutes). Overall, the peripheral effects of the peptides cannot be excluded.

Introduction

Kyotorphin (KTP, Fig. 1) is an endogenous analgesic neuropeptide (L-tyrosyl-L-arginine, L-Tyr-L-Arg) that has been proposed to induce Met-enkephalin release from nerve terminals in the brain.[1,2] The name kyotorphin was given in relation to Kyoto, the city where it was isolated from bovine brain by Takagi and colleagues in 1979,[2] with a suffix to mirror an endorphin-like substance. Kyotorphin was subsequently found in the brain of other mammals, including humans.[3]

The analgesic potency of kyotorphin administered directly to the brain is about 4.2 fold higher than naturally occurring opioid peptides.[4] However, when administered systemically, it shows activity only briefly, at a high dose of 200 mg kg^{-1}.[5] The limited capacity to cross the blood–brain barrier (BBB), putatively related to both insufficient lipophilicity and susceptibility to enzymatic degradation, narrows the pharmacological applications of KTP.

Strategies to enhance central nervous system targeting by chemical modification of KTP into more lipophilic analogues have been explored.[5,6] Accordingly, a direct correlation between improved interaction with lipid bilayers and analgesic activity for KTP derivatives has been reported.[7] Aiming to

[a] *Centro de Ciências e Tecnologias Nucleares, Instituto Superior Técnico, Universidade de Lisboa, Estrada Nacional 10 (ao km 139,7), 2695-066 Bobadela LRS, Portugal. E-mail: cristinaoliveira@ctn.tecnico.ulisboa.pt*
[b] *Instituto de Medicina Molecular, Faculdade de Medicina de Lisboa, Av. Professor Egas Moniz, 1649-028 Lisboa, Portugal*
[c] *Faculdade de Medicina do Porto, Departamento de Biologia Experimental, Universidade do Porto, 4200-319 Porto, Portugal*
[d] *Instituto de Biologia Celular e Molecular, Rua Campo Alegre, 4150-180 Porto, Portugal*
[e] *Laboratori d'Innovació en Processos i Productes de Síntesi Orgànica (LIPPSO), Departament de Química, Universitat de Girona, Campus Montilivi, 17071 Girona, Spain*

† The authors declare no competing interests.

‡ Electronic supplementary information (ESI) available. See DOI: 10.1039/c6md00028b

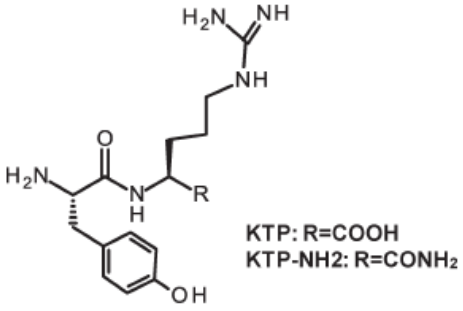

Fig. 1 Chemical structures of kyotorphin (KTP) and KTP-amide (KTP-NH_2).

increase the lipophilicity of KTP, Ribeiro and colleagues performed two main structural modifications of the peptide sequence (Fig. 1).[8,9] The first consisted of amidation, resulting in the derivative KTP-amide (KTP-NH_2), which presents improved lipophilicity and good analgesic ability following systemic administration in acute and chronic pain models.[7] To further improve the biological potential of KTP-NH_2, a second modification was made at the N-terminus by grafting ibuprofen (a lipophilic nonsteroidal anti-inflammatory drug, NSAID). This innovative combination resulted in a more lipophilic peptide, IbKTP-NH_2, with higher analgesic potency.[9]

The metabolic impact of kyotorphin derivatives is known to be minimal[10] and no histological hepatic lesions are detected at effective doses *in vivo*;[8] however, other focal toxicological effects in the organs in which the drugs eventually accumulate cannot be completely excluded. Although electrostatic effects favor the interaction with the BBB,[11] there is a generalized interaction with all endothelial surfaces throughout the body. This ubiquitous interaction of the drugs with virtually all the organs makes biodistribution data particularly relevant for their safety profiling. Thus, considering that such data would be also of key relevance to deduce the toxicity of the drugs, it would be important to determine the biological fate of the peptides and, simultaneously, assess their ability to cross the BBB.

In the work described herein we report on the radioiodination of KTP-NH_2 with ^{125}I as well as the assessment of the interaction of the resulting radioiodinated peptide with the BBB through permeation studies in bEnd.3 cell lines. We will also report on the biodistribution studies of the radioiodinated peptide in an adequate rat model. Moreover, to check whether the incorporation of iodine into the tyrosyl residue of KTP-NH_2 would affect its analgesic efficacy, KTP-NH_2 was also iodinated with non-radioactive sodium iodide and the analgesic efficacy of the two resulting iodinated species was evaluated in acute pain models.

Results and discussion

Radioiodination of KTP-NH_2

Radioiodination of the tyrosine residue in KTP-NH_2 was accomplished with [^{125}I]NaI/chloramine-T following a reported oxidative radioiodination procedure commonly used for direct radioiodination of proteins and peptides (Scheme 1).[12]

This method afforded almost exclusively the mono-radioiodinated derivative [^{125}I]MIK (Fig. 2). A small amount of the labelled di-iodinated derivative [^{125}I]DIK was also formed but has been efficiently removed by HPLC purification. [^{125}I]MIK was obtained in high radiochemical purity (>98%) after reconstitution in saline (Fig. 3).

The chemical identity of [^{125}I]MIK was ascertained by comparing its HPLC radioactive profile (γ detection) to that of the inactive analogue MIK (UV–Vis detection) (Fig. 3), which was synthesized as described below.

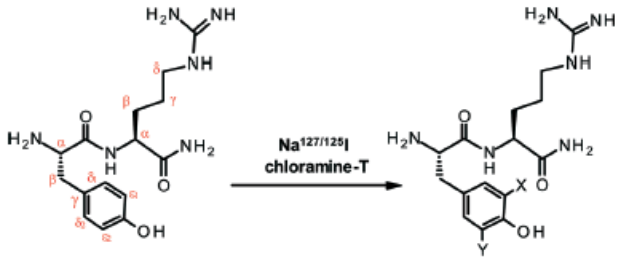

Scheme 1 Synthesis of radioiodinated and iodinated KTP-NH_2 derivatives (MIK and DIK).

The radioactive peptide [^{125}I]MIK is stable when stored in saline up to 1 week at 4 °C as demonstrated by HPLC analyses of samples collected at different time points. Furthermore, it is also stable in human serum up to 1 h at 37 °C as only a small amount of radioiodide (<5%), resulting from deiodination, was detected in the HPLC chromatograms after the incubation period. The lipophilicity of [^{125}I]MIK was assessed using octanol/PBS distribution coefficients (log $P_{o/w}$) defined as the concentration ratio of the compounds in the octanol phase and in the aqueous phase at physiological pH. The log $P_{o/w}$ found was −1.80 ± 0.03 at pH 7.4.

Iodination of KTP-NH_2

The tyrosine residue in KTP-NH_2 was iodinated with sodium iodide (NaI), following the general direct oxidative iodination procedure previously described for the preparation of [^{125}I]MIK. Unlike radioiodination, where the mono-radioiodinated derivative was the main species, in the case of iodination with $Na^{127}I$ both mono- and di-iodinated KTP-NH_2 derivatives (MIK and DIK, respectively) were obtained in moderate chemical yields (≈30%) when using equimolar amounts of peptide and sodium iodide. The iodinated peptides were separated and purified by silica gel column chromatography and their chemical purity (>98%) was ascertained by HPLC analysis (Fig. 4).

MIK and DIK were structurally characterized by mass spectrometry (ESI-MS) and ^{1}H-NMR spectroscopy, which was crucial for the elucidation of the substitution pattern of the aromatic rings. The ^{1}H-NMR spectrum of MIK presents a doublet at δ 7.51 ppm with a meta coupling constant (^4J = 2.1 Hz) assigned to the aromatic δ_1 proton and a doublet at δ 6.72 ppm with an ortho coupling constant (^3J = 8.1 Hz) assigned to the aromatic δ_2 proton. The doublet of doublets at δ 7.01 ppm with ortho and meta coupling constants (^3J = 8.1 Hz, ^4J = 2.1 Hz) is assigned to the ε_1 aryl proton. The di-iodinated compound shows only one singlet at δ 7.68 ppm, corresponding to the δ_1 and δ_2 protons, confirming the double iodination at the aromatic ring.

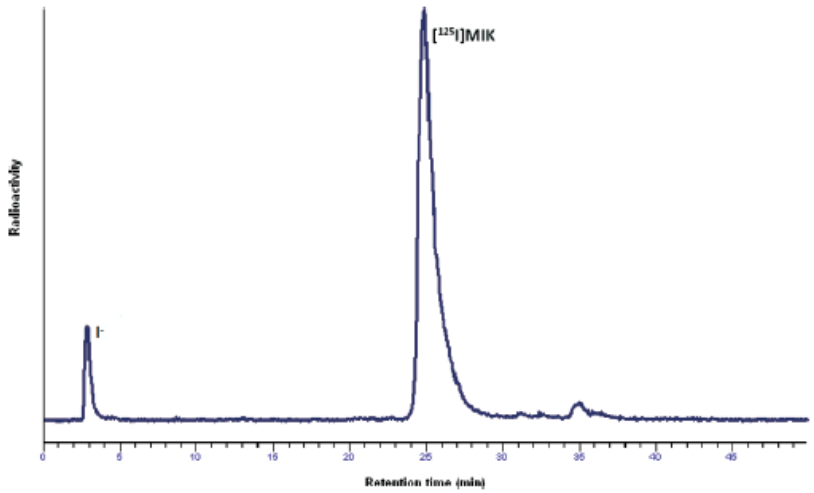

Fig. 2 HPLC radiochromatogram of the radioiodination mixture. HPLC chromatographic conditions: C18 analytical RP-HPLC column eluted with a linear gradient of acetonitrile/water containing 0.1% TFA running from 0% to 30% acetonitrile over 60 min with a flow rate of 1 mL min^{-1}. The radioactive eluting compounds were monitored by γ-detection.

Integrity and permeation of the BBB cellular model

The monolayers of the bEnd.3 cell line from mouse brain cultures used in this study mimic the *in vivo* BBB properties, namely the expression of tight junction proteins (occludin, claudin-5, zonula occludens-1) and the von Willebrand factor, which were imaged by immunofluorescence techniques (Fig. 5). Accordingly, the trans-endothelial electrical resistance (TEER), measured with an electrical resistance system (ERS) with a current-passing and a voltage-measuring electrode (Millicell-ERS), was 63 Ohm, which is characteristic of cell lines.[13] Astrocytes and pericytes were not detected in bEnd.3 cultures.

Permeation across this BBB model was measured in a Transwell setup, in which two compartments are separated by the cell monolayer supported on a filter. Considering that the activity retained by the filter support, with or without cells, was negligible (<5%), the P_R value of [^{125}I]MIK (0.49 ± 0.07; mean ± SD) obtained from data in Fig. 6 demonstrates the significant translocation of [^{125}I]MIK across the cellular model of the BBB, which is in good agreement with the improved lipophilicity and good analgesic ability observed after systemic administration in acute and chronic pain models for KTP-amide (KTP-NH_2).[8]

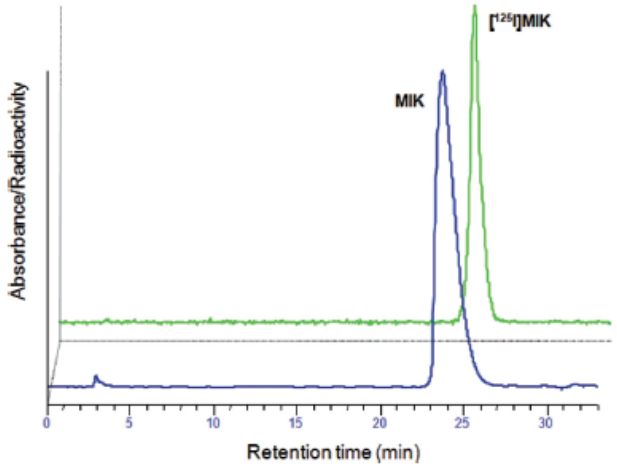

Fig. 3 HPLC radiochromatograms of the co-elution of purified radioiodinated [^{125}I]MIK with its non-radioactive analogue, MIK, with simultaneous (–) UV (280 nm) and (–) radioactivity detection.

Animal biodistribution and *in vivo* stability studies

The biological behavior of [^{125}I]MIK was evaluated through biodistribution studies in Sprague-Dawley male rats at 5 min and 10 min post-injection. The results of these studies, expressed in % of injected activity per gram of organ (%I.A. g^{-1}), are summarized in Table 1.

The low levels of radioactivity detected in blood (0.5 ± 0.2% I.A. g^{-1} at 5 min and 0.68 ± 0.05% I.A. g^{-1} at 10 min) indicated that [^{125}I]MIK presents rapid blood clearance. The relatively high levels of radioactivity found in the intestines (1.6 ± 0.1% I.A. g^{-1} at 5 min and 1.06 ± 0.08% I.A. g^{-1} at 10 min) suggest that [^{125}I]MIK is mainly excreted by the hepatobiliary tract. The relatively high uptake in liver (0.9 ± 0.2% I.A. g^{-1} at 5 min and 1.06 ± 0.08% I.A. g^{-1} at 10 min) probably reflects some enzymatic dehalogenation of [^{125}I]MIK by deiodinases, which are particularly abundant in hepatocyte microsomes.[14,15]

The low brain uptake (0.03 ± 0.01% I.A. g^{-1} and 0.07 ± 0.01% I.A. g^{-1} at 5 and 10 min, respectively) suggests that only a small fraction of [^{125}I]MIK crosses the BBB. This finding could be attributed in part to the hydrophilic character of [^{125}I]MIK (log $P_{o/w}$ = −1.80 ± 0.03). Since free radioiodide is taken up by the thyroid, the *in vivo* radiochemical stability of [^{125}I]MIK was evaluated by measuring the radioactivity in that

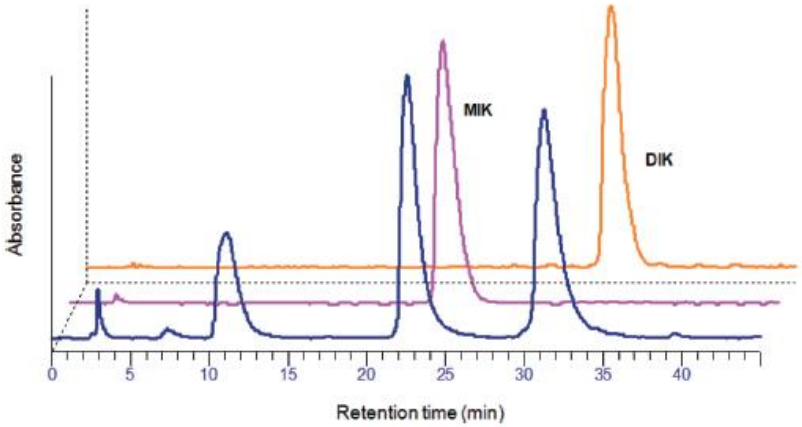

Fig. 4 HPLC chromatogram of the iodinated KTP-NH_2 mixture (–). HPLC analysis of the mono-iodinated peptide, MIK (–), and the di-iodinated peptide, DIK (–), after column chromatography purification. HPLC chromatographic conditions as described above. The products were detected spectrophotometrically at 280 nm.

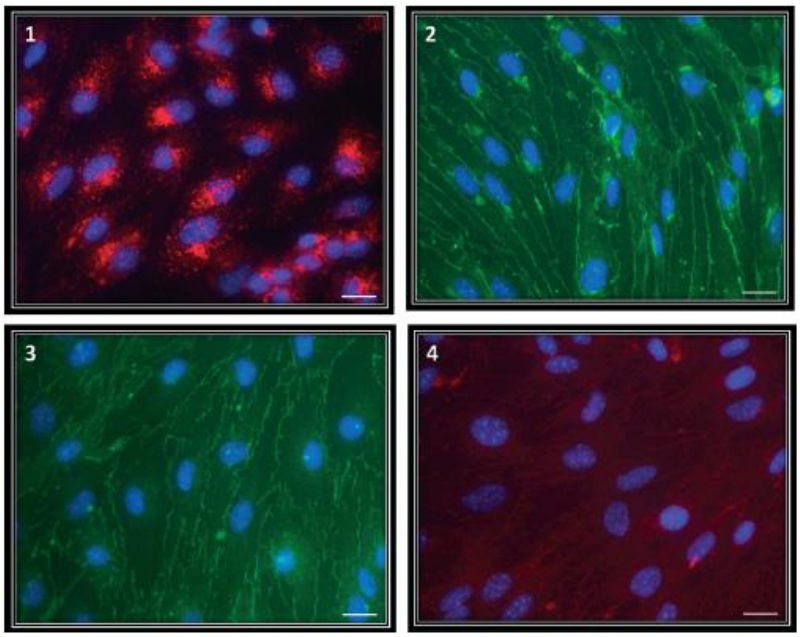

Fig. 5 Immunofluorescence microscopy images of the confluent capillary endothelial cell line from mouse brain (bEnd.3) stained for the von Willebrand factor (red) (1), junction associated protein claudin-5 (green) (2), occludin (green) (3), and zonula occludens-1 (red) (4). Nuclear staining with DAPI (blue); objective magnification, ×40; scale bar, 10 μm.

organ. Indeed, relevant accumulation of ^{125}I was found in the thyroid (2.7 ± 0.3% I.A. g^{-1} at 5 min post-injection), reflecting the hydrolysis of the iodine–tyrosine bond by liver deiodinases *in vivo*.

The radiochemical stability of [^{125}I]MIK was also studied in rat blood serum and rat tissue homogenates (kidney and liver). Analysis of plasma samples by RP-HPLC after appropriate work-up showed that intact [^{125}I]MIK accounted for 72.5% of the total radioactivity at 5 min post-injection, whereas the remaining radioactivity was associated with free radioiodide (I^-). These findings were subsequently confirmed by the low amount of [^{125}I]MIK found in the liver and kidney homogenates from rats sacrificed 10 min after administration of the radiopeptide. No further radiometabolites were found in the radiochromatograms.

Analgesic efficacy evaluation

To determine if iodine substitution causes major changes in the pharmacological efficacy of KTP-NH_2, the analgesic effect of mono-iodinated KTP-NH_2 (MIK, 44.42 mg kg^{-1} = 96 μmol

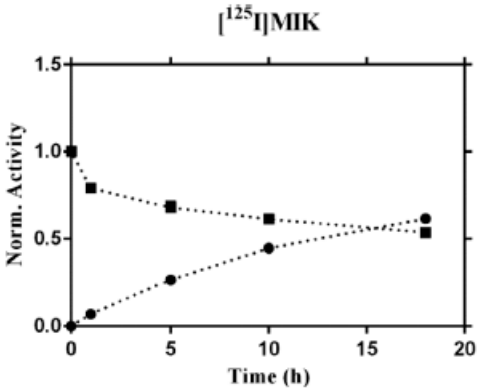

Fig. 6 Activity kinetics of [^{125}I]MIK. Activity at apical (squares) and basal (circles) compartments result from translocation of [^{125}I]MIK from the apical to basal compartment until an equal concentration is reached. Each point is an average of three independent measures. Data shown as mean ± SD. Lines are a guide to the eyes.

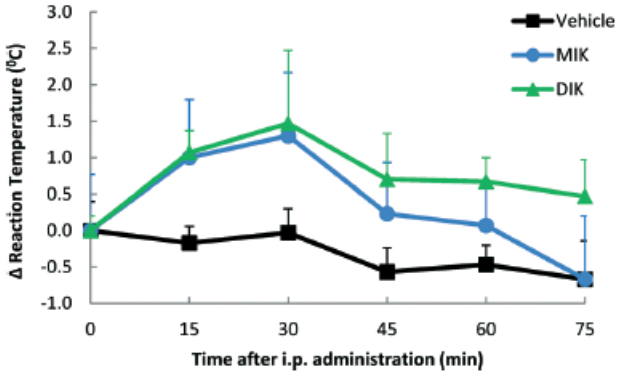

Fig. 7 MIK and DIK analgesic action. Inhibition of acute nociceptive responses in a hot plate test following systemic administration of MIK and DIK, 96 μmol kg^{-1}, in Wistar Han male rats. Results are shown as the variation of the behavioral responses at each evaluation time point in relation to the baseline values (time 0) obtained immediately before injection. In all experiments, n = 3 animals per group. Data shown as mean ± SD.

Table 1 Biodistribution data in the most relevant organs, expressed as %I.A. g^{-1}, at 5 min and 10 min after intraperitoneal administration of [^{125}I]MIK in Sprague-Dawley male rats (n = 3)

	Time after administration	
	5 min	10 min
Organ	%I.A. g^{-1}	%I.A. g^{-1}
Blood	0.5 ± 0.2	0.68 ± 0.05
Liver	0.9 ± 0.2	0.88 ± 0.02
Intestines	1.6 ± 0.1	1.06 ± 0.08
Spleen	1.1 ± 0.2	0.33 ± 0.04
Heart	0.26 ± 0.04	0.32 ± 0.04
Lung	0.5 ± 0.3	0.35 ± 0.05
Kidney	0.5 ± 0.2	0.57 ± 0.17
Muscle	0.28 ± 0.01	0.26 ± 0.06
Femur	0.22 ± 0.08	0.27 ± 0.06
Brain	0.03 ± 0.01	0.07 ± 0.01
Thyroid	2.7 ± 0.3	0.7 ± 0.2
Stomach	0.48 ± 0.04	0.98 ± 0.08

kg^{-1}) and di-iodinated KTP-NH$_2$ (DIK, 56.47 mg kg^{-1} = 96 μmol kg^{-1}) was evaluated after i.p. administration in Wistar Han male rats. A similar nociception efficacy was observed for MIK and DIK groups. Yet, the results show that iodine delays that effect, with the maximal effect being transferred from 15 min after i.p. administration[8] to 30 min (Fig. 7).

Conclusions

The ability of [^{125}I]MIK to translocate the histological BBB model correlates well with the good analgesic ability observed after systemic administration in a chronic pain model for KTP-amide (KTP-NH$_2$). MIK injections lead to analgesia, although the peak of maximal efficacy (30 min in Fig. 7) is delayed comparatively to KTP-NH$_2$ (15 min),[8] and the overall effect lasts for a longer period. Although the results cannot by themselves exclude the peripheral effects of the dipeptide, they strongly suggest that, despite the potential to cross the BBB observed *in vitro*, [^{125}I]MIK deiodination is concomitant with analgesic action *in vivo*, the conjugation of both effects resulting in low accumulation of [^{125}I]MIK in the brain and delayed KTP-NH$_2$ action. The fact that only low radioactivity accumulation was found in the brain after systemic administration suggests that KTP-NH$_2$ action is mediated by a low effective dose inside the CNS, and that its analgesic potency is consistent with the original profile reported for kyotorphin: 4.2 fold higher efficacy than that of Met-enkephalin when administered directly into the brain. In conclusion, iodination resulted in a slow release-like process that converted KTP, a drug rapidly cleared and having a fast transient effect, into a pro drug having delayed and prolonged action.

Experimental section

General information

All commercial reagents and solvents were of analytical grade and were used without further purification. HPLC-grade solvents were used for HPLC purification and analysis. Proton and carbon nuclear magnetic resonance spectroscopy (^{1}H and ^{13}C) were performed on a Varian Unity 300 MHz spectrometer using CD_3OD as solvent. Electrospray ionization mass spectrometry (ESI-MS) was performed on a QITMS Brucker HCT mass spectrometer. Analytical thin-layer chromatography was run using Merck 60 F 254 silica gel plates and spots were visualized under UV light (254 nm). Purification of iodinated KTP-NH$_2$ derivatives was performed by column chromatography using silica gel (70–230 mesh) from Merck. High performance liquid chromatography (HPLC) analyses were performed on a Perkin-Elmer system equipped with a biocompatible quaternary pump (series 200), a UV/vis detector (SPD-10 AV, Shimadzu, UV detection at λ_{max} = 280 nm) and a radioactivity γ-detector (LB 509, Berthold). Purification and analysis of the final products were carried out by analytical reverse-phase HPLC on an EC-Nucleosil C18 column (250 × 4 mm, 5 μm, Macherey Nagel) with a linear gradient of

acetonitrile/water containing 0.1% TFA running from 0% to 30% acetonitrile over 60 min with a flow rate of 1 mL min^{-1}. Sodium [^{125}I]iodide was obtained from Perkin Elmer, USA, as a non-carrier added solution in 0.1 M aqueous NaOH. The synthesis of the amidated peptide KTP-NH_2 has been described elsewhere.[8,9]

Radioiodination of KTP-NH_2

To a solution of KTP-NH_2 (5 μg, 15 nmol) in phosphate buffered saline (PBS, 25 μl) was sequentially added 18–37 MBq (0.5–1 mCi) of [^{125}I]NaI and a solution of chloramine-T (25 μg, 89 nmol) in PBS (25 μL). The reaction was allowed to proceed for 40–90 s with constant mixing at room temperature before being quenched by addition of a solution of sodium metabisulphite (50 μg, 263 nmol) in PBS (50 μL). The pure mono-radioiodinated peptide ([^{125}I]MIK) was obtained after purification by analytical reverse-phase HPLC on an EC-Nucleosil C18 column (250 × 4 mm, 5 μm, Macherey Nagel) with a linear gradient of acetonitrile/water containing 0.1% TFA running from 0% to 30% acetonitrile over 60 min with a flow rate of 1 mL min^{-1} with simultaneous UV (λ_{max} = 280 nm) and radioactivity detection (γ detection). The fractions corresponding to the radioiodinated peptide were collected and evaporated under a nitrogen stream to remove acetonitrile. The remaining aqueous solution was then loaded onto a C18 Sep-Pak cartridge and eluted with 2–4 mL of a PBS : ethanol (1 : 1) solution. After removal of ethanol by evaporation under a nitrogen stream the PBS solution was kept at 4 °C.

In vitro stability studies

The *in vitro* stability of [^{125}I]MIK was assessed in saline and human serum by HPLC analysis. Saline: the radioiodinated peptide (200 μL, 11 kBq μL^{-1}) was incubated in saline at 4 °C for 1 week. Aliquots were taken immediately before incubation as well as at various time points during incubation. Human serum: the radioiodinated peptide (400 μL, 11 kBq μL^{-1}) was incubated in human serum (1.6 mL) at 37 °C. Aliquots were taken (200 μL) at various time intervals during incubation (0, 15 min and 1 h) and treated with absolute ethanol (400 μL) at 4 °C to precipitate the proteins. Samples were centrifuged at 3000 rpm for 10 min at 4 °C. The supernatants were separated from the precipitate and analyzed by HPLC.

Lipophilicity determination

Log $P_{o/w}$ was determined by a 'shake flask' method using the back-extraction technique. The radioiodinated compound was added to a mixture of octanol (1 mL) and PBS, pH 7.4 (1 mL) previously saturated in each other by stirring the mixture. The mixture was vortexed and centrifuged (3000 rpm, 10 min, rt) to allow for phase separation. Aliquots of both octanol and PBS, pH 7.4, were counted for radioactivity in a gamma counter. A 0.5 mL aliquot of PBS, pH 7.4, layer was added to an equal volume of octanol and the extraction and counting was repeated as above. The log $P_{o/w}$ value was calculated by dividing the counts in octanol by those in the buffer and the results were expressed as log $P_{o/w}$.

Iodination of KTP-NH_2

To a solution of KTP-NH_2 (100 mg, 0.30 mmol) in PBS (600 μL) was added a solution of sodium iodide (35 mg, 0.23 mmol) in PBS (200 μL), followed by a solution of chloramine-T (69 mg, 0.24 mmol) in the same buffer (600 μL). The reaction was allowed to proceed for 1–2 min at room temperature with constant mixing. Thereafter, it was quenched by the addition of a solution of sodium metabisulphite (57 mg, 0.30 mmol) in PBS (500 μL). The resulting crude was purified by column chromatography on silica gel using MeOH/$CHCl_3$/25% NH_4OH (5 : 1 : 0.2) as an eluent to give a colorless solid after evaporation to dryness, which was further identified as corresponding to the di-iodinated KTP-NH_2 (DIK, 40 mg, 23% yield). Further elution with MeOH/25% NH_4OH (5 : 0.2) afforded mono-iodinated KTP-NH_2 as a colorless solid (MIK, 29 mg, 21% yield). Unreacted KTP-NH_2 was recovered from the column by elution with MeOH/25% NH_4OH (8 : 0.2).

Mono-iodinated KTP-NH_2 (MIK). ^{1}H NMR (CD_3OD, 300 MHz) δ 1.43–1.88 (m, 4H, $-(CH_2)_2$, arginine) 2.81–2.83 (m, 2H, $-CH_2$, tyrosine), 3.09–3.24 (m, 2H, $-NHCH_2$), 3.58–3.62 (m, 1H, −CH, tyrosine), 4.25–4.30 (m, 1H, −CH, arginine), 6.72 (d, ^3J = 8.1 Hz, 1H, $-CH_{aryl}$, $\varepsilon_{1tyrosine}$), 7.01 (dd, ^3J = 8.1 Hz, ^4J = 2.1 Hz, 1H, $-CH_{aryl}$, $\delta_{1tyrosine}$), 7.51 (d, ^4J = 2.1 Hz, 1H, $-CH_{aryl}$, $\delta_{2tyrosine}$); ^{13}C NMR (CD_3OD, 75 MHz) δ 26.20, 30.44, 40.54, 42.00, 53.68, 57.52, 86.40, 116.41, 130.04, 131.76, 140.93, 158.79, 158.71, 176.35, 176.70; ESI/MS (+) $C_{15}H_{23}N_6O_3I$ (463.69) (*m*/*z*) 463.1 $[M + H]^+$.

Di-iodinated KTP-NH_2 (DIK). ^{1}H NMR (CD_3OD, 300 MHz) δ 1.65–1.85 (m, 4H, $-(CH_2)_2$, arginine), 2.89 (dd, J = 14.4 Hz, J = 8.4 Hz, 1H, of the $-CH_2$ tyrosine), 3.11–3.31 (m, 3H, $-NHCH_2$ and 1H, of the $-CH_2$ tyrosine), 4.08–4.12 (m, 1H, −CH tyrosine), 4.38–4.42 (m, 1H, −CH, arginine), 7.68 (s, 2H, $-CH_{aryl}$); ^{13}C NMR (CD_3OD, 75 MHz) δ 25.04, 29.45, 40.79, 52.86, 54.28, 84.54, 130.03, 140.47, 144.95, 155.48, 157.53, 168.21, 174.37; ^{13}C NMR (CD_3OD, 75 MHz) δ 25.04, 29.45, 40.79, 52.86, 54.28, 84.54, 130.03, 140.47, 144.95, 155.48, 157.53, 168.21, 174.37; ESI/MS (+) $C_{15}H_{22}N_6O_3I_2$ (589.19) (*m*/*z*) 589.0 $[M + H]^+$.

Cell culture assays

bEnd.3 cell culture. A brain endothelial cell line from mouse (bEnd.3, ATCC CRL-2299) was used as an *in vitro* BBB model. For culturing, bEnd.3 cells were seeded in 25 cm^2 culture flasks in a concentration of 1.0 × 10^4 cells cm^{-2} and grown in Dulbecco's Modified Eagle's Medium (DMEM; ATCC; LGC Standards S.L.U., Barcelona, Spain) supplemented with 10% (v/v) fetal bovine serum and penicillin/streptomycin (100 U mL^{-1}) (both from Gibco, Life Technologies). Cells were kept in a humidified atmosphere of 5% CO_2 at 37 °C and the culture medium was changed every 2–3 days. After 5–6 days, 80% confluent bEnd.3 cells were trypsinized

using trypsin/EDTA (0.25% w/v; Life Technologies) for immunocytochemical studies and permeation assays.

Immunocytochemical bEnd.3 studies

The endothelial morphology of bEnd.3 was routinely confirmed by both contrast phase microscopy and immunocytochemistry protocols using markers of the tight junction complex such as occludin, zonula occludens-1, and claudin-5, and the von Willebrand factor (VWF), which is a specific endothelial cell marker. Antibodies against glial fibrillary acidic protein (GFAP) and α-smooth muscle actin (α-SMA) were used to rule out the presence of astrocytes and pericytes, respectively.

Briefly, cells were seeded onto glass coverslips in 24-well microplates (Costar, Corning Incorporated, NY, USA) and grown to confluence. Then, confluent cells were washed, fixed for 10 min in 1% paraformaldehyde, washed 3 times in PBS, permeabilized for 10 min in 0.2% Triton X-100 in PBS (PBS-Tx), rewashed and blocked for 1 h in 10% Bovine Serum Albumin (BSA) in PBS-Tx before staining. Cells were then incubated for 3 h with the primary antibody of interest: rabbit anti occludin (71–1500), rabbit anti zonula-occludens-1 (61–7300), and rabbit anti claudin-5 (34–1600), all from Life Technologies; rabbit IgG anti VWF (sc-14 014) from Santa Cruz Technologies, Texas, USA; mouse anti GFAP (IF03L) from Merck, Darmstadt, Germany; and mouse anti α-smooth muscle actin (MCA5781GA) from ABD Serotec, Oxford, UK.

The dilution of primary antibodies was 1 : 200 and 1 : 300 for anti-occludin. The cells were washed in PBS and then incubated for 1 h with a fluorescein-conjugated secondary antibody: Alexa Fluor 594 goat anti-rabbit IgG (A11012) and Alexa Fluor 488 goat anti-mouse IgG (A11017) from Life Technologies (dilution of 1 : 200), plus 10 min with DAPI (nuclei dye), followed by extensive rinsing before mounting in Fluoro-Mount (Sigma Aldrich, Deisehnhofen, Germany). Omission of the primary antibody served as negative control. Cells were observed using a Leica DM5000B fluorescence microscope [40× HCX PL FLUOTAR dry objective (NA 0.75)].

Permeation bEnd.3 studies

For permeability determination assays, 3000 bEnd.3 cells were seeded in 24-well Transwell filters (6.5 mm, 0.4 μm pore, transparent polyester membrane insert) filled with culture medium and maintained in a humidified atmosphere of 5% CO_2 at 37 °C. The culture medium was changed every 2 days. At day 6, cells reached confluence and 3 days later (day 9), coincident with maximal expression of tight junctions and the highest trans-endothelial resistance, transport assays were performed.

Permeation studies were carried out for 18 h and were performed in triplicate. Both sides of the Transwell chamber were carefully washed with pre-warmed culture medium. The basal compartment was filled with 800 μL of culture medium and the apical compartment was loaded with 200 μL of the radioiodinated peptide diluted in culture medium. The apical compartment was placed on top of the base being separated by a filter with or without cells (sample *vs.* blank filter). The apparatus was then incubated at 37 °C with 5% CO_2 for different time intervals. After incubation, the apparatus was disassembled and the basal and apical solutions, as well as the filter support, were transferred to radioimmunoassay test tubes and immediately read or kept at room temperature until use. The dose tested was 37 KBq per 200 μL (1 μCi per 200 μL).

Relative permeability calculation. The relative permeability calculation is described elsewhere.[16] Briefly, the activity of the drug at the apical compartment was plotted against time, and the slope, m, of the linear part of the curves was calculated for blank filters and filters covered with cells. Sample permeability (P_s) and blank permeability (P_b) may be simply calculated according to:[17]

$$P_x = m_x \cdot \frac{V}{A} \quad (1)$$

where x refers to sample (s) or blank (b), V is the basal volume, and A the area of the filter.

Because the permeability depends on the porosity of the support filter, its absolute value is of limited comparability with other experimental setups. The relative permeability, $P_R = P_s/P_b$, is a more robust parameter for comparison purposes. Experimentally, it reads:

$$P_R = \frac{P_s}{P_b} = \frac{m_s}{m_b} \quad (2)$$

P_R was calculated considering the first 10 hours.

Animal studies

All described experiments were carried out in compliance with the National law and with the European Community guidelines (Directive 2010/63/EU) for Animal Care and Ethics for Animal Experiments and were approved by National Authority. Healthy Sprague-Dawley or Wistar Han adult male rats (Charles River, Spain) were used according to the type of procedure (see details on the following sections). The animals were housed together in groups (within each strain) with unrestricted access to water and food, and under controlled conditions (22 ± 2 °C; lights on between 7:00 a.m. and 7:00 p.m.). Biodistribution studies and analgesia testing were conducted during the light period of the 12 : 12 h cycle.

Biodistribution and *in vivo* stability assays

Biodistribution studies were carried out on healthy Sprague-Dawley male rats obtained from Charles River, Spain. The animals were injected intraperitoneally with 11 MBq (30 μCi) of [^{125}I]MIK reconstituted in 250 μL of physiological saline. The injected activity was assumed to be the difference between the measured radioactivity in the syringe before and after injection. The animals were maintained on normal diet *ad libitum* and were sacrificed by excess anesthesia with

using trypsin/EDTA (0.25% w/v; Life Technologies) for immunocytochemical studies and permeation assays.

Immunocytochemical bEnd.3 studies

The endothelial morphology of bEnd.3 was routinely confirmed by both contrast phase microscopy and immunocytochemistry protocols using markers of the tight junction complex such as occludin, zonula occludens-1, and claudin-5, and the von Willebrand factor (VWF), which is a specific endothelial cell marker. Antibodies against glial fibrillary acidic protein (GFAP) and α-smooth muscle actin (α-SMA) were used to rule out the presence of astrocytes and pericytes, respectively.

Briefly, cells were seeded onto glass coverslips in 24-well microplates (Costar, Corning Incorporated, NY, USA) and grown to confluence. Then, confluent cells were washed, fixed for 10 min in 1% paraformaldehyde, washed 3 times in PBS, permeabilized for 10 min in 0.2% Triton X-100 in PBS (PBS-Tx), rewashed and blocked for 1 h in 10% Bovine Serum Albumin (BSA) in PBS-Tx before staining. Cells were then incubated for 3 h with the primary antibody of interest: rabbit anti occludin (71–1500), rabbit anti zonula-occludens-1 (61–7300), and rabbit anti claudin-5 (34–1600), all from Life Technologies; rabbit IgG anti VWF (sc-14 014) from Santa Cruz Technologies, Texas, USA; mouse anti GFAP (IF03L) from Merck, Darmstadt, Germany; and mouse anti α-smooth muscle actin (MCA5781GA) from ABD Serotec, Oxford, UK.

The dilution of primary antibodies was 1 : 200 and 1 : 300 for anti-occludin. The cells were washed in PBS and then incubated for 1 h with a fluorescein-conjugated secondary antibody: Alexa Fluor 594 goat anti-rabbit IgG (A11012) and Alexa Fluor 488 goat anti-mouse IgG (A11017) from Life Technologies (dilution of 1 : 200), plus 10 min with DAPI (nuclei dye), followed by extensive rinsing before mounting in Fluoro-Mount (Sigma Aldrich, Deisehnhofen, Germany). Omission of the primary antibody served as negative control. Cells were observed using a Leica DM5000B fluorescence microscope [40× HCX PL FLUOTAR dry objective (NA 0.75)].

Permeation bEnd.3 studies

For permeability determination assays, 3000 bEnd.3 cells were seeded in 24-well Transwell filters (6.5 mm, 0.4 μm pore, transparent polyester membrane insert) filled with culture medium and maintained in a humidified atmosphere of 5% CO_2 at 37 °C. The culture medium was changed every 2 days. At day 6, cells reached confluence and 3 days later (day 9), coincident with maximal expression of tight junctions and the highest trans-endothelial resistance, transport assays were performed.

Permeation studies were carried out for 18 h and were performed in triplicate. Both sides of the Transwell chamber were carefully washed with pre-warmed culture medium. The basal compartment was filled with 800 μL of culture medium and the apical compartment was loaded with 200 μL of the radioiodinated peptide diluted in culture medium. The apical compartment was placed on top of the base being separated by a filter with or without cells (sample *vs.* blank filter). The apparatus was then incubated at 37 °C with 5% CO_2 for different time intervals. After incubation, the apparatus was disassembled and the basal and apical solutions, as well as the filter support, were transferred to radioimmunoassay test tubes and immediately read or kept at room temperature until use. The dose tested was 37 KBq per 200 μL (1 μCi per 200 μL).

Relative permeability calculation. The relative permeability calculation is described elsewhere.[16] Briefly, the activity of the drug at the apical compartment was plotted against time, and the slope, m, of the linear part of the curves was calculated for blank filters and filters covered with cells. Sample permeability (P_s) and blank permeability (P_b) may be simply calculated according to:[17]

$$P_x = m_x \cdot \frac{V}{A} \quad (1)$$

where x refers to sample (s) or blank (b), V is the basal volume, and A the area of the filter.

Because the permeability depends on the porosity of the support filter, its absolute value is of limited comparability with other experimental setups. The relative permeability, $P_R = P_s/P_b$, is a more robust parameter for comparison purposes. Experimentally, it reads:

$$P_R = \frac{P_s}{P_b} = \frac{m_s}{m_b} \quad (2)$$

P_R was calculated considering the first 10 hours.

Animal studies

All described experiments were carried out in compliance with the National law and with the European Community guidelines (Directive 2010/63/EU) for Animal Care and Ethics for Animal Experiments and were approved by National Authority. Healthy Sprague-Dawley or Wistar Han adult male rats (Charles River, Spain) were used according to the type of procedure (see details on the following sections). The animals were housed together in groups (within each strain) with unrestricted access to water and food, and under controlled conditions (22 ± 2 °C; lights on between 7:00 a.m. and 7:00 p.m.). Biodistribution studies and analgesia testing were conducted during the light period of the 12 : 12 h cycle.

Biodistribution and *in vivo* stability assays

Biodistribution studies were carried out on healthy Sprague-Dawley male rats obtained from Charles River, Spain. The animals were injected intraperitoneally with 11 MBq (30 μCi) of [^{125}I]MIK reconstituted in 250 μL of physiological saline. The injected activity was assumed to be the difference between the measured radioactivity in the syringe before and after injection. The animals were maintained on normal diet *ad libitum* and were sacrificed by excess anesthesia with

isofluorane at 5 and 10 min post injection with a radiotracer. The most relevant organs (Table 1) were removed, weighed and the activity was measured in a gamma counter. Results were expressed as percent of injected activity per gram of organ (% I.A. g^{-1}) and presented as mean values ± SD (standard deviation). Whole animal body radioactivity excretion was not quantified.

The *in vivo* stability was assessed in rat blood serum, liver and kidney homogenates by HPLC analysis under the experimental conditions already described. Serum: the blood collected from rats, at the sacrifice time points 5 and 10 min, after injection was centrifuged at 3000 rpm for 15 min at 4 °C and the serum was separated. Afterwards, 100 μL aliquots of serum were treated with 200 μL of ethanol to precipitate the proteins. Samples were cooled at 4 °C and centrifuged at 4000 rpm for 15 min. Supernatant was collected and filtered through a Millipore Millex GV filter (0.22 μm) prior to RP-HPLC analysis. Liver homogenates: the rats were injected with 100 μL bolus of each radioiodinated preparation, as described for biodistribution studies. The animals were kept on normal diet *ad libitum*. Immediately after sacrifice the liver was excised and rapidly rinsed and placed in chilled 50 mM TRIS/0.2 M sucrose buffer, pH = 7.4, where it was homogenized. Aliquots (in duplicate) of the liver homogenate were treated with ethanol in 2 : 1 EtOH : aliquot (v/v). The samples were then centrifuged at 25 000 rpm for 15 min at 4 °C, filtered through Millex GV (0.22 μm) and analysed by HPLC following the same procedure.

Analgesic efficacy evaluation

The analgesic efficacy of the mono- and di-iodinated KTP-NH_2 derivatives (MIK and DIK, respectively) was evaluated in Wistar Han male rats by a hot plate test. The dose tested for each compound was 96 μmol kg^{-1} according to the analgesic action profile of KTP-NH_2.[8] This corresponds to 44.42 mg kg^{-1} for MIK and 56.47 mg kg^{-1} for DIK (considering MW (MIK) = 462.69 g mol^{-1} and MW (DIK) = 588.19 g mol^{-1}). MIK and DIK compounds were dissolved in physiological saline solution (vehicle: 0.9% NaCl containing 6.7% dimethyl sulfoxide, DMSO). The animals were divided into groups according to the injected compound (single i.p. injection in a dosing volume of 1 mL kg^{-1} body weight): MIK, DIK or vehicle (saline solution: control group).

For the hot plate test, the animals were previously habituated to the experimenter, the animal room and the apparatus for the days preceding the behavioral tests. The animals were placed on an aluminium surface inside a Plexiglas box (12 cm diameter; 22.5 cm high) of an IITC Life Sciences Analgesimeter (San Fernando Valley, CA, USA). The initial temperature was 35 °C, and the rate of increasing temperature was 9 °C min^{-1} with a cut-off temperature of 52.5 °C. The temperature to elicit hind paw licking or jumping was recorded. The animals' response was assessed before i.p. administration of MIK, DIK or saline solution (basal values) and every 15 min for 75 min after i.p. injections. The results were represented as the difference between the values registered at each time after treatment and the basal values (zero time). In all experiments, $n = 3$ animals per group.

Acknowledgements

C2TN/IST authors gratefully acknowledge the FCT support through the UID/Multi/04349/2013 project. The authors thank Dr. Célia Fernandes for mass spectroscopy analysis, which was carried out on a QITMS instrument, acquired with the support of the Programa Nacional de Reequipamento Científico (Contract REDE/1503/REM/2005- ITN) of FCT and is part of RNEM-Rede Nacional de Espectrometria de Massa.

Notes and references

1 H. Takagi, H. Shiomi, H. Ueda and H. Amano, *Nature*, 1979, 282, 410.
2 H. Takagi, H. Shiomi, H. Ueda and H. Amano, *Eur. J. Pharmacol.*, 1979, 55, 109.
3 K. Nishimura, K. Kaya, T. Hazato, H. Ueda, M. Satoh and H. Takagi, *Masui*, 1991, 40, 1686.
4 H. Shiomi, H. Ueda and H. Takagi, *Neuropharmacology*, 1981, 20, 633.
5 P. Chen, N. Bodor, W. M. Wu and L. Prokai, *J. Med. Chem.*, 1998, 41, 3773.
6 S. C. Lopes, C. M. Soares, A. M. Baptista, E. Goormaghtigh, B. J. Cabral and M. A. Castanho, *J. Phys. Chem. B*, 2006, 110, 3385.
7 S. C. Lopes, A. Fedorov and M. A. Castanho, *ChemMedChem*, 2006, 1, 723.
8 M. Ribeiro, A. Pinto, M. Pinto, M. Heras, I. Martins, A. Correia, E. Bardaji, I. Tavares and M. Castanho, *Br. J. Pharmacol.*, 2011, 163, 964.
9 M. M. B. Ribeiro, A. R. T. Pinto, M. M. Domingues, I. Serrano, M. Heras, E. R. Bardaji, I. Tavares and M. A. Castanho, *Mol. Pharmaceutics*, 2011, 8, 1929.
10 M. M. B. Ribeiro, S. Sá Santos, D. S. C. Sousa, M. Oliveira, S. M. Santos, M. Heras, E. Bardaji, I. Tavares and M. A. R. B. Castanho, *Amino Acids*, 2013, 45, 171.
11 M. M. B. Ribeiro, M. M. Domingues, J. M. Freire, N. C. Santos and M. A. R. B. Castanho, *Front. Cell. Neurosci.*, 2012, 6, 44.
12 V. Hunter and F. Greenwood, *Nature*, 1962, 194, 495.
13 B. B. Weksler, E. A. Subileau, N. Perrière, P. Charneau, K. Holloway, M. Levequ, H. Tricoire-Leignel, A. Nicotra, S. Bourdoulous, P. Turowski, D. K. Male, F. Roux, J. Greenwood, I. A. Romero and P. O. Couraud, *FASEB J.*, 2005, 19, 1872.
14 S. L. Morrell, J. A. Fuchs and J. L. Holtzman, *J. Pharmacol. Exp. Ther.*, 2000, 294, 308.
15 K. Sorimachi, A. Niwa and Y. Yosihiro, *Biochim. Biophys. Acta*, 1980, 630, 469–475.
16 I. D. Serrano, V. G. Ramu, A. R. Pinto, J. M. Freire, I. Tavares, M. Heras, E. R. Bardaji and M. A. Castanho, *Biopolymers*, 2014, 104, 1.
17 I. D. Serrano, J. M. Freire, M. V. Carvalho, M. Neves, M. N. Melo and M. A. Castanho, *Mini-Rev. Med. Chem.*, 2014, 14, 99.

^{1}H NMR (CD_3OD, 300 MHz)
Mono-iodinated KTP-NH_2 (MIK)

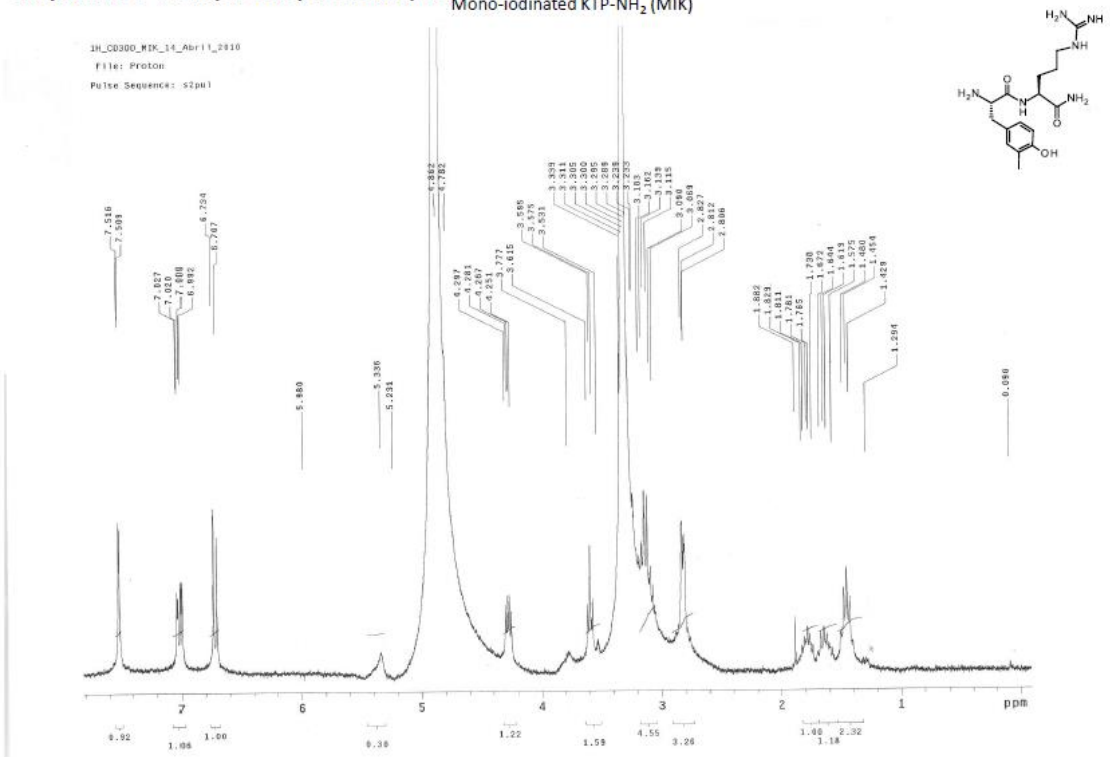

1

^{1}H NMR (CD_3OD, 300 MHz)
Mono-iodinated KTP-NH_2 (MIK)

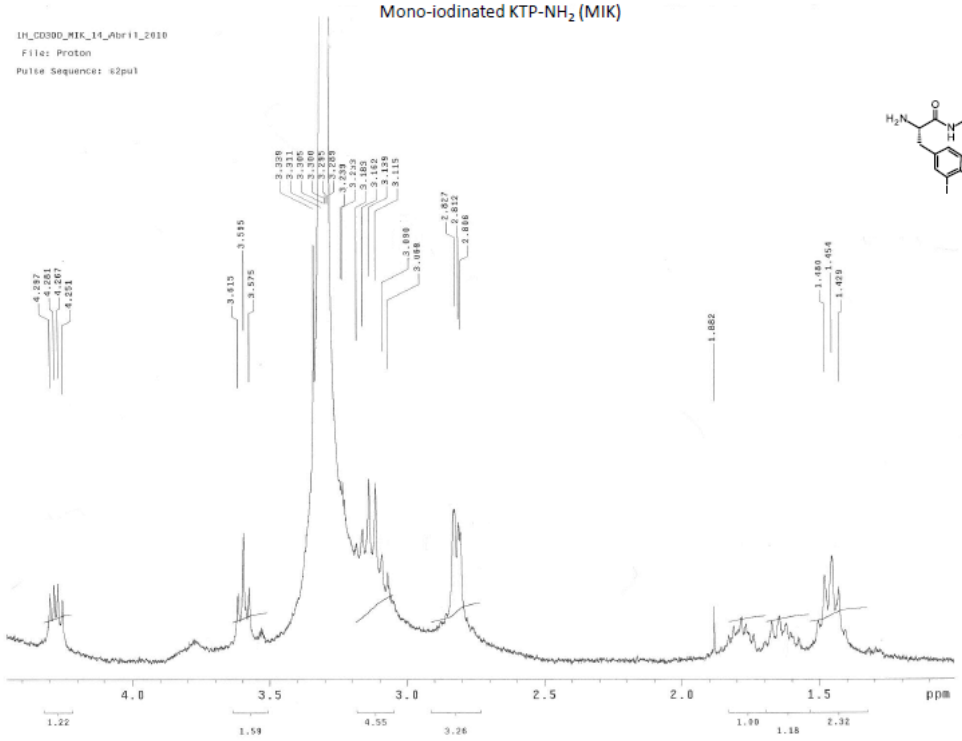

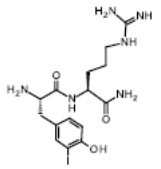

2

^{1}H NMR (CD_3OD, 300 MHz)
Mono-iodinated KTP-NH_2 (MIK)

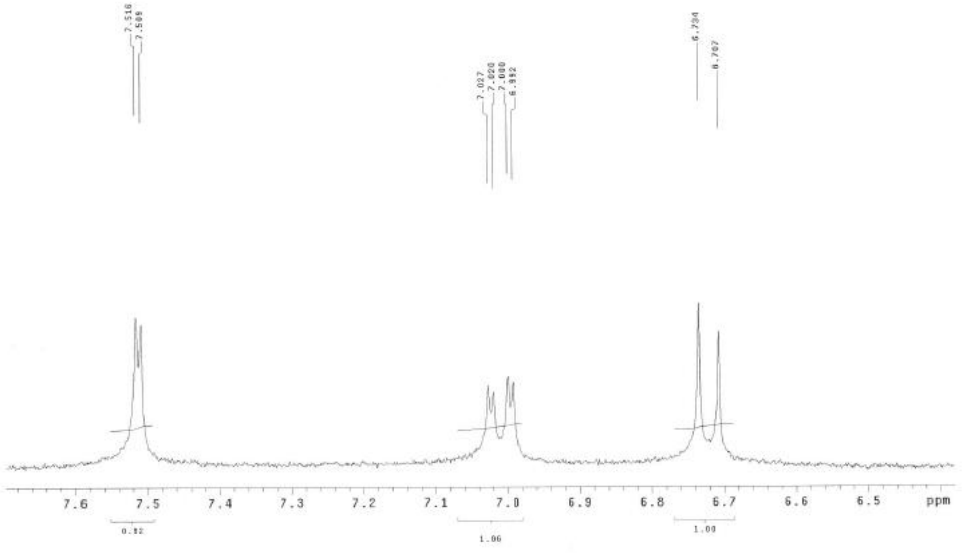

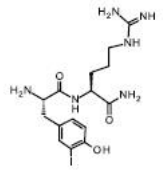

3

^{1}H NMR (CD_3OD, 300 MHz)
Di-iodinated KTP-NH_2 (DIK)

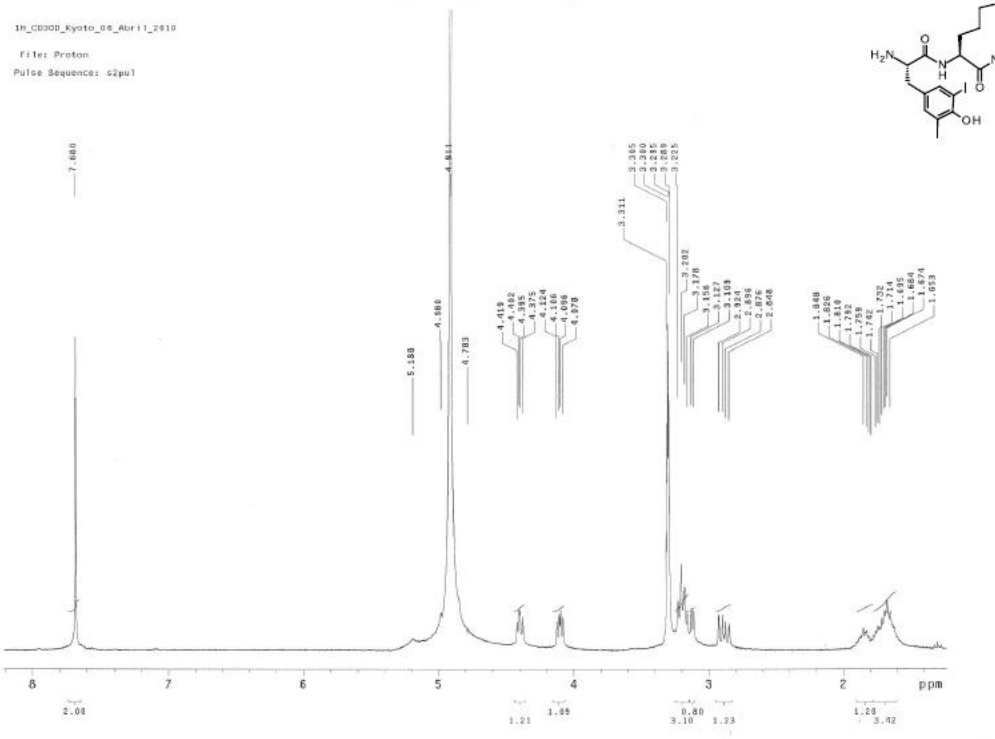

4

^{1}H NMR (CD_3OD, 300 MHz)
Di-iodinated KTP-NH_2 (DIK)

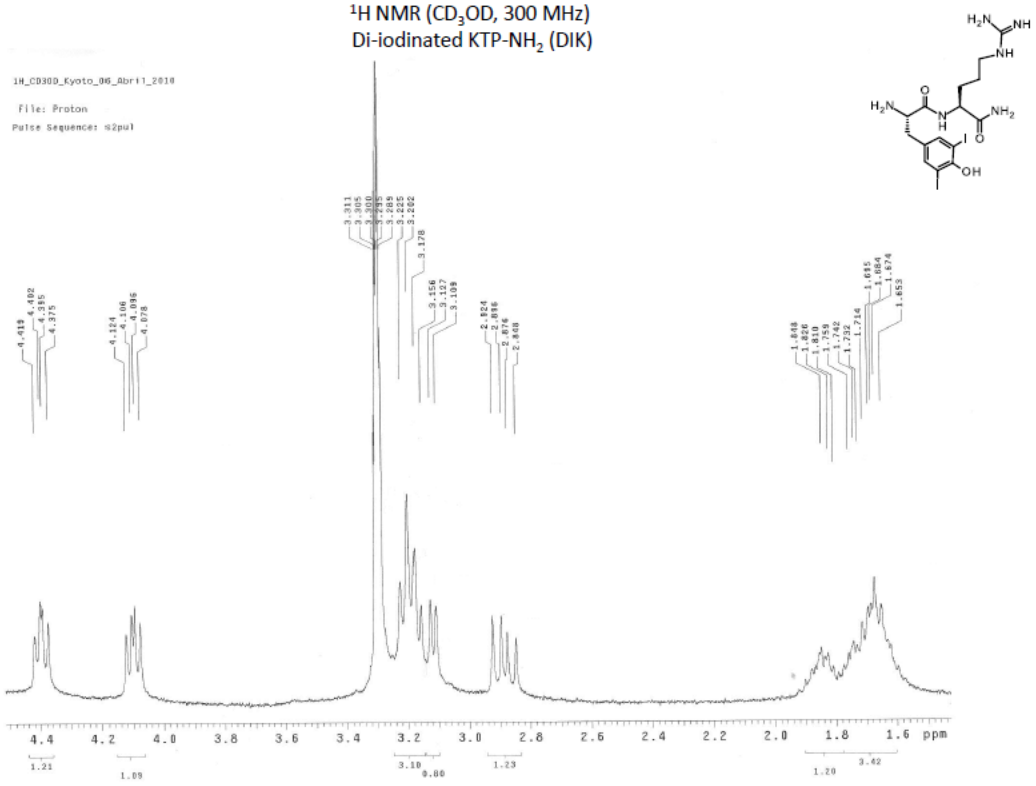

5

^{13}C NMR (CD_3OD, 75 MHz)
Mono-iodinated KTP-NH_2 (MIK)

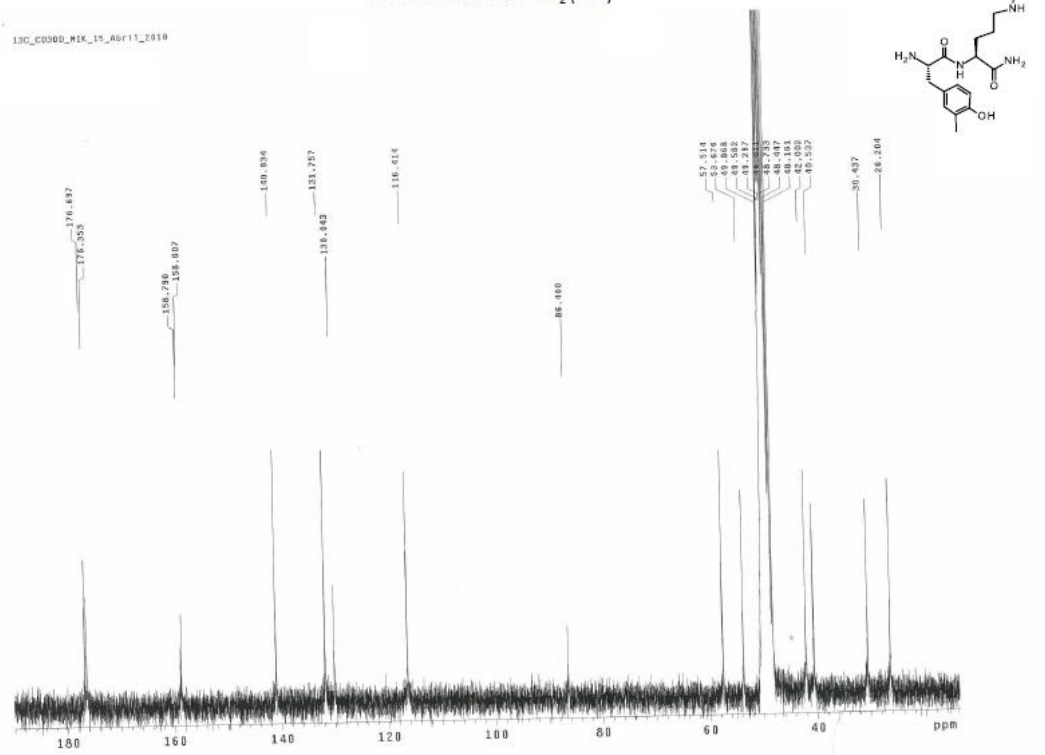

6

^{13}C NMR (CD_3OD, 75 MHz)
Mono-iodinated KTP-NH_2 (MIK)

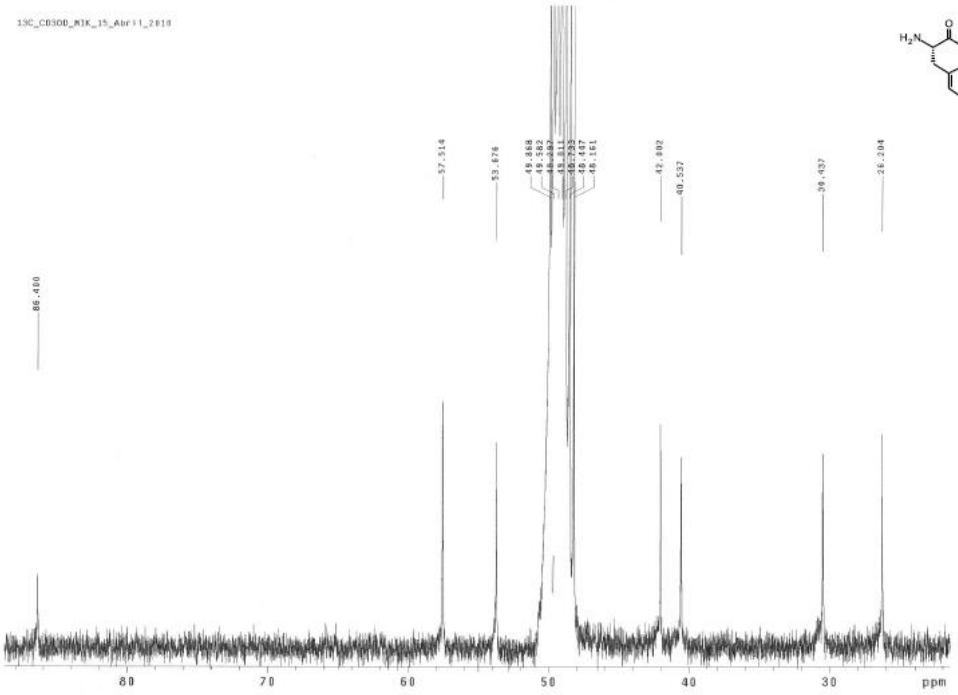

7

^{13}C NMR (CD_3OD, 75 MHz)
Mono-iodinated KTP-NH_2 (MIK)

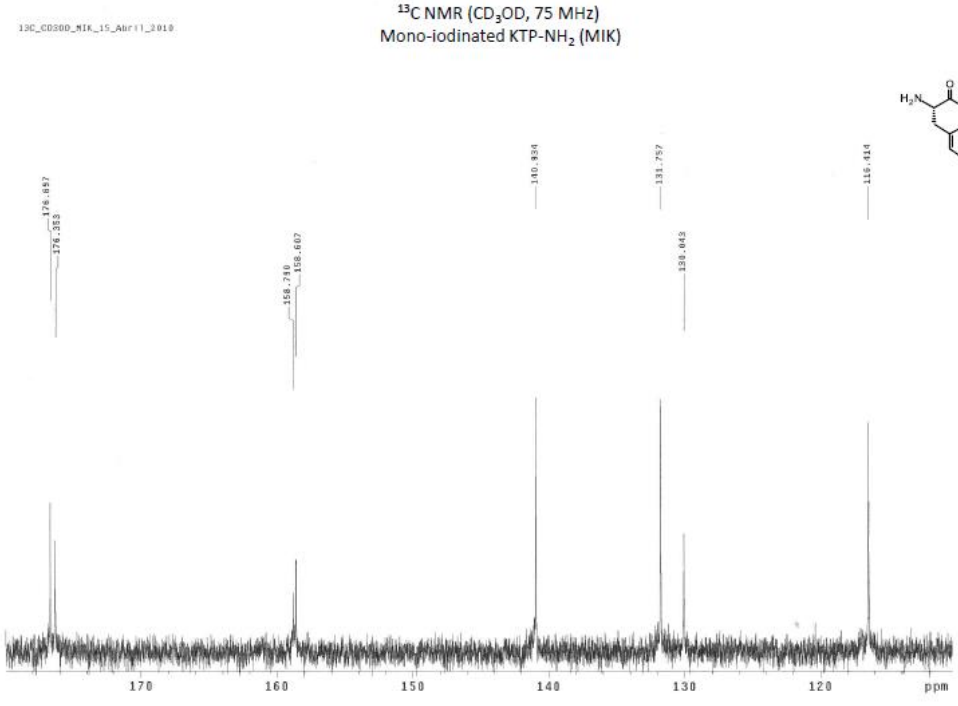

)

8

^{13}C NMR (CD_3OD, 75 MHz)
Di-iodinated KTP-NH_2 (DIK)

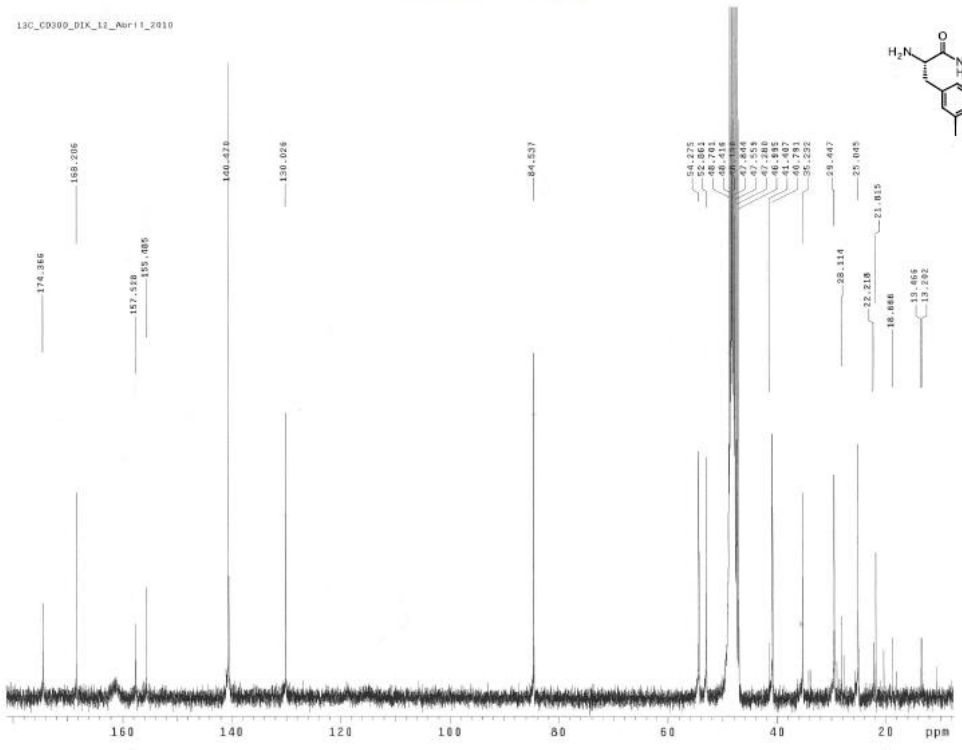

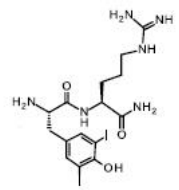

9

^{13}C NMR (CD_3OD, 75 MHz)
Di-iodinated KTP-NH_2 (DIK)

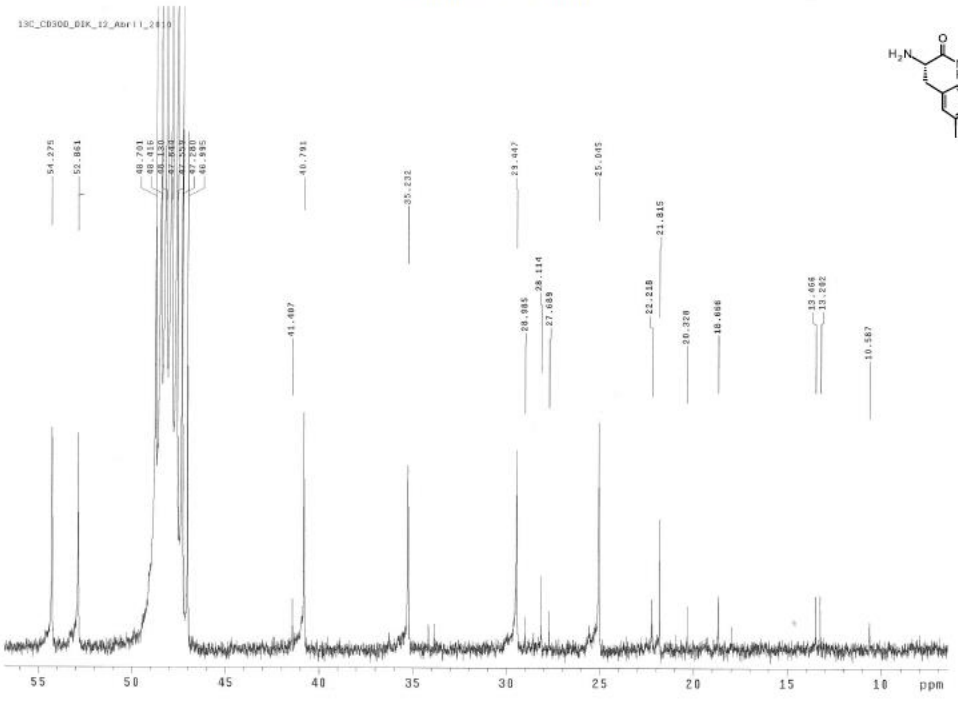

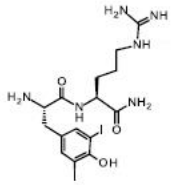

10

^{13}C NMR (CD_3OD, 75 MHz)
Di-iodinated KTP-NH_2 (DIK)

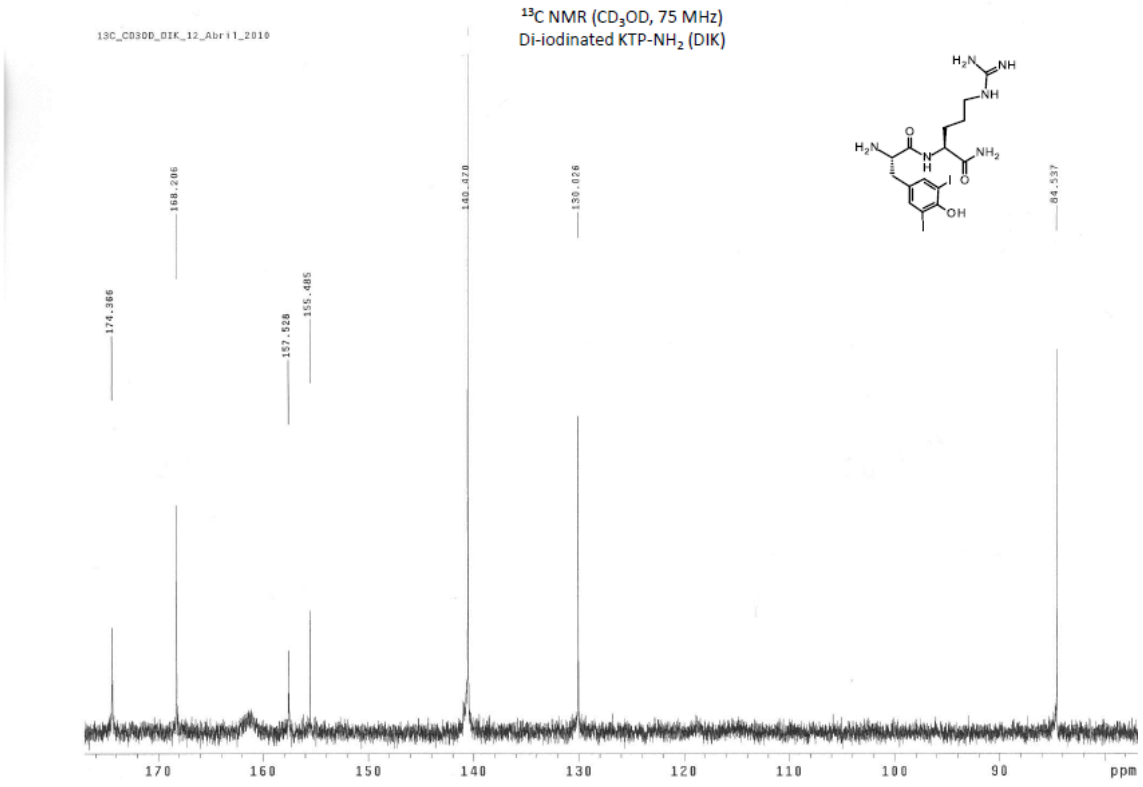

11

Mono-iodinated KTP-NH_2 (MIK)

Generic Display Report

Analysis Info

Analysis Name	C:\Data\MIK_Cristina_P2.d	Acquisition Date	12/05/2010 17:54:45
Method	DEF_MS_NEW.M	Operator	Administrator
Sample Name	MIK_Cristina	Instrument	HCT
Comment	C15H23N6O3I CH3OH		

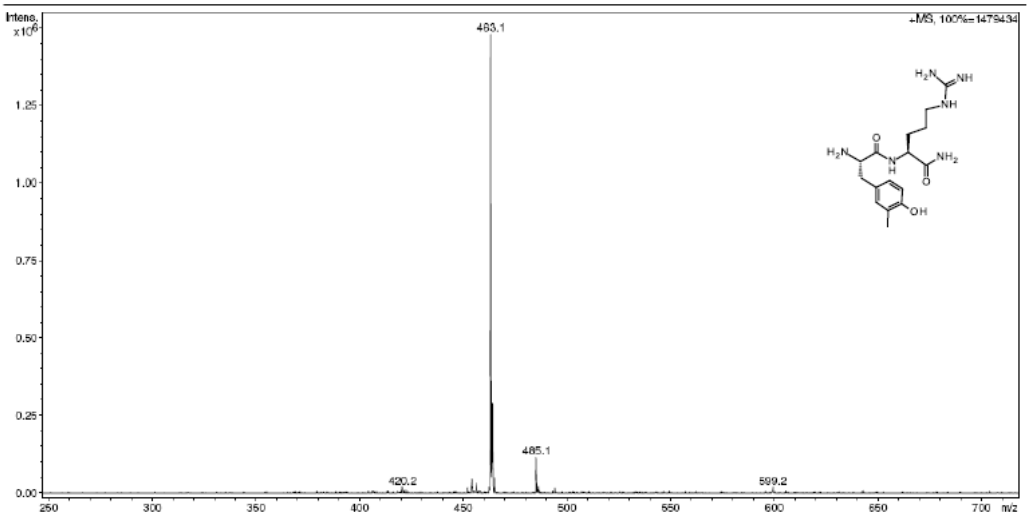

12

Di-iodinated KTP-NH_2 (DIK)

Generic Display Report

Analysis Info			
Analysis Name	C:\Data\DIK_Cristina_P.d	Acquisition Date	12/05/2010 17:33:59
Method	DEF_MS_NEW.M		
Sample Name	DIK_Cristina	Operator	Administrator
Comment	C15H22N8O3I2 CH3OH	Instrument	HCT

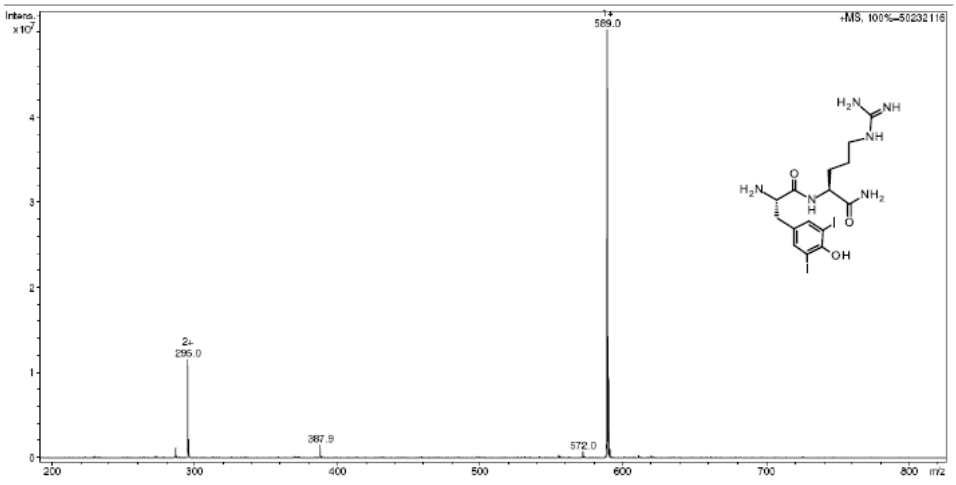

Appendix 2

SUPPLEMENTARY MATERIAL

Endothelium-mediated action of analog derivatives of the endogenous neuropeptide kyotorphin (Tyrosil-arginine): Mechanistic insights from permeation and effects on microcirculation.

Juliana Perazzo[§], Mônica Lopes-Ferreira[†], Sónia Sá Santos[§], Isa Serrano[§], Antónia Pinto[§], Carla Lima[†], Eduard Bardají[‡], Isaura Tavares[#], Montserrat Heras[‡], Kátia Conceição[ϕ], Miguel A. R. B. Castanho[§]*.*

§- Instituto de Medicina Molecular, Faculdade de Medicina da Universidade de Lisboa, Av. Professor Egas Moniz, 1649-028 Lisboa, Portugal;
†- Unidade de Imunorregulação, Laboratório Especial de Toxinologia Aplicada, Instituto Butantan, Av. Vital Brasil 1500 São Paulo, Brazil;
‡- Laboratori d'Innovació en processos i Productes de Síntesi Orgànica (LIPPSO), Department de Química, Universitat de Girona, Campus Montilivi, 17071 Girona, Spain.
#- Instituto de Biologia Molecular e Celular, Porto, Portugal; i3S - Instituto de Inovação e Investigação em Saúde, Universidade do Porto, Porto, Portugal; Departamento de Biologia Experimental, Faculdade de Medicina, Universidade do Porto, Portugal.
ϕ- Departamento de Ciências e Tecnologia, Universidade Federal de São Paulo, UNIFESP, Rua Talim, 330, São José dos Campos, Brazil.

Table of contents

^{1}H-NMR (400 MHz, D_2O) of KTP-NH_2-DD

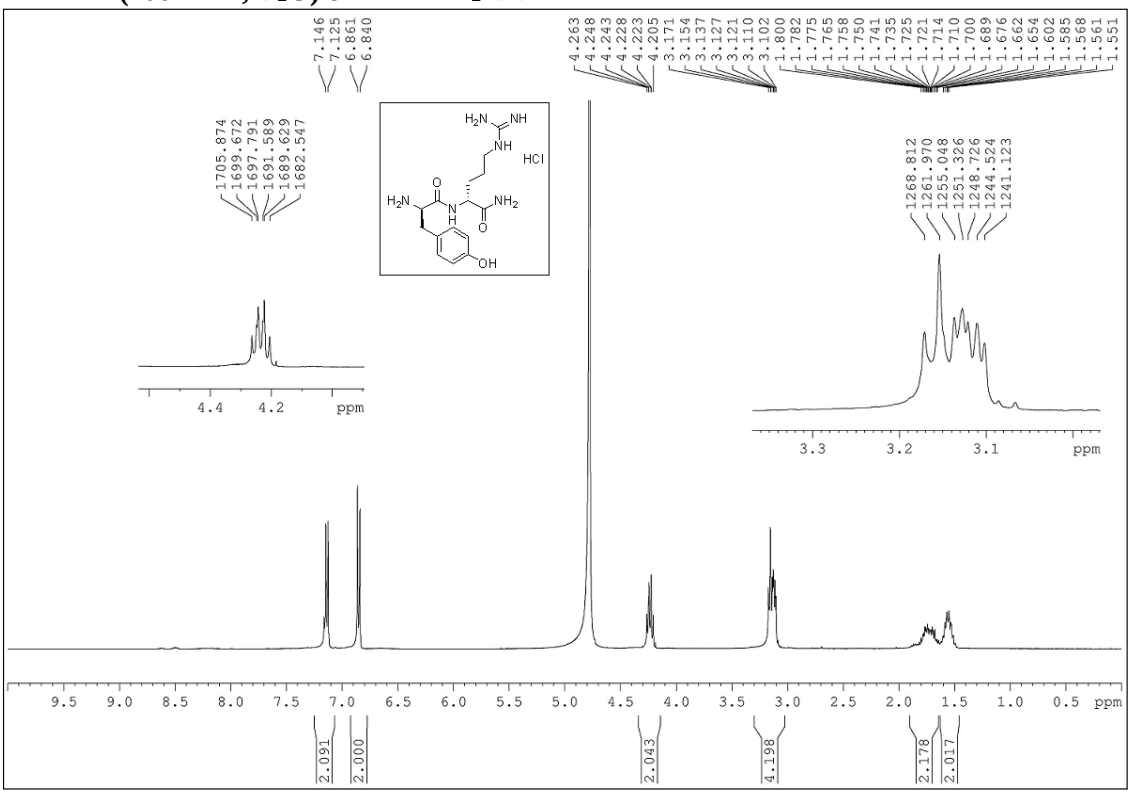

HPLC of KTP-NH_2-DD

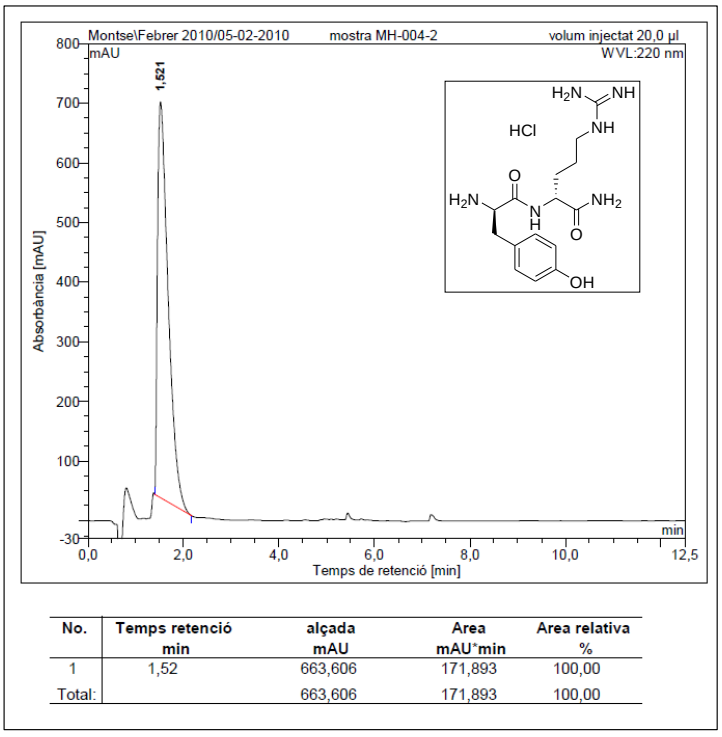

No.	Temps retenció min	alçada mAU	Area mAU*min	Area relativa %
1	1,52	663,606	171,893	100,00
Total:		663,606	171,893	100,00

^{1}H-NMR (400 MHz, D_2O) of KTP-NH_2-LD

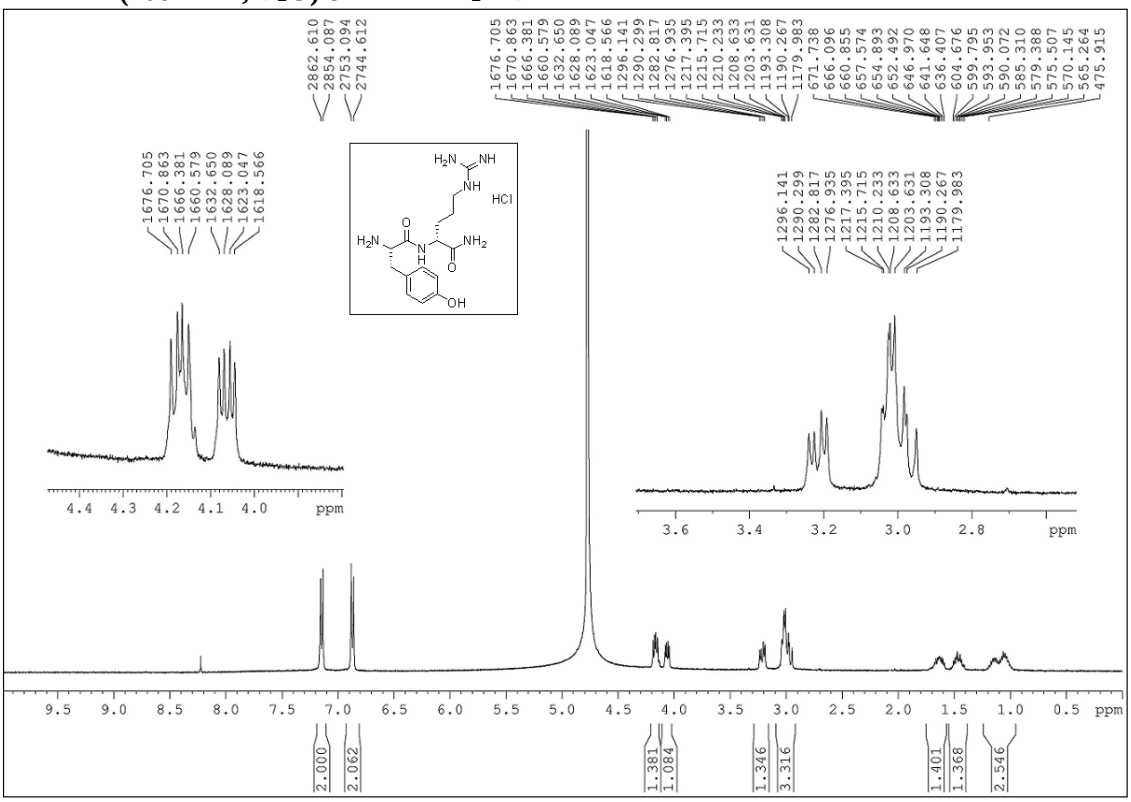

HPLC of KTP-NH_2-LD

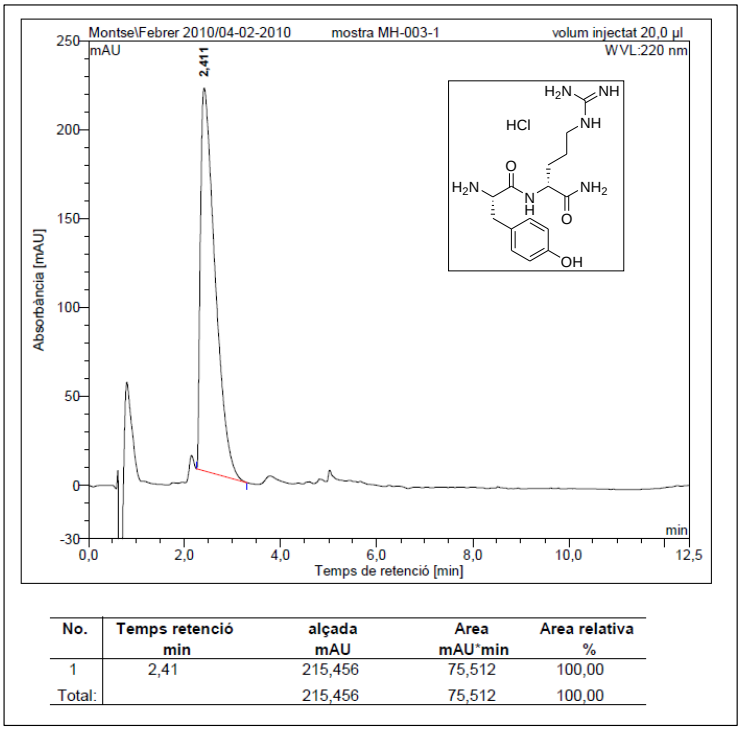

No.	Temps retenció min	alçada mAU	Area mAU*min	Area relativa %
1	2,41	215,456	75,512	100,00
Total:		215,456	75,512	100,00

^{1}H-NMR (400 MHz, DMSO-*d6* + a drop D_2O) of Boc-D-Tyr(Bzl)-Arg-NH_2

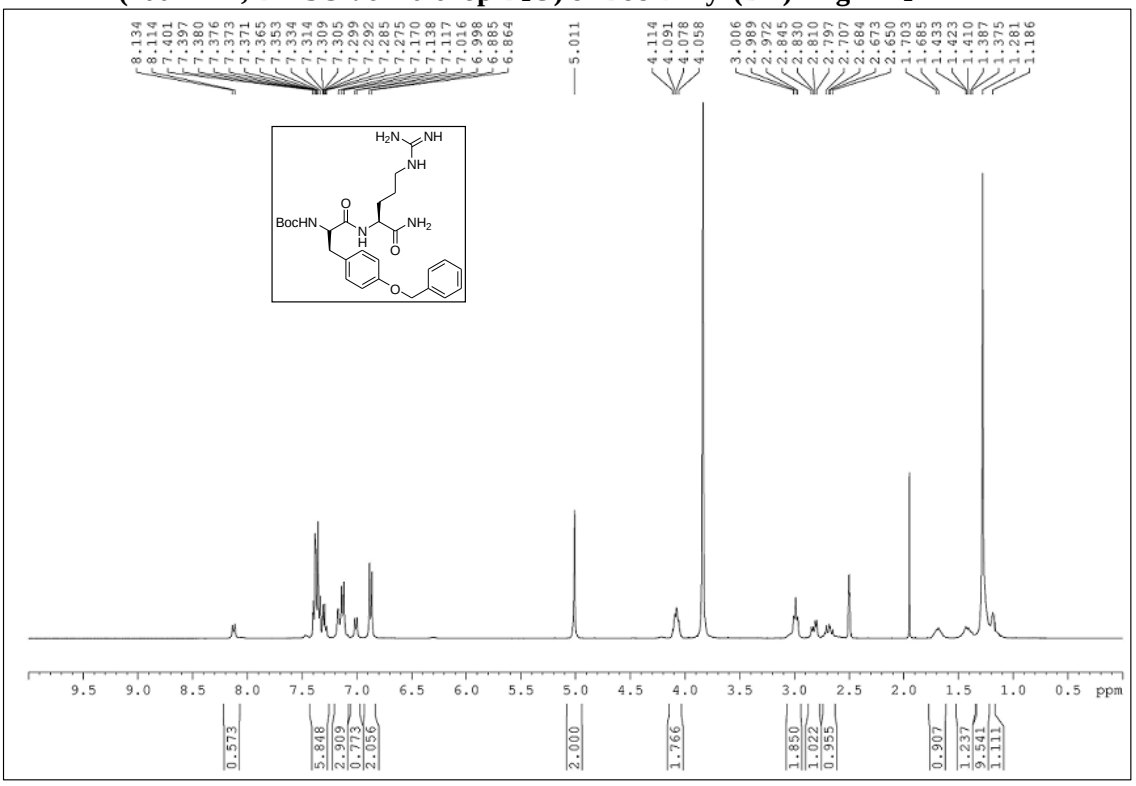

^{13}C-NMR (100 MHz, DMSO-*d6*) and dept experiment of Boc-D-Tyr(Bzl)-Arg-NH_2

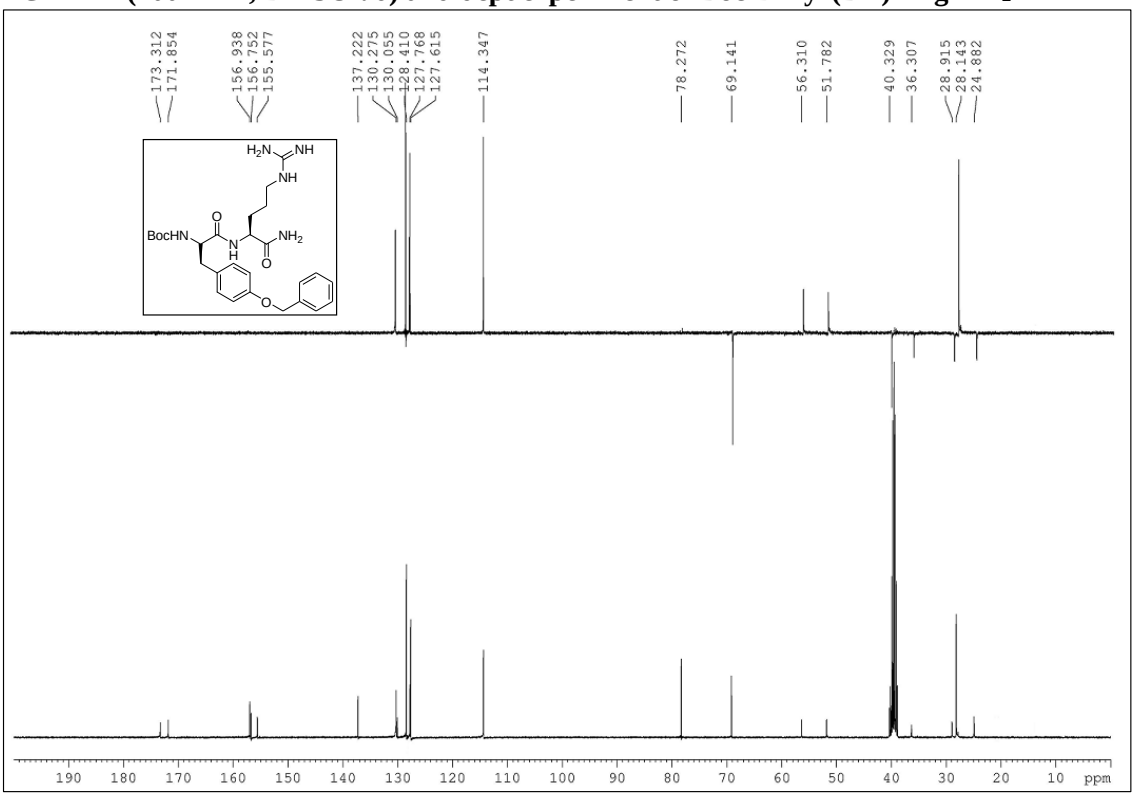

HRMS (ESI) of Boc-D-Tyr(Bzl)-Arg-NH_2

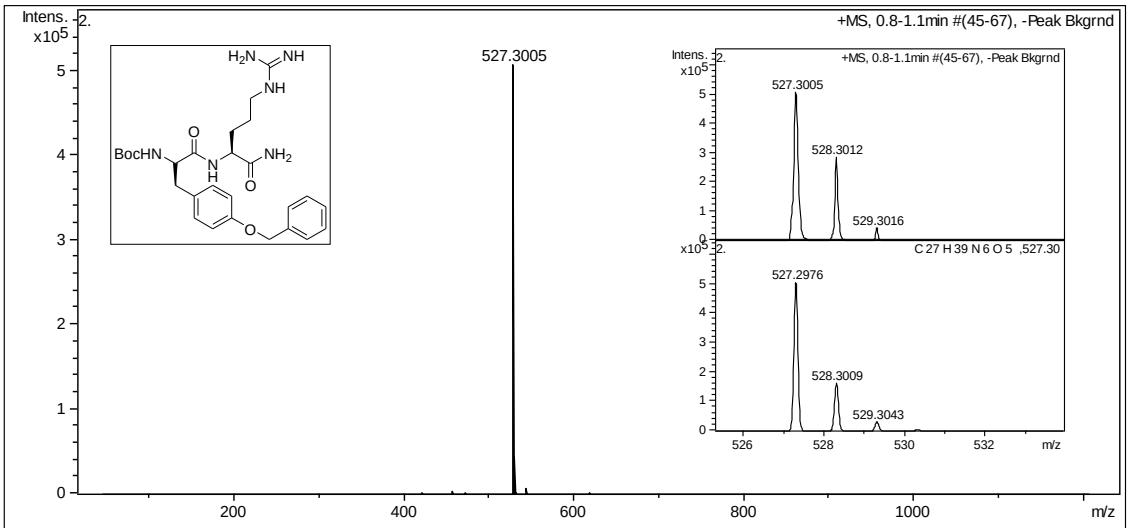

Meas. m/z	Formula	m/z	err [mDa]	err [ppm]	mSigma
527.3005	C 27 H 39 N 6 O 5	527.2976	-2.9	-5.5	120.0

^{1}H-NMR (400 MHz, D_2O) of KTP-NH_2-DL

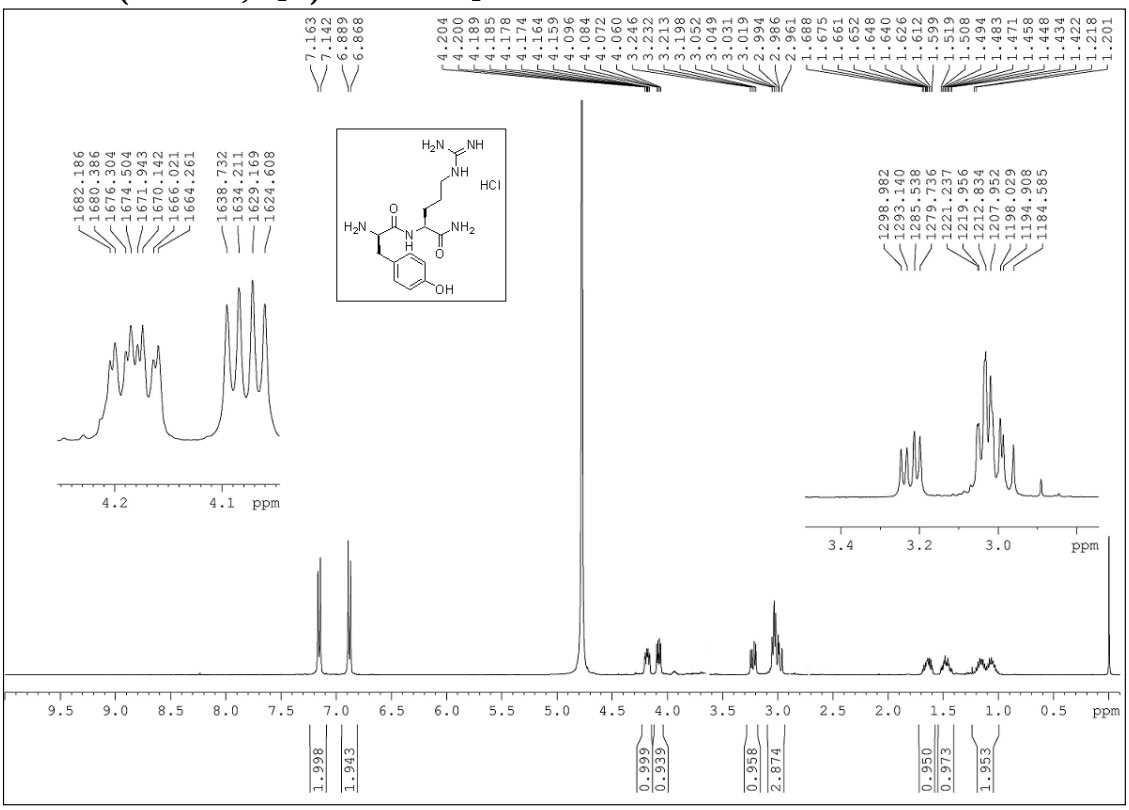

COSY experiment of KTP-NH_2-DL

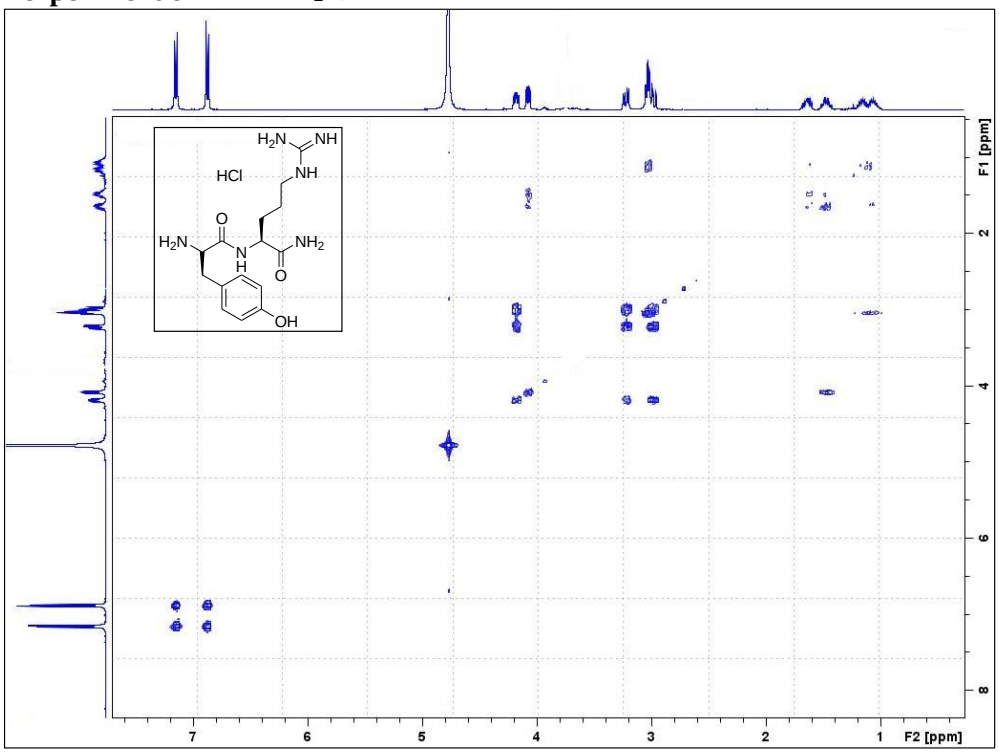

^{13}C-NMR (100 MHz, D_2O) and dept experiment of KTP-NH_2-DL

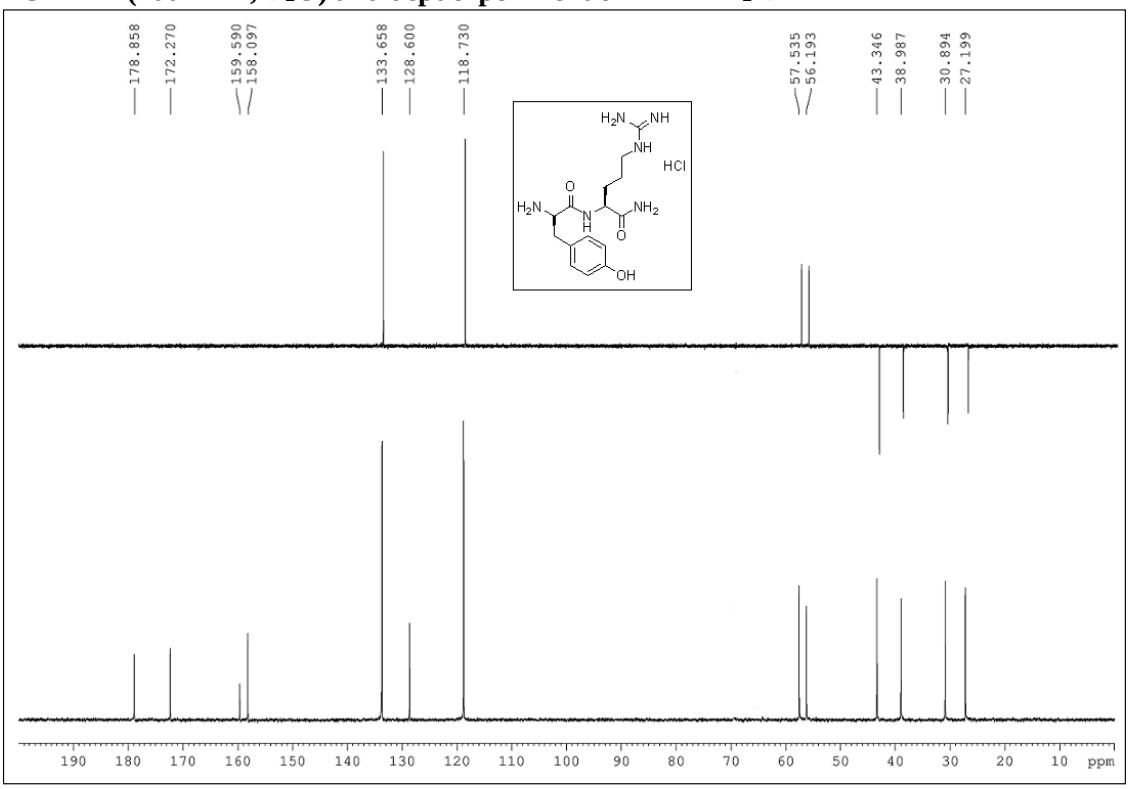

HRMS (ESI) of KTP-NH$_2$-DL

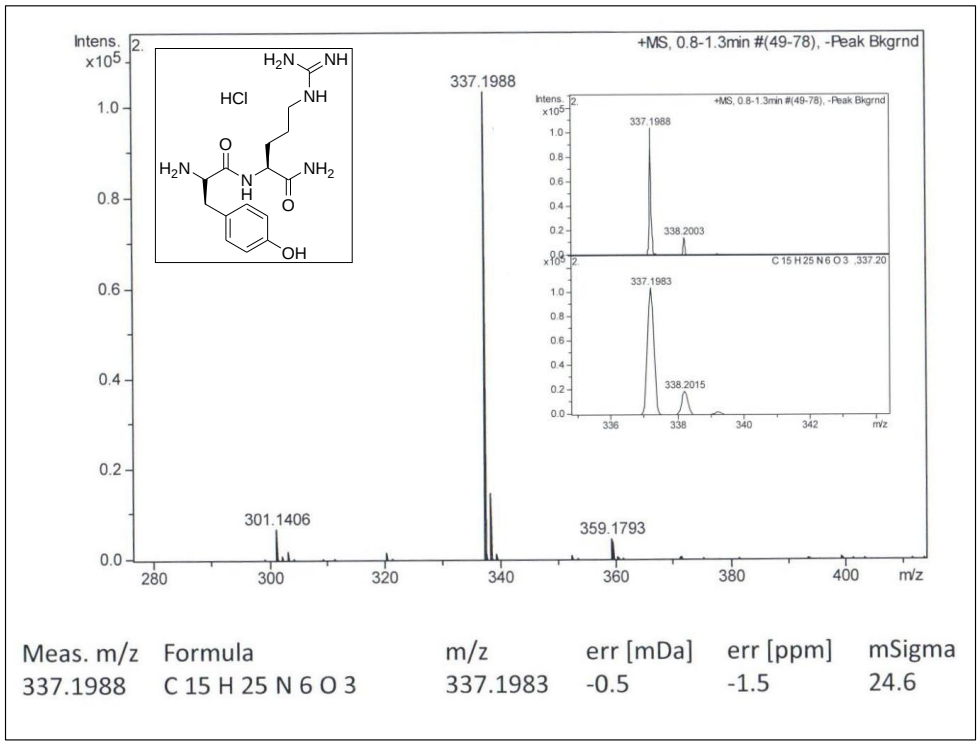

Meas. m/z	Formula	m/z	err [mDa]	err [ppm]	mSigma
337.1988	C 15 H 25 N 6 O 3	337.1983	-0.5	-1.5	24.6

HPLC of KTP-NH$_2$-DL

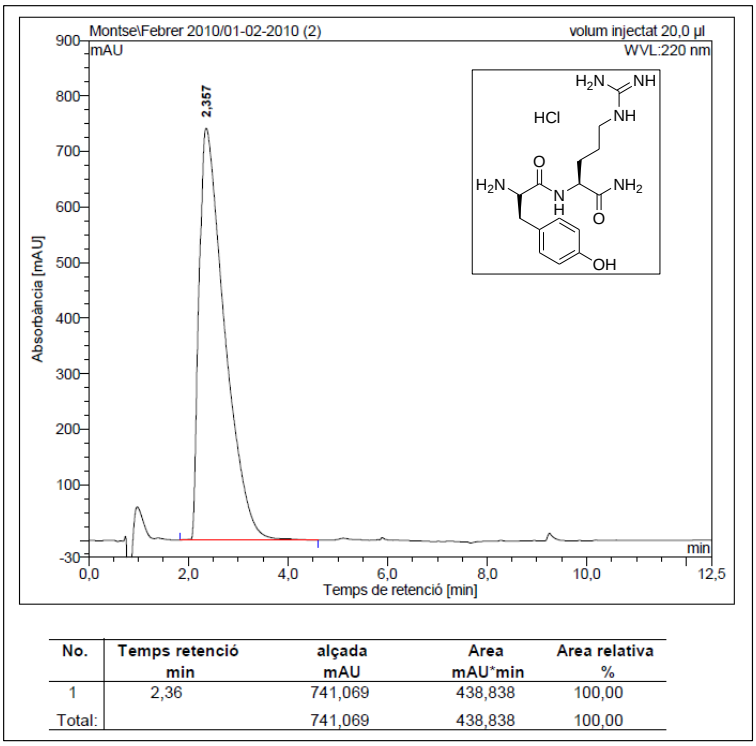

No.	Temps retenció min	alçada mAU	Area mAU*min	Area relativa %
1	2,36	741,069	438,838	100,00
Total:		741,069	438,838	100,00

^{1}H-NMR (400 MHz, DMSO-*d6*, 110 ºC) of Boc-N-Me-Tyr(Bzl)-D-Arg-NH$_2$

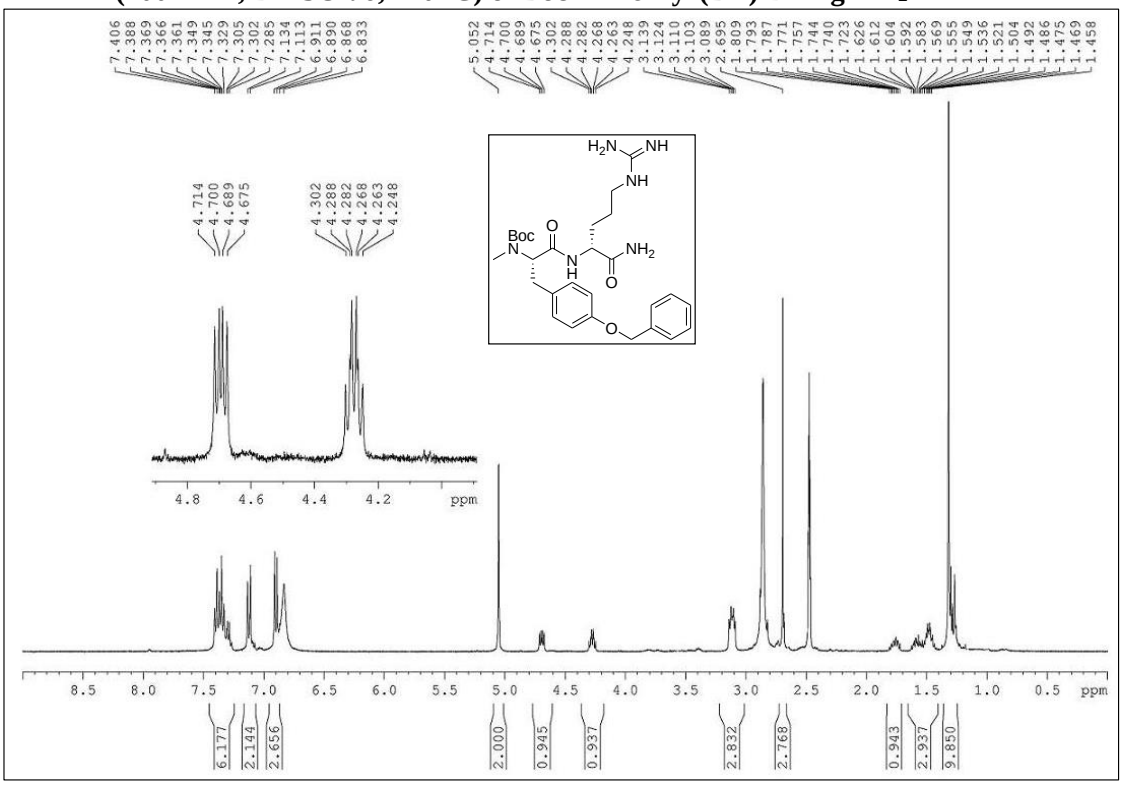

^{13}C-NMR (100 MHz, DMSO-*d$_6$*, 80 ºC) dept experiment of Boc-N-Me-Tyr(Bzl)-D-Arg-NH$_2$

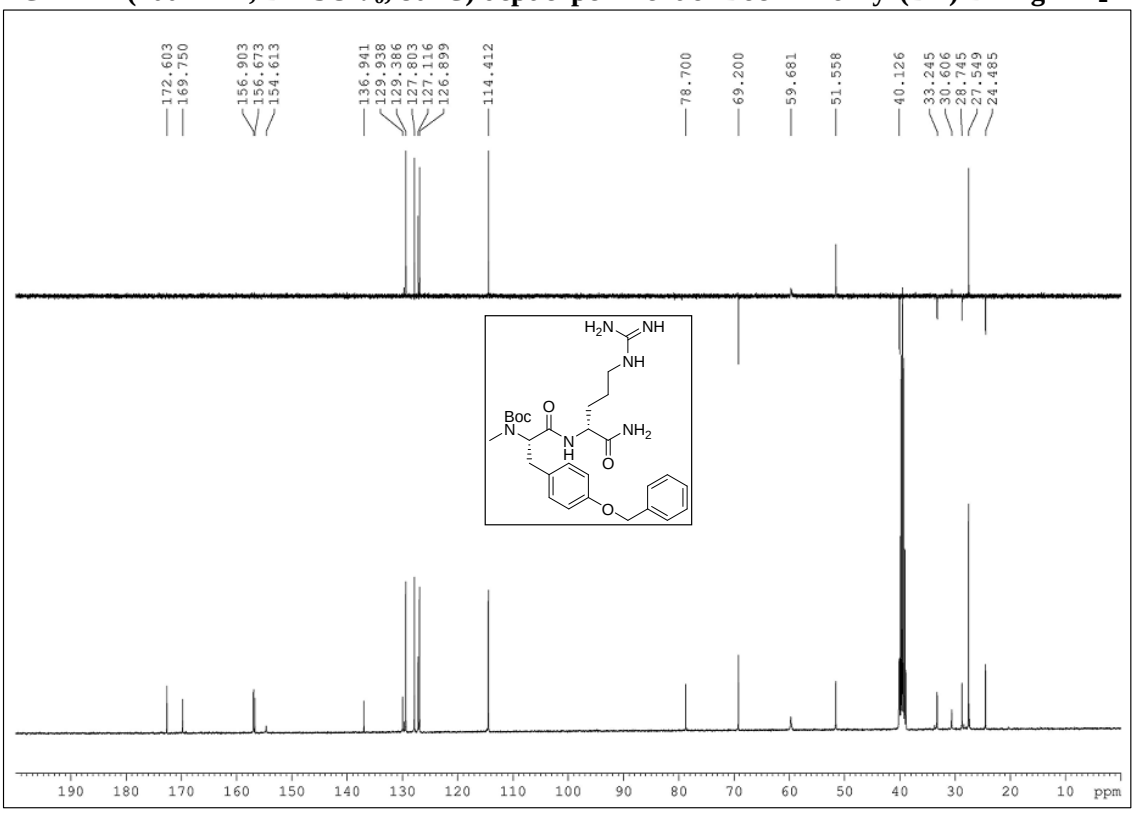

HRMS (ESI) of Boc-N-Me-Tyr(Bzl)-D-Arg-NH_2

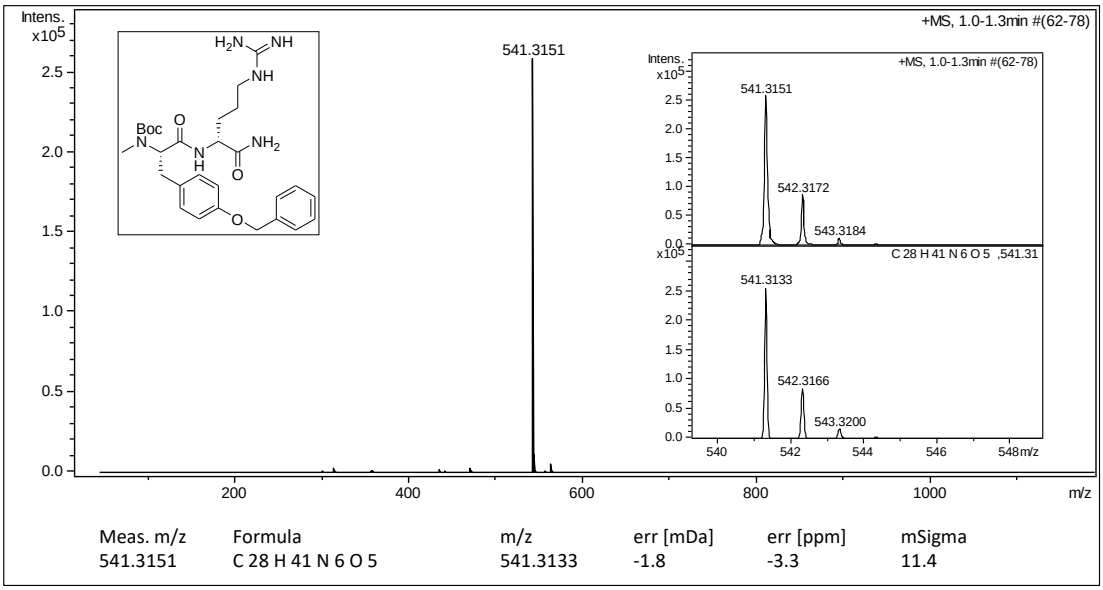

Meas. m/z	Formula	m/z	err [mDa]	err [ppm]	mSigma
541.3151	C 28 H 41 N 6 O 5	541.3133	-1.8	-3.3	11.4

^{1}H-NMR (400 MHz, D_2O) of Me-KTP-NH_2-LD

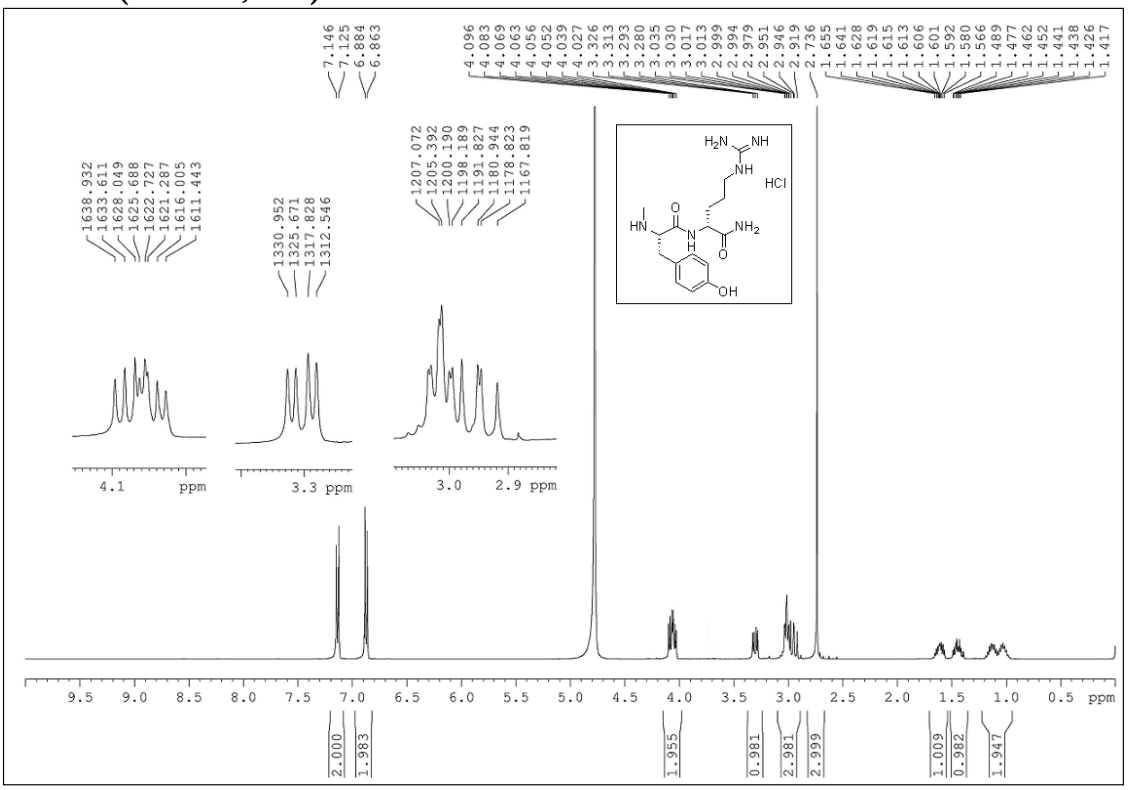

COSY experiment of Me-KTP-NH_2-LD

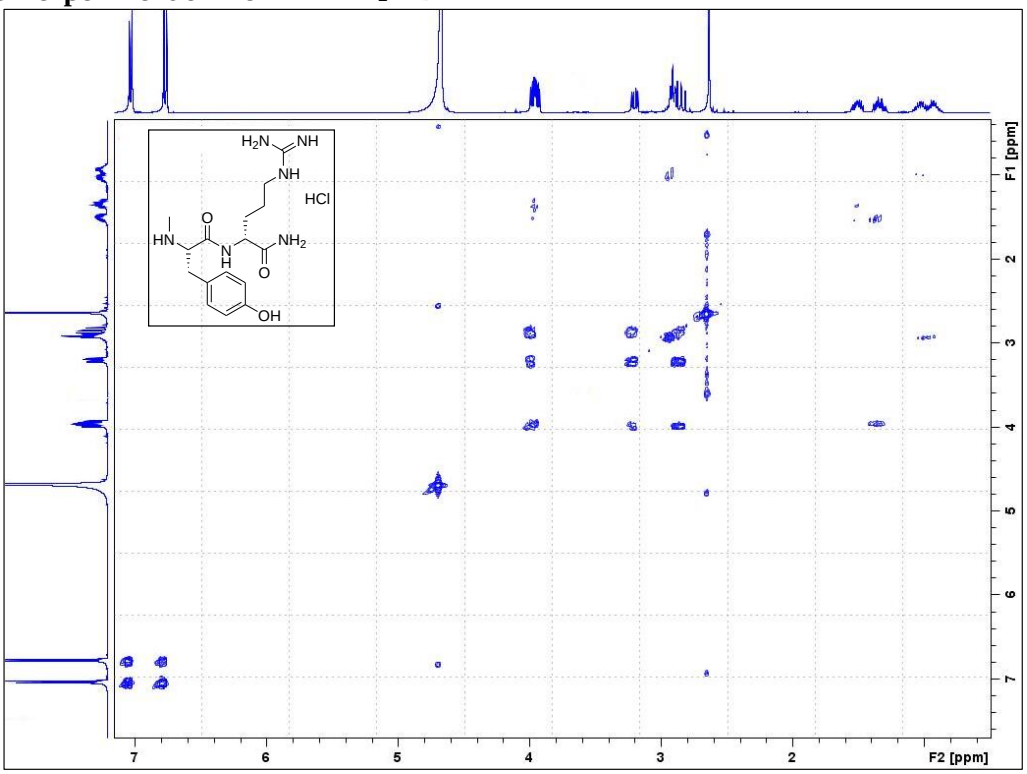

^{13}C-NMR (100 MHz, D_2O) and dept experiment of Me-KTP-NH_2-LD

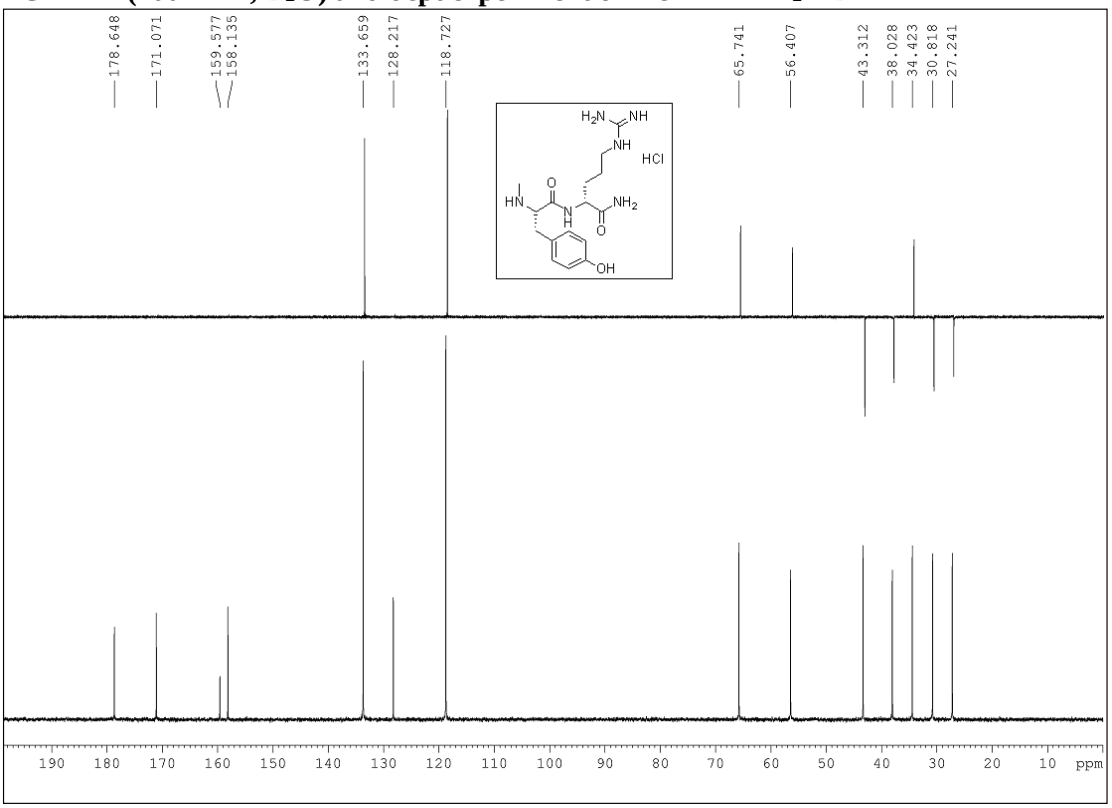

HRMS (ESI) of Me-KTP-NH_2-LD

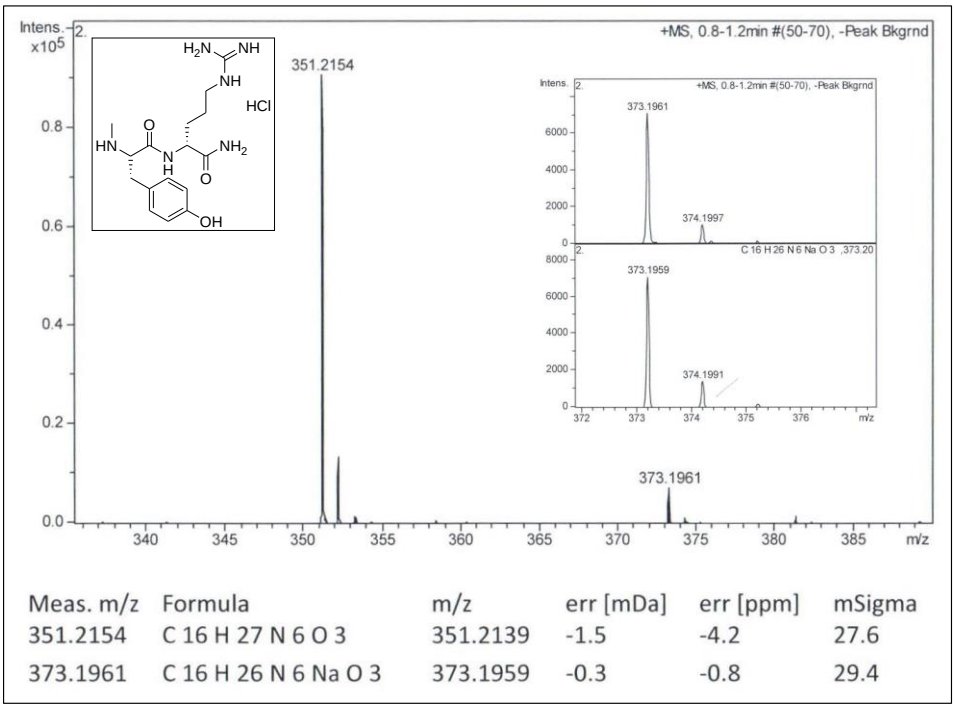

Meas. m/z	Formula	m/z	err [mDa]	err [ppm]	mSigma
351.2154	C 16 H 27 N 6 O 3	351.2139	-1.5	-4.2	27.6
373.1961	C 16 H 26 N 6 Na O 3	373.1959	-0.3	-0.8	29.4

HPLC of Me-KTP-NH_2-LD

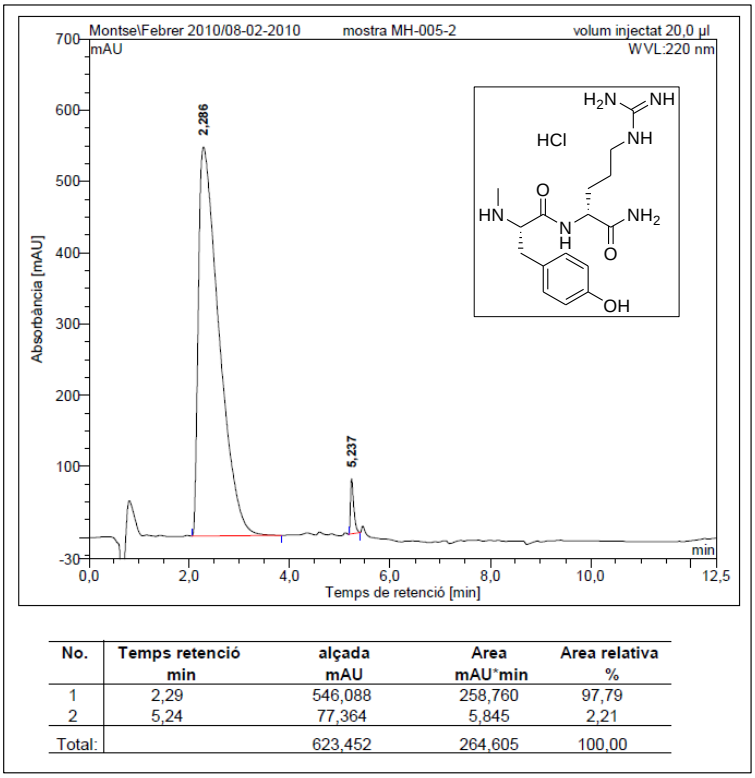

No.	Temps retenció min	alçada mAU	Area mAU*min	Area relativa %
1	2,29	546,088	258,760	97,79
2	5,24	77,364	5,845	2,21
Total:		623,452	264,605	100,00

^{1}H-NMR (400 MHz, DMSO-*d6*, 80 ºC) of Boc-N-Me-Tyr(Bzl)- Arg-NH$_2$

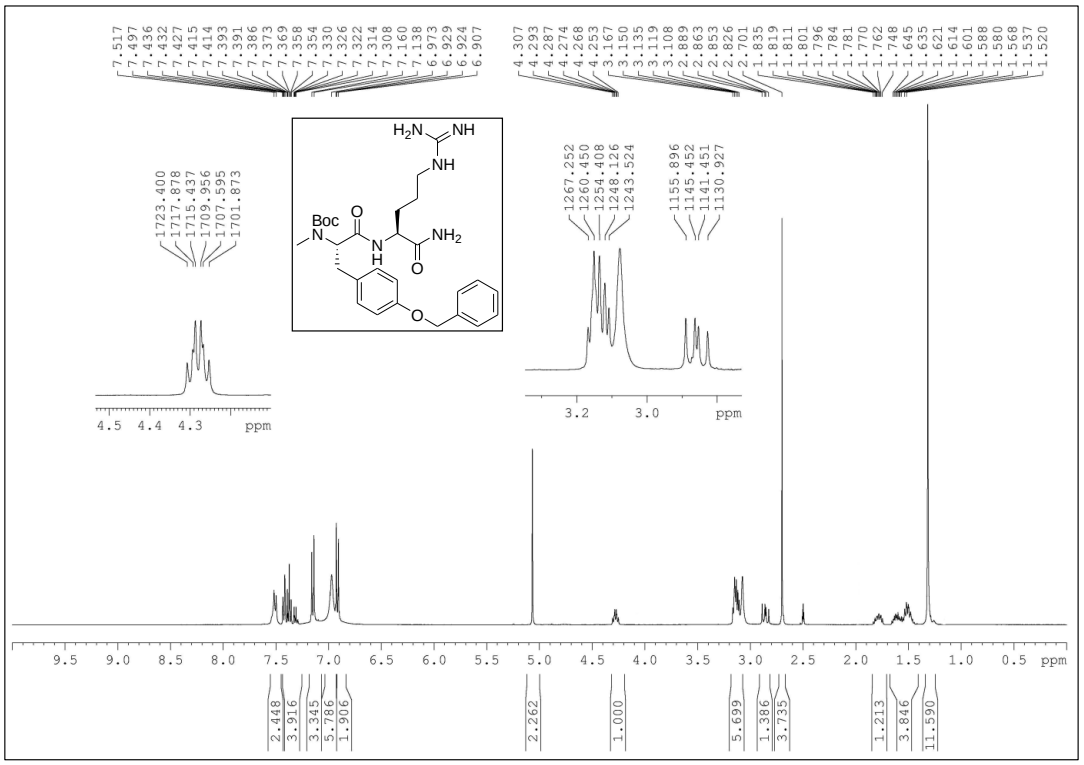

^{13}C-NMR (100 MHz, DMSO-*d6*, 80 ºC) dept experiment of Boc-N-Me-Tyr(Bzl)-Arg-NH$_2$

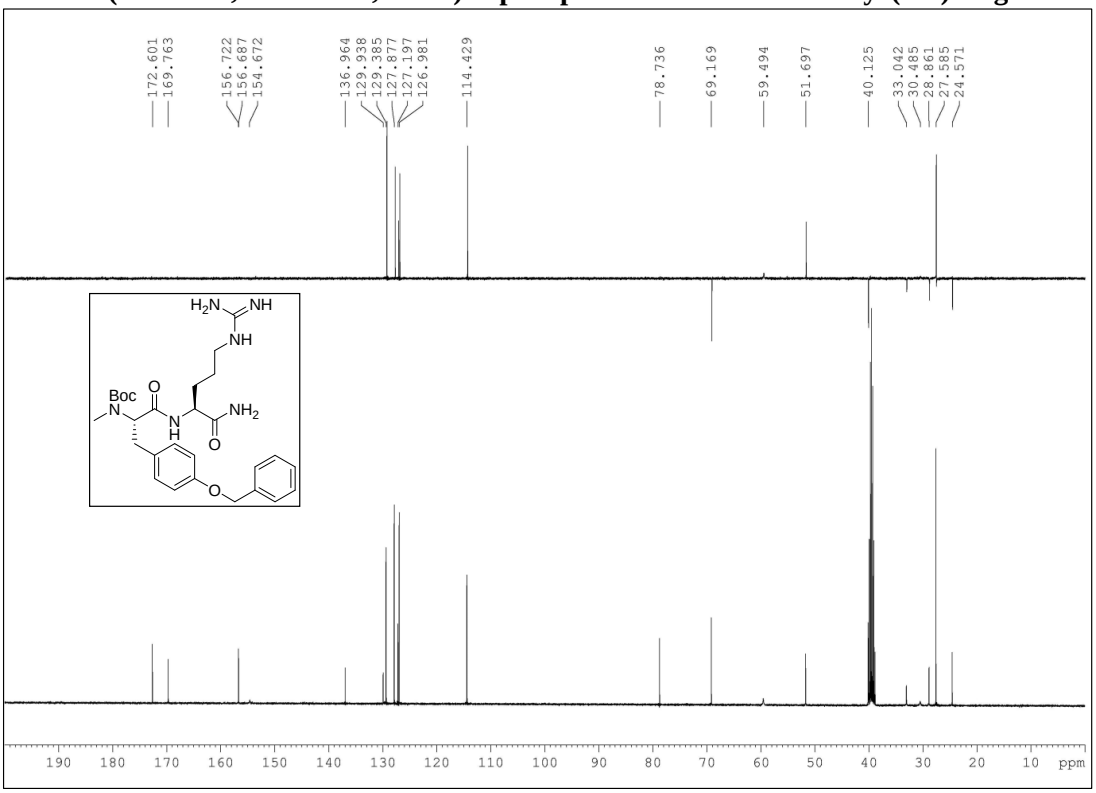

HRMS (ESI) of Boc-N-Me-Tyr(Bzl)-Arg-NH_2

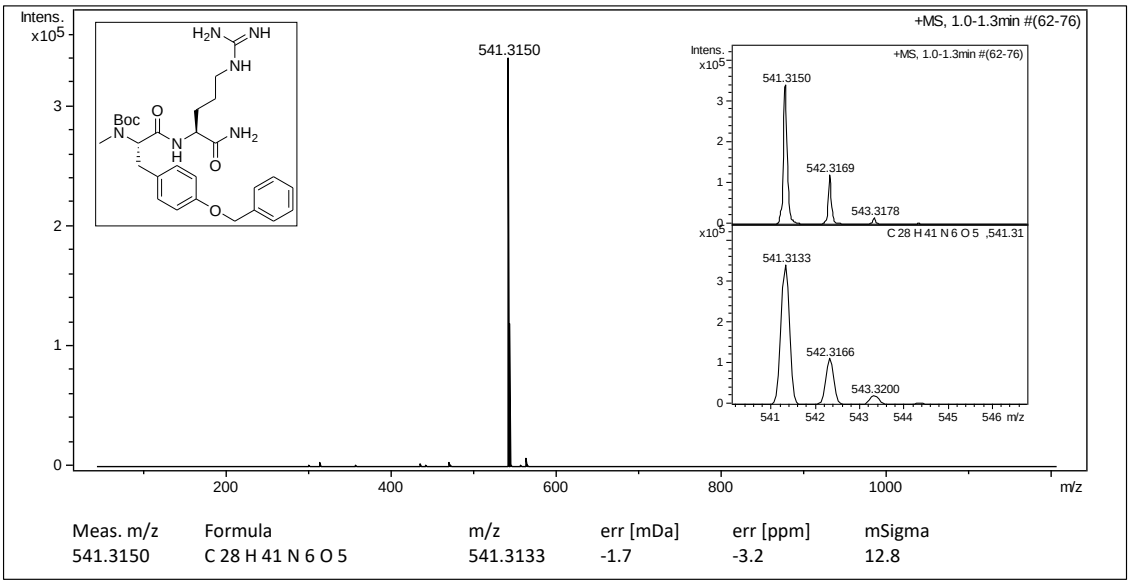

Meas. m/z	Formula	m/z	err [mDa]	err [ppm]	mSigma
541.3150	C 28 H 41 N 6 O 5	541.3133	-1.7	-3.2	12.8

^{1}H-NMR (400 MHz, D_2O) of Me-KTP-NH_2

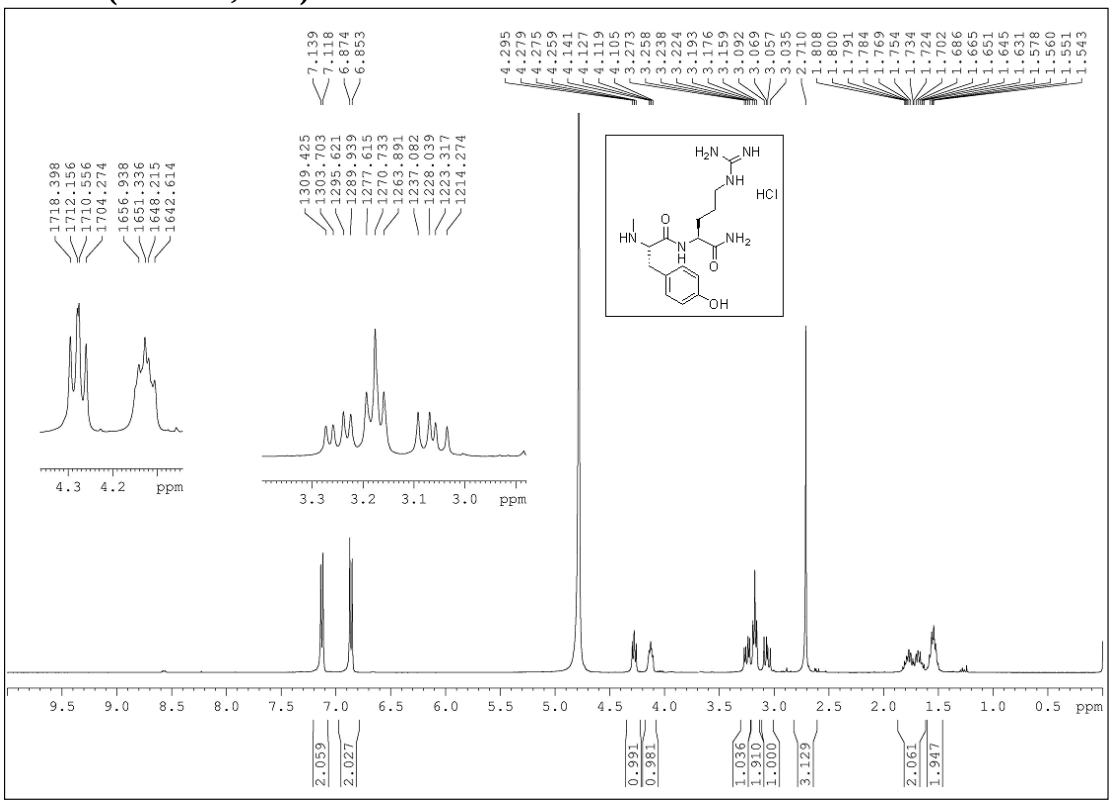

COSY experiment of Me-KTP-NH_2

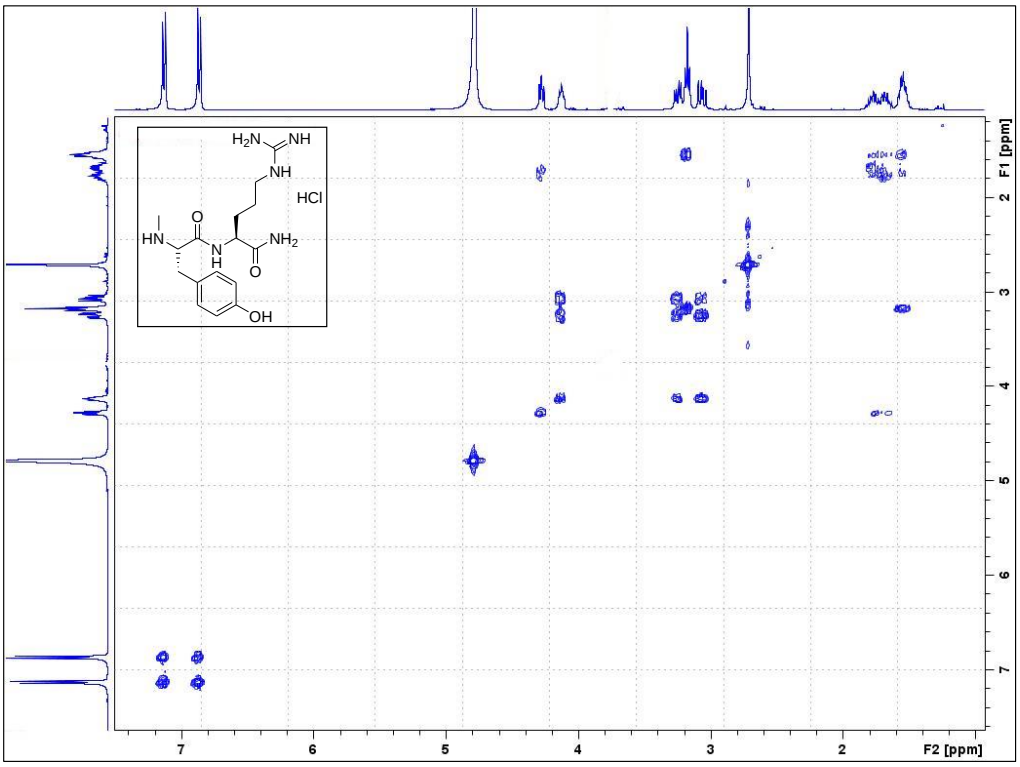

^{13}C-NMR (100 MHz, D_2O) and dept experiment of Me- KTP-NH_2

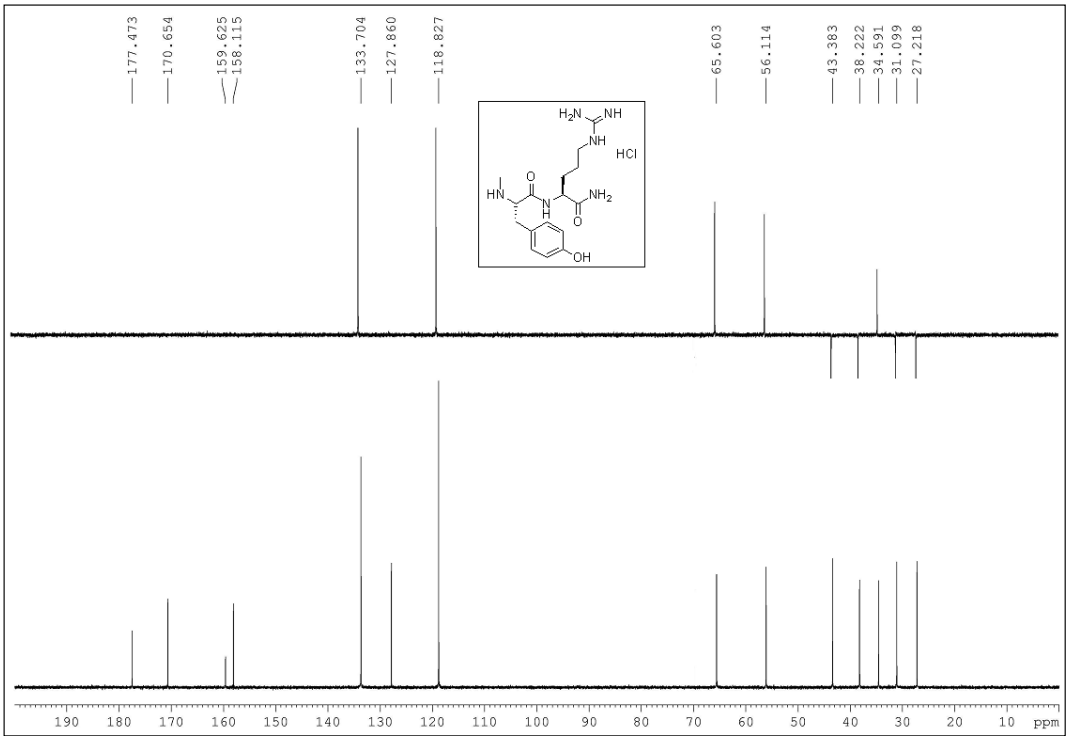

HRMS (ESI) of Me- KTP-NH$_2$

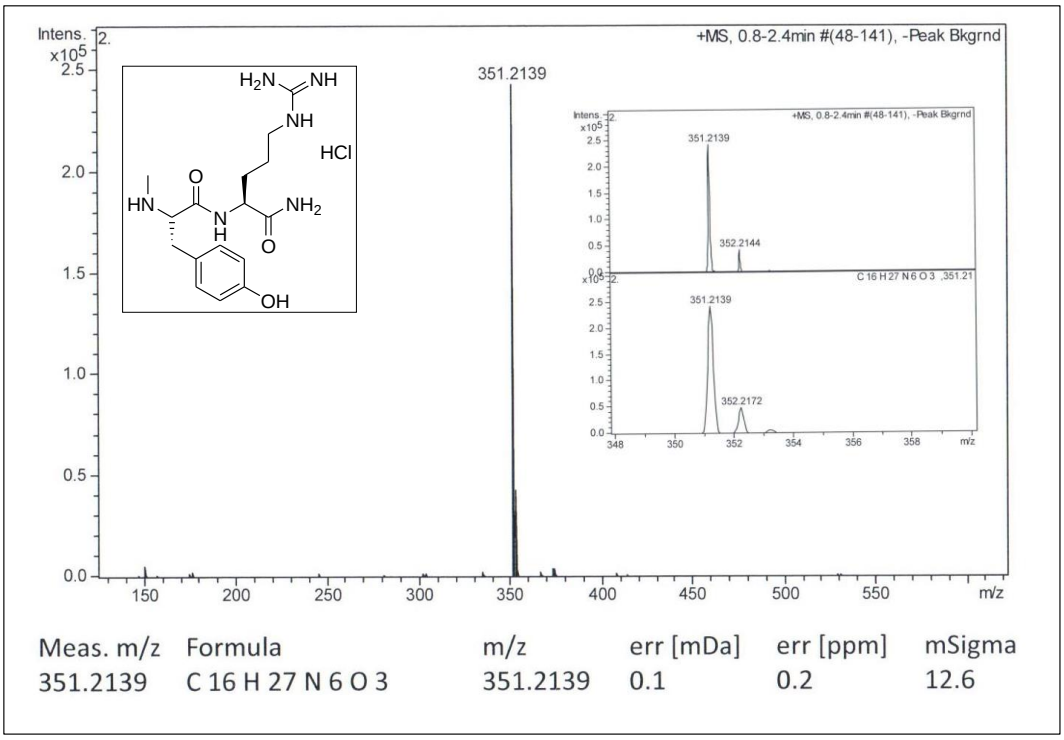

HPLC of Me- KTP-NH$_2$

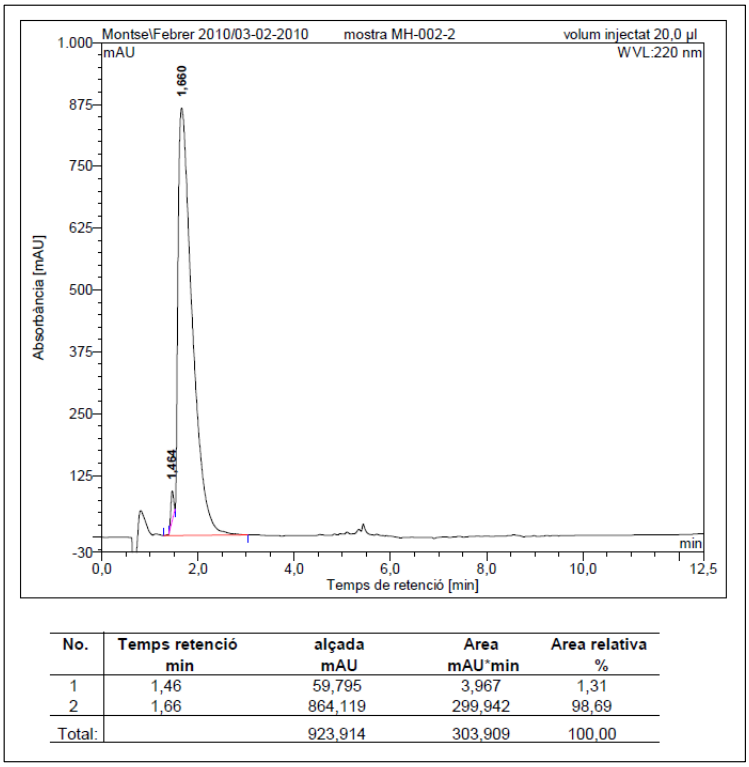

No.	Temps retenció min	alçada mAU	Area mAU*min	Area relativa %
1	1,46	59,795	3,967	1,31
2	1,66	864,119	299,942	98,69
Total:		923,914	303,909	100,00

Measure of relative permeability in permeation studies

Relative permeability was measured using the transwell setup and data analysis methodology described in references S1 and S2.

Relative permeability was calculated by dividing the slope of the kinetics of the Tyr residues fluorescence intensity in the apical compartment in lipid-covered filters by the same measurement in lipid-free filters, over a 10h period (Figure S1).

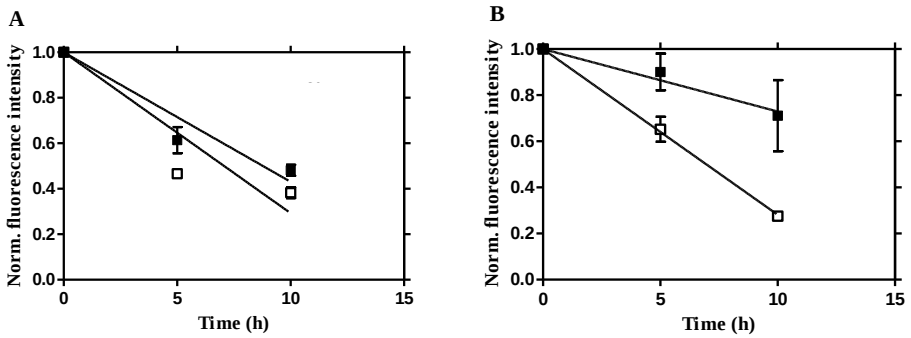

Figure S1: *Normalized fluorescence intensity plotted against time in lipid-covered (solid squares) and lipid-free filters (empty squares). Me-KTP-NH₂ (A) and KTP-NH₂-DL (B) are examples of highly and poorly permeable drugs, respectively.*

As shown in Table S1, means of P_R ranged from 0.38 to 0.81. Comparing to KTP-NH₂, the P_R of Me-KTP-NH₂-LL was significantly higher, whereas there were no significant differences with Me-KTP-NH₂-LD, KTP-NH₂-DL or KTP.

Table S1: *Relative permeability of Me-KTP-NH₂, Me-KTP-NH₂-LD, KTP-NH₂-DL, KTP, and KTP-NH₂. Data showed as means ± SD; each group is an average of three independent measures. ***P < 0.001, and ns not significant, versus KTP-NH₂. One-way ANOVA P < 0.0001, followed by Tukey's post test.*

Kyotorphin derivatives	Relative permeability (P_R)
Me-KTP-NH₂	0.805±0.092 ***
Me-KTP-NH₂-LD	0.659±0.028 ns
KTP	0.583±0.059 ns
KTP-NH₂	0.489±0.060
KTP-NH₂-DL	0.377±0.065 ns

REFERENCES

S1. Serrano, I.D., Freire, J.M., Carvalho, M.V., Neves, M., Melo, M. N., and Castanho, M.A.R.B. (2014) The Mechanisms and Quantification of the Selective Permeability in Transport Across Biological Barriers: the Example of Kyotorphin, *Mini Reviews in Medicinal Chemistry 14*, 99-110.

S2. Serrano, I. D., Ramu, V. G., Pinto, A. R., Freire, J. M., Tavares, I., Heras, M., Bardaji, E. R., and Castanho, M. A. (2015) Correlation between membrane translocation and analgesic efficacy in kyotorphin derivatives, *Biopolymers 104*, 1-10.